南京师范大学

博 士 学 位 论 文

界面问题的非匹配网格的有限元方法

研 究 生： 刘盎然

指导教师： 陈金如 教授

研究生学号： 160901007

培养单位： 数学科学学院

一级学科： 数学

二级学科： 计算数学

完成时间： 2020 年 3 月 25 日

学位论文独创性声明

本人郑重声明：所提交的学位论文是本人在导师指导下进行的研究工作和取得的研究成果。本论文中除引文外，所有实验、数据和有关材料是真实的。本论文中除引文和致谢的内容外，不包含其他人或其它机构已经发表或撰写过的研究成果。其它同志对本研究所做的贡献均已在论文中作了声明并表示了谢意。

学位论文作者签名：　　　　日　　期：2020年5月26日

学位论文使用授权声明

研究生在校攻读学位期间论文工作的知识产权单位属南京师范大学。学校有权保存本学位论文的电子和纸质文档，可以借阅或上网公布本学位论文的部分或全部内容，可以采用影印、复印等手段保存、汇编本学位论文。学校可以向国家有关机关或机构送交论文的电子和纸质文档，允许论文被查阅和借阅。（保密论文在解密后遵守此规定）

学位论文作者签名：　　　　指导教师签名：

日　　期：2020年5月26日　　日　　期：2020年5月26日

Interface-unfitted Finite Element Methods for Interface Problems

by

Angran Liu

A Dissertation Submitted to the Graduate Faculty of
Nanjing Normal University
in Partial Fulfillment of the
Requirements for the Degree of

Doctor of Philosophy
in
Mathematics

School of Mathematical Sciences

Supervisor

Professor Jinru Chen

Nanjing
May 2020

Contents

目 录

摘要

界面问题广泛的存在于实际生活和应用中，如流体力学的诸多问题，细胞变形和血液流动，复合材料的研究和生物科学等等。通常涉及求解耦合的偏微分方程组。本文致力于用有限元方法研究界面问题。

根据网格单元和界面之间的拓扑关系，界面问题的有限元方法 (FEMs) 可分为两大类，即界面匹配网格方法和界面非匹配网格方法。界面匹配网格方法的优点在于可以直接应用传统的有限元方法，并且可以得到最优误差估计。然而，在界面较为复杂或者随时间演变的情况下，网格剖分的工作量就会相当巨大。并且当界面结构变化时，例如破裂或者合并，此时生成匹配网格的界面是非常困难的。因此，界面非匹配网格方法就成了一个越来越重要的研究方向。

主流的界面非匹配网格方法主要有两种，扩展有限元法 (XFEMs) 和浸入界面有限元方法 (IFEMs)。扩展有限元方法有许多分支，但是只有Nitshce–扩展有限元方法有着严格的理论估计。该方法中，由于解的连续性被破坏，因此需要在离散的弱形式里边加上额外的惩罚项。对于浸入界面有限元方法，它的基函数构造依赖于界面跳跃条件，从而使得误差分析变得非常困难。到目前为止只有二阶椭圆问题具有完整的理论分析。这两种方法都是基于对有限元空间进行修正，但是又各自有相应的缺点。

在本文中，我们首先应用P_1/CR浸入界面有限元方法研究弹性界面问题。我们利用单元上的点值进行构造相应的有限元空间，并且给出了理论上插值误差的估计。之后又利用单元边界上的积分平均值构造相应的浸入界面有限元方法，也给出了插值误差的理论分析。最后还结合了部分加罚的方法，给出了两种方法的有限元误差的理论分析。接下来，结合扩展有限元方法，我们进一步研究了一种新的界面非匹配网格方法，增扩有限元方法。并且把非协调的增扩有限元方法应用于弹性问题的混合元形式，并解决了弹性界面方程出现的闭锁现象问题。在最后，对于Stokes界面问题，我们给出了一种CR元浸入界面有限元方法，构造了相应的有限元空间并给出插值误差和有限元误差的理论估计。

关键词：界面非匹配网格方法; 弹性界面问题; 浸入界面有限元方法; 增扩有限元方法; Stokes界面问题。

Abstract

Interface problems widely exist in actual life and applications, such as many research of composite materials, blood flow and cell deformation, biological science and fluid mechanics and so on. It usually involves solving coupled partial differential equations. In this dissertation, we use the finite element method to study these interface problems.

According to the topological relationship between the grid and the interface, the finite element methods (FEMs) of the interface problem can be divided into two categories, the interface-fitted FEMs and interface-unfitted FEMs. The advantage of interface-fitted FEMs is that the traditional finite element methods can be directly applied and the optimal error estimates can be also obtained. However, when the interface becomes complex or evolves with time, the work of mesh generation will be huge. And when the interface structure changes, such as cracking or merging, it is very difficult to generate meshes that fit the interface. Therefore, interface-unfitted FEMs have become an increasingly important research direction.

There are mainly two kinds of interface-unfitted methods, extended finite element methods (XFEMs) and immersed finite element methods (IFEMs). The XFEMs have many branches, but only Nitshce-XFEM has a strict theoretical analysis. In this method, because the continuity of solution is broken, additional penalty terms always need to be added in the discrete weak form. For immersed finite element method, its basic functions construction depends on the interface jump condition, which makes the error estimates very difficult. So far, only the second order elliptic interface problem has complete theoretical analysis. Both methods are based on the modification of finite element space, but they have their own shortcomings.

In this paper, we first propose the P_1/CR IFEM to study the elasticity interface problem. We use points values as degrees of freedom on elements, give corresponding finite element space and the theoretical estimate of interpolation error. After that, for the method which uses integral average values on the edges of elements as degrees of freedom, we also present the interpolation capability analysis. Finally, the theoretical analysis of the finite element errors of these two kinds of methods are given by combining the partial penalty method. Then, combining the extend finite element method, we develop a new interface-unfitted method, enriched finite element method. We apply it on the mixed element form of elasticity interface problem with a non-conforming enriched finite element method and solve the phenomenon of locking. At last, for stokes interface problem, a CR immersed finite element method is presented. We give the construction of the finite element space, the interpolation error estimate and finite element error estimate.

Keywords: interface-unfitted method; elasticity interface problem; immersed finite element method; enriched finite element method; Stokes interface problem.

Chapter 1 Introduction

1.1 Model problems and applications

The multi-phase interface problems are caused by the interaction of many mediums and physical fields, which are widely used in daily life. To name only a few, the simulation of the blood flow in the human hearts, the elasticity interface problems describing various material behaviors, composite materials problems, Darcy-Stokes coupled models, moving interface problems, fluid-structure interaction problems. Therefore, interface problems are widely used in biomechanics and fluid mechanics.

Some characteristics of differential equations describing interface problems, for instance, discontinuous coefficients or solutions in the equations, irregularity solving sub-regional, interface or interfacial motions, greatly increase the difficulty of solving interface problems numerically. If we still use the traditional numerical methods, the accuracy will be lost, so that the traditional numerical methods are no longer applicable to the interface problems.

Nowadays, interface problems have attracted more and more attention and became a hot research topic in scientific and engineering computing. Many scholars have developed many numerical methods to solve interface problems [8, 37, 50, 51, 69]. In this dissertation, We mainly study two kinds of interface model problems. Let Ω be a bounded convex polygon in $\mathbb{R}^2$ and separated by a C^2-continuous interface Γ into two sub-domains Ω^+ and Ω^-, as the Fig. 1-1.

Elasticity interface problem:

$$\begin{aligned} -\nabla \cdot \boldsymbol{\sigma}(\boldsymbol{u}) = \boldsymbol{f} &\quad \text{in } \Omega^+ \cup \Omega^-, \\ [\boldsymbol{u}] = \mathbf{0},\ [\boldsymbol{\sigma}(\boldsymbol{u})\boldsymbol{n}_\Gamma] = \boldsymbol{g} &\quad \text{on } \Gamma, \\ \boldsymbol{u} = \mathbf{0} &\quad \text{on } \partial\Omega, \end{aligned} \tag{1.1.1}$$

where

$$\boldsymbol{\sigma}(\boldsymbol{u}) = 2\mu\boldsymbol{\epsilon}(\boldsymbol{u}) + \lambda tr(\boldsymbol{\epsilon}(\boldsymbol{u}))\boldsymbol{I},$$

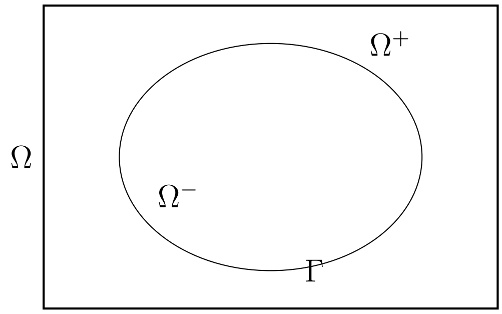

Figure 1-1 A skeleton of the geometry of an interface problem.

is the stress tensor. $\boldsymbol{I}$ is the identity matrix. $\boldsymbol{\epsilon}(\boldsymbol{u}) = \frac{1}{2}\left(\nabla \boldsymbol{u} + (\nabla \boldsymbol{u})^t\right)$ is the strain tensor with the trace being $tr(\boldsymbol{\epsilon}) = \Sigma_{i=1}^{2}\epsilon_{ii}$. The elasticity interface problems occur in many applications, for instance, the minimum compliance-design, the microstructural evolution numerical simulations, the atomic interactions and the kinetics of the crystalline materials.

Stokes interface problem:

$$\begin{aligned} -\nabla \cdot (\mu \boldsymbol{\epsilon}(\boldsymbol{u}) - p\boldsymbol{I}) = \boldsymbol{f} \quad & \text{in } \Omega^+ \cup \Omega^-, \\ \nabla \cdot \boldsymbol{u} = 0 \quad & \text{in } \Omega^+ \cup \Omega^-, \\ [\boldsymbol{u}] = \boldsymbol{0},\ [(\mu \boldsymbol{\epsilon}(\boldsymbol{u}) - p\boldsymbol{I})\boldsymbol{n}_\Gamma] = \boldsymbol{g} \quad & \text{on } \Gamma, \\ \boldsymbol{u} = \boldsymbol{0} \quad & \text{on } \partial\Omega, \end{aligned} \tag{1.1.2}$$

The most important motivation for investigate the Stokes interface problem (cf. [4, 6, 12, 44, 45, 58]) comes from the two-phase incompressible flows. These problems are modeled by Navier-Stokes equations with discontinuous viscosity and density coefficients. The Stokes equations can be adopted as a reasonable model instead of Navier-Stokes equations when the viscosities of two-phase flows are high.

In above equations, boldface characters are used to define vector-valued or matrix-valued functions. The coefficient functions $\mu(x, y)$ and $\lambda(x, y)$ are discontinuous across the interface Γ. The jump $[v] := (v|_{\Omega^+})|_\Gamma - (v|_{\Omega^-})|_\Gamma$ for any v belongs to H^1 in each sub-domain, $\boldsymbol{n}_\Gamma$ is the unit normal vector of Γ which points from Ω^+ to

Ω^-.

1.2 A simple overview of FEMs for interface problems

It is not necessary to give a complete overview of the interface problems, instead we only focus on those literatures which are close to our works. Some results from earlier papers are also included for completeness. In consideration of the vastness of the interface problems literature, I must apologize for the possible omission of references to works which may be relevant to this thesis.

According to the topological relationship between the grid and the interface, there are two kinds of finite element methods (FEMs) to solve interface problems numerically, i.e., interface-fitted mesh methods [26, 69] and interface-unfitted mesh methods [37, 51, 53]. The advantages of interface-fitted FEMs are easy to analysis and ability to use the conventional FEMs. In 1982, Xu [69] analyzed second order elliptic interface problems with homogeneous jump conditions and gave a quasi optimal error estimate. Then Bramble and King [14] considered nonhomogeneous jump conditions case and obtained an optimal error estimate. Chen and Zou [26] also applied the interface-fitted method to solve parabolic interface problems with fixed interfaces. However, it may be difficult and time consuming to generate an interface-fitted mesh for problems with complex interfaces, especially for moving interface problems. The mesh conform to the interface requires remeshing as the interface evolves with time, and leads to significant complications when topological changes occur such as breakup or coalescence. Therefore, interface-unfitted FEMs have become an increasingly important research direction.

There are mainly two types of interface-unfitted FEMs, the extended finite element method and the immersed finite element method. Both of the two methods modify finite element spaces in order to get optimal interpolation error estimate. The extended finite element method (XFEM) has been successfully applied to a wide range of engineering problems, it was originally introduced in [10] to solve the elastic crack problems. The most important feature of XFEM is the basis functions can be discontinuous across the interface. We refer to [31] and the references therein for a historical account of XFEM. In [37], A. Hansbo and P. Hansbo proposed the Nitsche-XFEM (or cut FEM), which is a combination of XFEM and Nitsche's method. After that, Hansbo et al. [39] studied the isoP_2-P_1 extended finite element pair and applied a ghost penalty term around the interface to avoid instabilities. Cattaneo [24] considered the extended P_1-P_1 pair and MINI element pair, the Brezzi-Pitkäranta stabilizations are added in the entire domain and the vicinity of the interface, respectively. For getting an optimal error estimate of the high-contrast interface problems, Burman and Guzman et al. proposed a robust Nitshce-XFEM in [21] which are independent of the diffusion coefficients. Kirchhart, Gross and Reusken [48] applied a standard P_2 finite element space and the extended P_1 finite element space for the velocity and the pressure, respectively, and given a strict analysis for the uniform inf-sup stability result. However, the interpolation error for the velocity is not optimal since the standard P_2 finite element velocity space was used. However, in XFEM, the system matrix can be ill-conditioned when the interface elements are cut with very small intersections. To overcome this difficult, a ghost penalty method is applied in [20, 22, 23] for elliptic interface problems and Stokes interface problems. Because the basis functions of Nitsche-XFEM are discontinuous across the interface, penalty terms (not only stabilization terms) are always needed to guarantee the consistency of the finite element formulations.

Immersed finite element method (IFEM) is first proposed by Li in [50]. The key idea of this method is to modify the basis functions in interface elements such that the interface jump conditions are satisfied. Li et al. extended the same idea to the two-dimensional elliptic problem [51]. After that, many other authors also made significant contribution in connection with IFEMs, interface problems with homogeneous jump conditions (cf. [40, 42, 50, 51, 71]), interface problems with nonhomogeneous jump conditions (cf. [34, 41]). But the finite element error estimates of IFEMs are difficult, until 2015 that the optimal error estimate of two-dimensional elliptic interface problem is obtained by Lin etc. in [53]. They proposed a partially penalized IFE method, which added penalty terms on the edges which cut by the interface to obtain an optimal error estimate. However, Lin employed a piecewise H^3 regularity assumption for the exact solution to the interface problem to prove the optimal convergence of the immersed finite element solutions. In [36], Guo improved the error estimation for the partially penalized IFEM under the standard piecewise H^2 regularity assumption for the exact solution.

Since the construction of IFEM basis functions depends largely on interface jump conditions, the interpolation error analysis of elasticity interface problems is not easy. When the velocity is a vector and the components are coupled together in interface jump conditions, the error estimate is more difficult. In particular, for elasticity interface problems, a nonconforming linear IFE space and a conforming IFE space are developed in [34, 71], respectively, by extending the IFE shape functions to the neighborhood interface elements. In [56], a bilinear IFE space on a rectangular Cartesian mesh is presented. A nonconforming IFE space using the rotated Q_1 polynomials is discussed in [54]. In [59], Qin developed a P_1/CR nonconforming immersed finite element method. However, there are no theoretical results for the approximation capability and finite element error estimate in all above researches. For Stokes interface problems, there is even less work to apply this method. Only Adjerid etc. [2] proposed a immersed Q_1/Q_0 finite element method, the optimal convergence rate was merely obtained by numerical experiments.

In this thesis, we mainly study the unfitted-meshes finite element method for elasticity interface problems and Stokes interface problems. For elasticity interface problems, we propose a nonconforming P_1/CR IFE method by using midpoint values on edges as degrees of freedom for CR elements. The nonconforming P_1/CR finite element method is first proposed by R. Kouhia and R. Stenberg in [49]. It consist of conforming P_1 element for one component of the displacement and linear nonconforming element for the other component. The nonconforming P_1/CR finite elements can naturally overcome the locking phenomenon and do not require stabilization term when solving the almost incompressible elastic problems. Moreover, even though it is a nonconforming finite elements method, its degrees of freedom is only around two thirds of those of existing methods. In [59], Qin combined this method with IFEM and developed a P_1/CR IFEM, the construction method of the basis functions of interface elements is presented and the unique solvability of the basis functions is obtained. Furthermore, we give the approximation capability and optimal approximation error estimate in L^2 norm and H^1 semi-norm of the P_1/CR IFE spaces. By adding partially penalty terms on the edges of interface elements, the optimal convergence is also derived in the energy norm. In addition, through some numerical experiments, we observe expected convergence rates. To our best knowledge, it is the first optimal approximation result for IFE method for planar elasticity interface problems. In order to solve the locking phenomenon in the elasticity problem, we develop a new nonconforming enriched finite element method, which can be roughly viewed as a combination of XFEM and IFEM. The conforming enriched finite element method was applied in elliptic interface problems and Stokes interface problems by Wang and Chen in [65, 66] respectively. This method maintains both advantages of IFEM and XFEM. We propose a nonconforming enriched finite element method for elasticity interface problems in mixed formulation and give corresponding theoretical proofs. At last, for Stokes interface problems, we present the construction of the basis functions the approximation capability of the CR IFEM and the corresponding finite element error estimate.

The dissertation is organized by first introducing some basic notation and definitions in Section 1.3. Then, in Chapter 2, we give the construction two kinds of P_1/CR IFEMs, corresponding approximation capability and the estimates of approximation error and finite element error. Chapter 3 comes to the nonconforming enriched finite element method for elasticity interface problems. In Chapter 4, the CR IFEM is applied to Stokes interface problems. Chapter 5 presents conclusions of our works and future expectations.

1.3 Notation and definitions

In the rest of this thesis, we will use the following notation and definitions. S-tandard notation will be adopted for Sobolev spaces, cf. [1, 17]. Let $\Omega \subset \mathbb{R}^d$ be a bounded domain with Lipschitz continuous boundary and $\mathcal{D}(\Omega)$ be the linear space of infinitely differentiable functions with compact support on Ω. Denote by $\mathcal{D}'(\Omega)$ the dual space of $\mathcal{D}(\Omega)$. $L^p(\Omega)$ is a Banach space consisting of p-th power integrable functions. The Sobolev Space of index (r, p) is defined by

$$W^{r,p}(\Omega) = \{v \in L^p(\Omega); D^\alpha v \in L^p(\Omega) \text{ if } |\alpha| \leq r\}$$

with the norm $\|v\|_{r,p,\Omega} = (\sum\limits_{|\alpha|\leq r} \|D^\alpha v\|_{p,\Omega}^p)^{1/p}$, where r and p are non-negative integers, $\alpha = (\alpha_1, \alpha_2, \cdots, \alpha_d)$ is a multi-integer and

$$D^\alpha = \frac{\partial^{|\alpha|}}{\partial x_1^{\alpha_1} \partial x_2^{\alpha_2} \cdots \partial x_d^{\alpha_d}}, \quad |\alpha| = \sum_{i=1}^{d} |\alpha_i|.$$

The domain Ω is separated by a smooth interface Γ into two sub-domains, i.e., $\Omega = \Omega_1 \cup \Omega_2 \cup \Gamma$. Let

$$W^{r,p}(\Omega^+ \cup \Omega^-) = \{v \in L^p(\Omega);\ v|_{\Omega^s} \in W^{r,p}(\Omega^s), s = +, -\},$$

be the broken Sobolev space of index (r, p) equipped with the norm and seminorm

$$\|v\|_{r,p,\Omega^+\cup\Omega^-} = (\|v\|^p_{r,p,\Omega^+} + \|v\|^p_{r,p,\Omega^-})^{1/p},$$

$$|v|_{r,p,\Omega^+\cup\Omega^-} = (|v|^p_{r,p,\Omega^+} + |v|^p_{r,p,\Omega^-})^{1/p}.$$

Furthermore, let $W_0^{r,p}(\Omega)$ be the closure of $\mathcal{D}(\Omega)$ in the norm $\|\cdot\|_{r,p,\Omega}$. Then we can denote

$$\tilde{W}^{r,p}(\Omega^+ \cup \Omega^-) = W_0^{1,p}(\Omega) \cap W^{r,p}(\Omega^+ \cup \Omega^-).$$

In the case $p = 2$, $\tilde{H}^r(\Omega^+ \cup \Omega^-)$ is used to represent $\tilde{W}^{r,2}(\Omega^+ \cup \Omega^-)$. Moreover, define bolder typeface be the vector parameter.

$\mathcal{T}_h$ is a regular and quasi-uniform triangulation of Ω and the mesh size $h = \max\{\text{diam } T : T \in \mathcal{T}_h\}$. $\mathcal{T}_h$ is assumed to be fitted to the boundary of the domain Ω. For each $\mathcal{T}_h$, we denote the set of interface elements and the set of non-interface elements of $\mathcal{T}_h$ by $\mathcal{T}_h^i$ and $\mathcal{T}_h^n$, respectively. Ω_h^I is defined as the domain of interface elements. Let $\mathcal{N}_h$ be the set of vertices and $\boldsymbol{\varepsilon}_h$ the set of interior edges. Moreover, $\boldsymbol{\varepsilon}_h^i$ and $\boldsymbol{\varepsilon}_h^n$ are defined as the sets of interior interface edges and interior non-interface edges, respectively. For every edge $e \in \boldsymbol{\varepsilon}_h$, let $\mathcal{T}_e = \{T \in \mathcal{T}_h; \partial T \cap e \neq \emptyset\}$ be the collection of triangles that share a common edge e. we assume that two elements $T_{e,1}$ and $T_{e,2}$ share the common edge e. For a function $\boldsymbol{u} \in \boldsymbol{H}^1(T_{e,1} \cup T_{e,2})$, we define its average and jump on e by

$$\{\boldsymbol{u}\} = \begin{cases} \frac{1}{2}((\boldsymbol{u}|_{T_{e,1}})|_e + (\boldsymbol{u}|_{T_{e,2}})|_e) & \text{if } e \in \boldsymbol{\varepsilon}_h, \\ (\boldsymbol{u}|_{T_e})|_e & \text{if } e \in \partial\Omega, \end{cases}$$

$$[\boldsymbol{u}] = \begin{cases} (\boldsymbol{u}|_{T_{e,1}})|_e - (\boldsymbol{u}|_{T_{e,2}})|_e & \text{if } e \in \boldsymbol{\varepsilon}_h, \\ (\boldsymbol{u}|_{T_e})|_e & \text{if } e \in \partial\Omega. \end{cases}$$

Similarly, we define $[\boldsymbol{u}]_\Gamma$ as the jump of a quantity across the Γ, such as $[\boldsymbol{u}]_\Gamma =$

$(\boldsymbol{u}^+ - \boldsymbol{u}^-)|_\Gamma$, where $\boldsymbol{u}^s = \boldsymbol{u}|_{\Omega^s}$, $s = +, -$. For simplicity, we will drop the subscript from the notation if there is no danger of causing confusion.

Define $\Gamma_T = \Gamma \cap T$, and the line segment is denoted by $\Gamma_{h,T}$ that connects the two points intersected by Γ and ∂T. Then $\Gamma_h = \bigcup_{T\in\mathcal{T}_h^i} \Gamma_{h,T}$ can be viewed as an discretization of Γ. We use $\boldsymbol{n}_\Gamma$ to represent the normal vector field of Γ and $\boldsymbol{n}_{\Gamma_h}$ to represent the normal vector field of Γ_h. Let Ω_h^s, $s = +, -$, be the two subregions divided by Γ_h. Denote by $\Omega_{h,E}^s$ the extension of Ω_h^s and $\Omega_{h,F}^s$ the shrink of Ω_h^s, i.e., $\Omega_{h,E}^s = \{\bar{T};\ \text{meas}(T \cap \Omega_h^s) \neq 0, T \in \mathcal{T}_h\}$ and $\Omega_{h,F}^s = \{\bar{T};\ T \subset \Omega_h^s, T \in \mathcal{T}_h\}$ $(s = +, -)$.

In this thesis, the constant is always independent of the mesh sizes of the triangulations and the location of the interface intersected with the mesh. To avoid the proliferation of constants, we adopt the notation $A \lesssim B$ to represent the statement $A \leq \text{constant} \times B$ without confusion. Furthermore, without loss of generality, we assume that interface elements and interface curve Γ satisfy the following hypotheses when the mesh size h is small enough.

(**H1**) The interface Γ can't intersect the boundary of any element at more than two points unless one edge is part of Γ.

(**H2**) If Γ intersects the boundary of an element at two points, these intersection points must be on different edges of this element.

Chapter 2 The immersed finite element methods for elasticity interface problems

We consider the elasticity interface problem

$$-\nabla \cdot \boldsymbol{\sigma}(\boldsymbol{u}) = \boldsymbol{f}, \quad \text{in } \Omega^- \cup \Omega^+, \tag{2.0.1}$$

$$\boldsymbol{u} = \boldsymbol{g}, \quad \text{on } \partial\Omega, \tag{2.0.2}$$

where $\boldsymbol{g} = (g_1, g_2)^t \in \boldsymbol{L}^2(\Omega)$, $\boldsymbol{u}$ is the displacement variable, $\boldsymbol{f} \in \boldsymbol{L}^2(\Omega)$ is the external force. The Lamé constants μ and λ are piecewise constants,

$$(\mu, \lambda) = \begin{cases} (\mu^-, \lambda^-), & \text{in } \Omega^-, \\ (\mu^+, \lambda^+), & \text{in } \Omega^+, \end{cases}$$

which are defined by the Young's module E and the Poisson ratio ν as

$$\mu = \frac{E}{2(1+\nu)}, \qquad \lambda = \frac{E\nu}{(1+\nu)(1-2\nu)}.$$

On the interface Γ, $\boldsymbol{u}$ satisfies the interface conditions

$$[\boldsymbol{u}]|_\Gamma = \mathbf{0}, \tag{2.0.3}$$

$$[\boldsymbol{\sigma}(\boldsymbol{u})\boldsymbol{n}]|_\Gamma = \mathbf{0}, \tag{2.0.4}$$

where $\boldsymbol{n} = (n_1, n_2)^t$ is the unit outer normal vector of the interface pointing from Ω^+ to Ω^-.

Multiplying $\boldsymbol{v} \in \boldsymbol{H}_0^1(\Omega)$ to the both sides of (2.0.1) and applying Green formula in each domain Ω^s $(s = +, -)$, we obtain

$$\int_{\Omega^s} \boldsymbol{\sigma}(\boldsymbol{u}) : \boldsymbol{\epsilon}(\boldsymbol{v}) d\boldsymbol{x} - \int_{\partial\Omega^s} \boldsymbol{\sigma}(\boldsymbol{u})\boldsymbol{n} \cdot \boldsymbol{v} ds = \int_{\Omega^s} \boldsymbol{f} \cdot \boldsymbol{v} d\boldsymbol{x}.$$

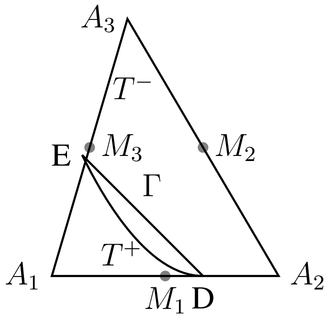

Figure 2-1 An interface triangle.

Summing over $s = +,\ -$ and applying the interface conditions, we have the weak form: find $\boldsymbol{u} \in V = \left\{\boldsymbol{\omega} \in \boldsymbol{H}^1(\Omega) \middle| \, \boldsymbol{\omega}|_{\partial\Omega} = \boldsymbol{g}\right\}$ such that

$$a(\boldsymbol{u}, \boldsymbol{v}) = (\boldsymbol{f}, \boldsymbol{v}), \quad \forall \boldsymbol{v} \in \boldsymbol{H}_0^1(\Omega), \tag{2.0.5}$$

where

$$a(\boldsymbol{u}, \boldsymbol{v}) = \int_\Omega \boldsymbol{\sigma}(\boldsymbol{u}) : \boldsymbol{\epsilon}(\boldsymbol{v}) d\boldsymbol{x}, \qquad (\boldsymbol{f}, \boldsymbol{v}) = \int_\Omega \boldsymbol{f} \cdot \boldsymbol{v} d\boldsymbol{x}.$$

2.1 The P_1/CR immersed finite element method

We present our P_1/CR IFE method, which is different from the method in [59] in the choosing of CR element degrees. In the non-interface element T, we use the standard P_1/CR finite element space $\boldsymbol{U}_h^n(T)$, which is locally defined by

$$\boldsymbol{U}_h^n(T) = \text{Span}\{\boldsymbol{\psi}_{j,T} : j = 1, \cdots, 6\}.$$

The local standard basis functions $\boldsymbol{\psi}_{j,T}$ ($j = 1, \cdots, 6$) are determined by the conditions

$$\boldsymbol{\psi}_{j,T}(A_i) = (\delta_{i,j},\ 0)^t, \qquad i,\ j = 1,\ 2,\ 3,$$

$$\boldsymbol{\psi}_{j,T}(M_i) = (0,\ \delta_{j-3,i})^t, \qquad i = 1,\ 2,\ 3,\ j = 4,\ 5,\ 6,$$

where A_i and M_i are the vertices and midpoints on edges of T respectively, and δ_{ij} is the Kronecker symbol. For the interface element T (see Fig.2-1), let $D = (x_d, y_d)$, $E = (x_e, y_e)$ be the intersections of the interface with T, the line segment $\overline{DE}$ separates element into two subelements T^+ and T^-. We use $\overline{DE}$ to approximate the curve $\widetilde{DE} = \Gamma \cap T$ so that the interface is perturbed by an $O(h^2)$ term. We only describe how to construct the basis functions on the reference interface element $\hat{T} = \triangle\, \hat{A}_1\hat{A}_2\hat{A}_3$, where

$$\hat{A}_1 = (0,0), \qquad \hat{A}_2 = (1,0), \qquad \hat{A}_3 = (0,1).$$

Suppose that $\hat{D} = (\hat{d}, 0)$ and $\hat{E} = (0, \hat{e})$, $0 < \hat{d}, \hat{e} < 1$.

Let $\hat{\boldsymbol{\phi}}_j = (\hat{\phi}_{1,j}, \hat{\phi}_{2,j})^t$, $j = 1, \cdots, 6$, be the P_1/CR IFE functions on $\hat{T}$, i.e.,

$$\hat{\boldsymbol{\phi}}_j = \begin{cases} \hat{\phi}_{1,j} = \begin{pmatrix} \hat{\phi}_{1,j}^+ \\ \hat{\phi}_{1,j}^- \end{pmatrix} = \begin{pmatrix} a_1^+ + b_1^+\hat{x} + c_1^+\hat{y} \\ a_1^- + b_1^-\hat{x} + c_1^-\hat{y} \end{pmatrix} & \begin{array}{l} \text{if } (\hat{x},\hat{y}) \in \hat{T}^+, \\ \text{if } (\hat{x},\hat{y}) \in \hat{T}^-, \end{array} \\ \hat{\phi}_{2,j} = \begin{pmatrix} \hat{\phi}_{2,j}^+ \\ \hat{\phi}_{2,j}^- \end{pmatrix} = \begin{pmatrix} a_2^+ + b_2^+\hat{x} + c_2^+\hat{y} \\ a_2^- + b_2^-\hat{x} + c_2^-\hat{y} \end{pmatrix} & \begin{array}{l} \text{if } (\hat{x},\hat{y}) \in \hat{T}^+, \\ \text{if } (\hat{x},\hat{y}) \in \hat{T}^-, \end{array} \end{cases} \tag{2.1.1}$$

where a_i^s, b_i^s, c_i^s ($i = 1,\ 2$ and $s = +, -$) are undetermined coefficients. We use the following 12 conditions to determine the basis function $\hat{\boldsymbol{\phi}}_j$ $(j = 1, \cdots, 6)$:
the values of $\hat{\phi}_{1,j}$ at the vertices,

$$\hat{\phi}_{1,j}(\hat{A}_i) = \delta_{ij}, \ \ i = 1, 2, 3; \tag{2.1.2}$$

the values of $\hat{\phi}_{2,j}$ at the midpoints of edges,

$$\hat{\phi}_{2,j}(\hat{M}_{i-3}) = \delta_{ij}, \ \ i = 4, 5, 6; \tag{2.1.3}$$

the continuity of the displacement at the $\hat{D}$ and $\hat{E}$,

$$\hat{\phi}_{i,j}^+(\hat{D}) = \hat{\phi}_{i,j}^-(\hat{D}), \ \ \hat{\phi}_{i,j}^+(\hat{E}) = \hat{\phi}_{i,j}^-(\hat{E}), \ \ i = 1, 2; \tag{2.1.4}$$

the weak traction continuity,

$$\begin{cases} \left[(\lambda + 2\mu)\frac{\partial \hat{\phi}_{1,j}}{\partial x}\bar{n}_1 + \lambda \frac{\partial \hat{\phi}_{2,j}}{\partial y}\bar{n}_1 + \mu\left(\frac{\partial \hat{\phi}_{1,j}}{\partial y} + \frac{\partial \hat{\phi}_{2,j}}{\partial x}\right)\bar{n}_2 \right] \Big|_{\overline{\hat{D}\hat{E}}} = 0, \\ \left[\mu\left(\frac{\partial \hat{\phi}_{1,j}}{\partial y} + \frac{\partial \hat{\phi}_{2,j}}{\partial x}\right)\bar{n}_1 + \lambda \frac{\partial \hat{\phi}_{1,j}}{\partial x}\bar{n}_2 + (\lambda + 2\mu)\frac{\partial \hat{\phi}_{2,j}}{\partial y}\bar{n}_2 \right] \Big|_{\overline{\hat{D}\hat{E}}} = 0, \end{cases} \tag{2.1.5}$$

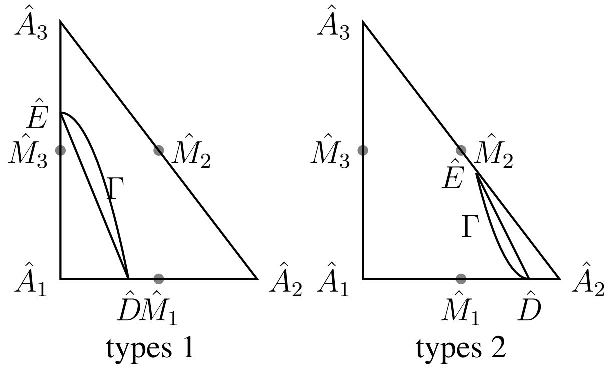

Figure 2-2 Two types of reference elements.

where $\bar{\boldsymbol{n}} = (\bar{n}_1, \bar{n}_2)$ is the unit outer normal to the segment $\overline{DE}$ pointing from T^+ to T^-. Due to the position variation of the interface Γ, the midpoints could be in T^+ or T^-. Hence, there are two types of interface elements, as in Fig. 3. In the remainder of this paper, we only consider the type 1, the other one can be treated in the same way. If the point D or E coincides with the midpoint M_i, the argument is similar. Combining the conditions (2.1.2) − (2.1.5), we could solve a_i^s, b_i^s, c_i^s $(i = 1,\ 2,\ s = +, -)$ by

$$\boldsymbol{A}\boldsymbol{\varphi} = \boldsymbol{b}, \tag{2.1.6}$$

where the matrix $\boldsymbol{A}$ is

$$\begin{pmatrix}
1 & 0 & 0 & 0 & 0 & 0 & 0 & 0 & 0 & 0 & 0 & 0 \\
0 & 0 & 0 & 1 & 1 & 0 & 0 & 0 & 0 & 0 & 0 & 0 \\
0 & 0 & 0 & 1 & 0 & 1 & 0 & 0 & 0 & 0 & 0 & 0 \\
1 & 0 & \hat{e} & -1 & 0 & -\hat{e} & 0 & 0 & 0 & 0 & 0 & 0 \\
1 & \hat{d} & 0 & -1 & -\hat{d} & 0 & 0 & 0 & 0 & 0 & 0 & 0 \\
0 & 0 & 0 & 0 & 0 & 0 & 1 & 1/2 & 0 & 0 & 0 & 0 \\
0 & 0 & 0 & 0 & 0 & 0 & 0 & 0 & 0 & 1 & 1/2 & 1/2 \\
0 & 0 & 0 & 0 & 0 & 0 & 0 & 0 & 0 & 1 & 0 & 1/2 \\
0 & 0 & 0 & 0 & 0 & 0 & 1 & \hat{d} & 0 & -1 & -\hat{d} & 0 \\
0 & 0 & 0 & 0 & 0 & 0 & 1 & 0 & \hat{e} & -1 & 0 & -\hat{e} \\
0 & a_{11,2} & a_{11,3} & 0 & a_{11,5} & a_{11,6} & 0 & a_{11,8} & a_{11,9} & 0 & a_{11,11} & a_{11,12} \\
0 & a_{12,2} & a_{12,3} & 0 & a_{12,5} & a_{12,6} & 0 & a_{12,8} & a_{12,9} & 0 & a_{12,11} & a_{12,12}
\end{pmatrix}$$

with

$$a_{11,2}=(\lambda^{+}+2\mu^{+})\hat{e},\ \ a_{11,3}=\mu^{+}\hat{d},\ \ a_{11,5}=-(\lambda^{-}+2\mu^{-})\hat{e},\ \ a_{11,6}=-\mu^{-}\hat{d},$$

$$a_{12,8}=\mu^{+}\hat{e},\ \ a_{12,9}=(\lambda^{+}+2\mu^{+})\hat{d},\ \ a_{12,11}=-\mu^{-}\hat{e},\ \ a_{12,12}=-(\lambda^{-}+2\mu^{-})\hat{d},$$

$$a_{11,8}=\mu^{+}\hat{d},\ \ a_{11,9}=\lambda^{+}\hat{e},\ \ a_{11,11}=-\mu^{-}\hat{d},\ \ a_{11,12}=-\lambda^{-}\hat{e},$$

$$a_{12,2}=\lambda^{+}\hat{d},\ \ a_{12,3}=\mu^{+}\hat{e},\ \ a_{12,5}=-\lambda^{-}\hat{d},\ \ a_{12,6}=-\mu^{-}\hat{e};$$

$$\boldsymbol{\varphi}=(a_1^+,b_1^+,c_1^+,a_1^-,b_1^-,c_1^-,a_2^+,b_2^+,c_2^+,a_2^-,b_2^-,c_2^-)^t,$$

$$\boldsymbol{b}=(\delta_{j,1},\delta_{j,2},\delta_{j,3},0,0,\delta_{j,4},\delta_{j,5},\delta_{j,6},0,0,0,0)^t.$$

For simplicity, denote the local basis functions $\boldsymbol{\phi}_j$ on the interface element T by $\boldsymbol{\phi}_{j,T}$. Then the local P_1/CR IFE space $\boldsymbol{U}_h^i(T)$ can be written as

$$\boldsymbol{U}_h^i(T)=\text{Span}\{\boldsymbol{\phi}_{j,T}:j=1,\cdots,6\}.$$

Now, we introduce the global IFE space for the planar elasticity interface problem,

$$\begin{aligned}\boldsymbol{U}_h(\Omega)=\big\{&\boldsymbol{u}_h=(u_{1,h},u_{2,h})^t\in\boldsymbol{L}^2(\Omega):\boldsymbol{u}_h\big|_T\in\boldsymbol{U}_h^{\alpha}(T),\ \alpha=i,n,\ \forall T\in\mathcal{T}_h;\\ &u_{1,h}\big|_{T_1}(A_j)=u_{1,h}\big|_{T_2}(A_j),\ j=1,2,\ \text{and}\ u_{2,h}\big|_{T_1}(m)=u_{2,h}\big|_{T_2}(m),\\ &\forall T_1\cap T_2=\overline{A_1A_2},\ m\ \text{is the midpoint of}\ \overline{A_1A_2},\ T_1,\ T_2\in\mathcal{T}_h\big\}.\end{aligned}$$

Our partially penalized P_1/CR IFE method for the problem (2.0.1)-(2.0.4) reads as: find $\boldsymbol{u}_h=(u_{1,h},u_{2,h})^t\in\boldsymbol{U}_{h,g}(\Omega)$ such that

$$a(\boldsymbol{u}_h,\boldsymbol{v}_h)=(\boldsymbol{f},\boldsymbol{v}_h),\quad\forall\boldsymbol{v}_h\in\boldsymbol{U}_{h,0}(\Omega),\tag{2.1.7}$$

where

$$\boldsymbol{U}_{h,g}(\Omega)=\big\{\boldsymbol{u}_h=(u_{1,h},u_{2,h})^t\in\boldsymbol{U}_h(\Omega),\ \text{if}\ \partial T\cap\partial\Omega=\overline{A_1A_2},$$

$$u_{1,h}|(A_i) = g_1(A_i),\ i = 1,\ 2,\ \text{and } u_{2,h}(m) = g_2(m),$$

$$m \text{ is the midpoint of } \overline{A_1A_2},\ T \in \mathcal{T}_h\},$$

$$a_h(\boldsymbol{u}_h, \boldsymbol{v}_h) = \sum_{T\in\mathcal{T}_h} \big(\boldsymbol{\sigma}(\boldsymbol{u}_h), \boldsymbol{\epsilon}(\boldsymbol{v}_h)\big)_T - \sum_{e\in\varepsilon_h^i} \big(\{\boldsymbol{\sigma}(\boldsymbol{u}_h)\boldsymbol{n}\}, [\boldsymbol{v}_h]\big)_e$$

$$- \sum_{e\in\varepsilon_h^i} \big(\{\boldsymbol{\sigma}(\boldsymbol{v}_h)\boldsymbol{n}\}, [\boldsymbol{u}_h]\big)_e + \sum_{e\in\varepsilon_h^i} h^{-1}((\mu+\lambda)[\boldsymbol{u}_h], [\boldsymbol{v}_h])_e,$$

$$(\boldsymbol{f}, \boldsymbol{v}_h) = \int_\Omega \boldsymbol{f}\cdot\boldsymbol{v}_h d\boldsymbol{x};$$

and

$$(\boldsymbol{\sigma}, \boldsymbol{\epsilon})_T = \int_T \boldsymbol{\sigma} : \boldsymbol{\epsilon} = \int_T \sum_{ij} \boldsymbol{\sigma}_{ij}\boldsymbol{\epsilon}_{ij}$$

for 2-tensors $\boldsymbol{\sigma}$, $\boldsymbol{\epsilon}$; $(\boldsymbol{v}, \boldsymbol{w})_e = \int_e \boldsymbol{v}\cdot\boldsymbol{w}$ for vectors $\boldsymbol{v}$, $\boldsymbol{w}$.

Remark 2.1.1. For general nonzero flux jump $\boldsymbol{g}$, we can never compute $\langle \boldsymbol{g}, \boldsymbol{v}_h\rangle_\Gamma$ exactly. Usually, we should replace $\langle \boldsymbol{g}, \boldsymbol{v}_h\rangle_\Gamma$ by $\langle g_h, \boldsymbol{v}_h\rangle_{\Gamma_h}$, where $\boldsymbol{g}_h$ is a linear interpolation or projection of $\boldsymbol{g}$. If we want to analyze the difference between $\langle \boldsymbol{g}, \boldsymbol{v}_h\rangle_\Gamma$ and $\langle \boldsymbol{g}_h, \boldsymbol{v}_h\rangle_{\Gamma_h}$, a higher smoothness of $\boldsymbol{g}$ is always needed. This work is already done by Chen and Zou on body-fitted meshes, see Lemma 2.2 in [26] for more details.

2.2 Some properties of the basis functions

Combining Theorem 2.3 in [52] with Lemma 3.3 in [72], we have following result.

Lemma 2.2.1. *Let $X = (x, y)^t$. The six functions $\boldsymbol{\phi}_j(X) \in \boldsymbol{U}_h^i(T)$ satisfy*

$$\sum_{j=1}^{6} \boldsymbol{\phi}_j(X) = I,$$

where I is a two-dimension identity matrix.

According to Theorem 2.4 in [52] and Theorem 3.2 in [72], the following lemma can be obtained.

Lemma 2.2.2. *For any $T \in \mathcal{T}_h^i$ and point $X \in T$,*

$$|\boldsymbol{\phi}_j(X)| \lesssim 1, \quad \|\nabla \boldsymbol{\phi}_j(X)\|_{0,T} \lesssim h^{-1}. \tag{2.2.1}$$

Theorem 2.2.1. *In an interface element T, any P_1/CR IFE function $\boldsymbol{\phi}(x,y) \in S_h^i(T)$ can be uniquely determined by its values at the vertices and midpoints of edges of T.*

Proof. We carry out the proof for $\hat{\boldsymbol{\phi}}(x,y)$. It is apparent from (2.1.6) that we only need to prove the matrix A is nonsingular. By direct calculations, we have

$$\begin{aligned}\det(\boldsymbol{A}) =& N_1(\mu^-)^2 + N_2(\mu^+)^2 + N_3\mu^-\lambda^- + N_4\mu^-\lambda^+ + N_5\mu^-\mu^+ \\ &+ N_6\mu^+\lambda^- + N_7(\lambda^+)^2 + N_8\lambda^-\lambda^+, \end{aligned} \tag{2.2.2}$$

where

$$N_1 = \frac{1}{2}\hat{e}^2\hat{d}^2(-2\hat{d}^2 + 4\hat{e}\hat{d} + \hat{d} - 2\hat{e}),$$

$$N_2 = \hat{d}^4(3\hat{e} - 2\hat{e}^2 - 1) + \hat{d}^3\hat{e}(4\hat{e}^2 - \hat{e} - 1) + 3\hat{e}^2\hat{d}^2(\hat{e} - 1) + \hat{d}\hat{e}^3(\hat{e} - 2) - \hat{e}^4,$$

$$N_3 = \frac{1}{2}\hat{e}^2\hat{d}\left(-\hat{d}^3 + \hat{d}^2(4\hat{e} + \frac{1}{2}) - \hat{d}\hat{e}(\hat{e} + 2) + \frac{1}{2}\hat{e}^2\right),$$

$$N_4 = \frac{1}{4}\hat{e}\hat{d}\left(\hat{d}^3(2\hat{e} - 1) + \hat{d}^2\hat{e}(1 - 8\hat{e}) + \hat{d}\hat{e}^2(2\hat{e} - 1) + 2\hat{e}^2 - \hat{e}^3\right),$$

$$N_5 = \frac{1}{2}\hat{e}\hat{d}\left(\hat{d}^3(4\hat{e} - 3) + \hat{d}^2(1 - 8\hat{e}^2) - \hat{d}\hat{e}^2 + 2\hat{e}^2 - \hat{e}^3\right),$$

$$N_6 = \frac{1}{4}\hat{e}\hat{d}\left(2\hat{d}^3(\hat{e} - 1) + \hat{d}^2(1 + 2\hat{e} - 8\hat{e}^2) + 2\hat{d}\hat{e}^2(\hat{e} - 1) + \hat{e}^2(3 - 2\hat{e})\right),$$

$$N_7 = -\frac{1}{3}N_8 = \frac{1}{4}\hat{e}^3\hat{d}.$$

Let $\mu^+ = k\mu^-$, $t = \frac{1}{1-2\nu}$. We can derive

$$\det(\boldsymbol{A}) = (\mu^-)^2\Big(t^2(k^2N_7 + kN_8) + t(-k^2N_7 + k(N_4 + N_6 - 2N_8) + N_3)$$

$$+ k^2(N_2 + N_7) + k(N_5 - N_4 - N_6 + N_8) + N_1 - N_3\Big)$$

$$= (\mu^-)^2(at^2 + bt + c).$$

Denote $F(t) = \det(\boldsymbol{A})$. Let $t_1 = \frac{-b-\sqrt{b^2-4ac}}{2a}$ and $t_2 = \frac{-b+\sqrt{b^2-4ac}}{2a}$ be the roots of $F(t) = 0$. If $a < 0$, since $t = \frac{1}{1-2\nu} > 1$, we know $t_1 > 1$, then

$$\sqrt{b^2 - 4ac} > -(2a + b).$$

If $(2a + b) < 0$, then $a + b + c > 0$. However, by direct calculation, we get $a + b + c = k^2(N_2 + N_7) + kN_5 + N_1 < 0$. It causes a contradiction. If $(2a + b) > 0$, $\sqrt{b^2 - 4ac} > -(2a + b)$ is always true. Since $a < 0$, we have $a + b > 2a + b > 0$, and it means $b > 0$. From $a + b + c < 0$ and $a + b > 0$, we can derive $c < 0$. Hence, combining with the conditions $0 < \hat{d} \leq 1$ and $0 < \hat{e} \leq 1$, we deduce that $F(t) = 0$ has a solution when the following inequality system holds:

$$\begin{cases} 0 < \hat{d} \leq 1,\ 0 < \hat{e} \leq 1, \\ a = k^2N_7 + kN_8 < 0,\ \ b^2 - 4ac \geq 0, \\ b = -k^2N_7 + k(N_4 + N_6 - 2N_8) + N_3 > 0, \\ c = k^2(N_2 + N_7) + k(N_5 - N_4 - N_6 + N_8) + N_1 - N_3 < 0, \\ 2a + b = k^2N_7 + k(N_4 + N_6) + N_3 > 0. \end{cases} \tag{2.2.3}$$

Similarly, if $a > 0$, according to the same argument, we derive that $F(t) = 0$ has a solution when the following inequality system holds:

$$\begin{cases} 0 < \hat{d} \leq 1,\ 0 < \hat{e} \leq 1, \\ a = k^2N_7 + kN_8 > 0,\ \ b^2 - 4ac \geq 0, \\ b = -k^2N_7 + k(N_4 + N_6 - 2N_8) + N_3 > 0, \\ c = k^2(N_2 + N_7) + k(N_5 - N_4 - N_6 + N_8) + N_1 - N_3 < 0. \end{cases} \tag{2.2.4}$$

By tedious calculation, we obtain that inequality systems (3.13) and (3.14) have no solution. It means $\det(\boldsymbol{A}) = F(t) \neq 0$, and the proof is completed. $\square$

2.3 Error estimates for the interpolation approximations

For any interface triangle T, define $(s=+,-)$

$$\tilde{\boldsymbol{H}}^2(T)=\left\{\boldsymbol{u}\in\boldsymbol{H}^1(T),\ \boldsymbol{u}|_{T^s}\in\boldsymbol{H}^2(T^s),\ [\boldsymbol{\sigma}(\boldsymbol{u})\boldsymbol{n}]=\boldsymbol{0}\text{ on }\Gamma\cap T\right\},$$

$$\tilde{\boldsymbol{C}}^2(T)=\left\{\boldsymbol{u}\in\boldsymbol{H}^1(T),\ \boldsymbol{u}|_{T^s}\in\boldsymbol{C}^2(T^s),\ [\boldsymbol{\sigma}(\boldsymbol{u})\boldsymbol{n}]=\boldsymbol{0}\text{ on }\Gamma\cap T\right\}.$$

Given any $\boldsymbol{u}\in\tilde{\boldsymbol{H}}^2(T)$, let

$$\|\boldsymbol{u}\|_{2,T}^2=\|\boldsymbol{u}\|_{1,T}^2+\|\boldsymbol{u}\|_{2,T^+}^2+\|\boldsymbol{u}\|_{2,T^-}^2,$$

$$|\boldsymbol{u}|_{2,T}^2=\|\boldsymbol{u}\|_{1,T}^2+|\boldsymbol{u}|_{2,T^+}^2+|\boldsymbol{u}|_{2,T^-}^2,$$

where $\|\cdot\|_{2,T^s}$ and $|\cdot|_{2,T^s}$ are the norms and semi-norms in $\boldsymbol{H}^2(T^s)$ $(s=+,-)$, respectively.

Define a local interpolation operator $I_{h,T}:\tilde{\boldsymbol{H}}^2(T)\to\boldsymbol{U}_h^i(T)$ as

$$I_{h,T}\boldsymbol{u}=\begin{cases}\sum_{j=1}^6 c_j\boldsymbol{\psi}_{j,T}, & \text{if } T \text{ is a non-interface element,}\\ \sum_{j=1}^6 c_j\boldsymbol{\phi}_{j,T}, & \text{if } T \text{ is an interface element,}\end{cases}$$

where

$$c_j=\begin{cases}u_1(A_j), & j=1,2,3,\\ u_2(M_{j-3}), & j=4,5,6.\end{cases}$$

For any $\boldsymbol{u}\in\tilde{\boldsymbol{H}}^2(T)$, the global IFE interpolation operator $I_h:\tilde{\boldsymbol{H}}^2(\Omega)\to\boldsymbol{U}_h(\Omega)$ is defined by

$$I_h\boldsymbol{u}|_T=I_{h,T}\boldsymbol{u},\qquad \forall T\in\mathcal{T}_h.$$

In any $T\in\mathcal{T}_h^n$, the error estimate of $I_h\boldsymbol{u}-\boldsymbol{u}$ can be obtained by the standard interpolation estimate. For an arbitrary interface element, the key is to establish suitable multi-point Taylor expansions for functions in $S_h^i(T)$ by formula

$$I_{h,T}\boldsymbol{u}(X)=\sum_{i=1}^3\boldsymbol{u}(A_i)\boldsymbol{\phi}_i(X)+\sum_{i=4}^6\boldsymbol{u}(M_{i-3})\boldsymbol{\phi}_i(X).$$

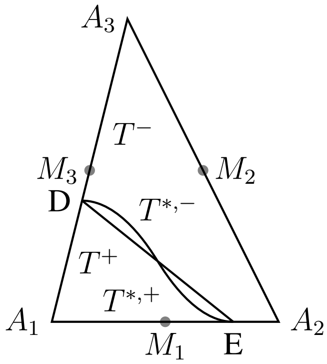

Figure 2-3 A separated interface element.

Denote by T^* the subset in T enclosed by the interface Γ and the line segment $\overline{DE}$, $T^{*,s} = T^s \backslash T^*$, $s = +, -$. Then, for any function $\boldsymbol{u} \in \tilde{\boldsymbol{H}}^2(T)$, the error estimate for $I_h\boldsymbol{u} - \boldsymbol{u}$ on T can be obtained by estimating in the three subsets $T^{*,-}$, $T^{*,+}$ and T^*. In this expansion, the most important thing is the relationship between $\nabla \boldsymbol{u}^+(X)$ and $\nabla \boldsymbol{u}^-(X)$. We start from the estimate on $T^{*,-}$. Let ($s = +, -$)

$$\rho^s = 2\mu^s + \lambda^s, \;\; L_u = \left(\frac{\partial u_1^-}{\partial x}, \; \frac{\partial u_1^-}{\partial y} + \frac{\partial u_2^-}{\partial x}, \; \frac{\partial u_2^-}{\partial y} \right)^t.$$

By tedious calculations, the following results hold.

Lemma 2.3.1. *Without loss of generality, assume $n_2 \neq 0$. Let $c_0 = \frac{n_2}{\mu^+\rho^+}$ and*

$$l_1 = c_0 n_1 \left(\rho^-(\mu^+ n_1^2 + \rho^+ n_2^2) - n_2^2 \lambda^- \right), \; l_2 = c_0 \mu^- n_2 (\mu^+ n_1^2 + \rho^+ n_2^2 - n_1^2),$$

$$l_3 = c_0 n_1 \left((\mu^+ n_1^2 + \rho^+ n_2^2)\lambda^- - n_2^2 \rho^- \right), \; l_4 = c_0 n_2 \left(\mu^+ \lambda^- - 2(\mu^+ + \lambda^+) n_1^2 \mu^- \right),$$

$$l_5 = c_0 \mu^- n_1 \left(\rho^+ n_1^2 - \lambda^+ n_2^2 \right), \; l_6 = c_0 n_2 \left(\mu^+ \rho^- + 2(\mu^+ + \lambda^+) n_1^2 \mu^- \right).$$

Given any point $X = (x, y) \in \Gamma \cap T$, assume that $\mathbf{u}(x, y)$ satisfies the interface jump conditions, then

$$\nabla \boldsymbol{u}^+(X) = \begin{pmatrix} \frac{\partial u_1^+(X)}{\partial x} & \frac{\partial u_1^+(X)}{\partial y} \\ \frac{\partial u_2^+(X)}{\partial x} & \frac{\partial u_2^+(X)}{\partial y} \end{pmatrix} = \begin{pmatrix} \frac{n_1}{n_2} L_f \cdot L_u(X) & L_f \cdot L_u(X) \\ \frac{n_1}{n_2} L_b \cdot L_u(X) & L_b \cdot L_u(X) \end{pmatrix}, \quad (2.3.1)$$

where

$$L_f = (l_1,\ l_2,\ l_3),\ \ L_b = (l_4,\ l_5,\ l_6).$$

Moreover,

$$[\nabla \boldsymbol{u}(X)] = \nabla \boldsymbol{u}^+(X) - \nabla \boldsymbol{u}^-(X) = \begin{pmatrix} G_{11}(X) & G_{12}(X) \\ G_{21}(X) & G_{22}(X) \end{pmatrix}, \tag{2.3.2}$$

where

$$G_{11} = \left(\frac{n_1}{n_2} L_f - (1,0,0)\right) \cdot L_u,\ \ G_{22} = (L_b - (0,0,1)) \cdot L_u,$$

$$G_{12} = L_f \cdot L_u - \frac{\partial u_1^-}{\partial y},\ \ G_{21} = \frac{n_1}{n_2} L_b \cdot L_u - \frac{\partial u_2^-}{\partial x}.$$

For any point $\overline{X} \in \overline{DE}$, Let $\bar{c}_0 = \frac{\bar{n}_2}{\mu^+\rho^+}$ and

$$\bar{l}_1 = \bar{c}_0 \bar{n}_1 \left(\rho^-(\mu^+\bar{n}_1^2 + \rho^+\bar{n}_2^2) - \bar{n}_2^2\lambda^-\right),\ \bar{l}_2 = \bar{c}_0 \mu^- \bar{n}_2(\mu^+\bar{n}_1^2 + \rho^+\bar{n}_2^2 - \bar{n}_1^2),$$

$$\bar{l}_3 = \bar{c}_0 \bar{n}_1 \left(\lambda^-(\mu^+\bar{n}_1^2 + \rho^+\bar{n}_2^2) - \bar{n}_2^2\rho^-\right),\ \bar{l}_4 = \bar{c}_0 \bar{n}_2 \left(\mu^+\lambda^- - 2(\mu^+ + \lambda^+)\bar{n}_1^2\mu^-\right),$$

$$\bar{l}_5 = \bar{c}_0 \mu^- \bar{n}_1 \left(\rho^+\bar{n}_1^2 - \lambda^+\bar{n}_2^2\right),\ \bar{l}_6 = \bar{c}_0 \bar{n}_2 \left(\mu^+\rho^- + 2(\mu^+ + \lambda^+)\bar{n}_1^2\mu^-\right).$$

We can obtain the expressions for $\nabla \boldsymbol{u}^+(\overline{X})$ and $[\nabla \boldsymbol{u}(\overline{X})]$ similarly.

Now we introduce a local coordinate system centered at the point D with one axis in the direction of $\overline{DE}$. Given any point (x, y), let (ξ, η) be its coordinate in this local coordinate system. We have

$$\begin{pmatrix} x \\ y \end{pmatrix} = \begin{pmatrix} x_D \\ y_D \end{pmatrix} + \begin{pmatrix} \cos(\theta_{DE}) & -\sin(\theta_{DE}) \\ \sin(\theta_{DE}) & \cos(\theta_{DE}) \end{pmatrix} \begin{pmatrix} \xi \\ \eta \end{pmatrix},$$

where (x_D, y_D) is the coordinates of the point D, θ_{DE} is the angle between $\overline{DE}$ and the x axis. Suppose that

$$\eta = \phi(\xi), \qquad \xi \in [0, |\overline{DE}|].$$

Then

$$|\phi(\xi)| \lesssim h^2, \qquad |\phi^{'}(\xi)| \lesssim h,$$

$$\bar{\boldsymbol{n}} = (0,1)^t, \qquad \boldsymbol{n} = \frac{1}{\sqrt{1+(\phi^{'}(\xi))^2}}(-\phi^{'}(\xi),1)^t.$$

Let $X \in T^{*,-}$, we assume that the line segments $\overline{A_iX}$ and $\overline{M_iX}$ $(i=2,3)$ don't intersect with the interface Γ and $\overline{DE}$, and the line segment $\overline{A_1X}$ ($\overline{M_1X}$) meets Γ and $\overline{DE}$ at $\tilde{A}$ ($\tilde{M}$) and $\bar{A}$ ($\bar{M}$) (see Fig.2-4), respectively. We have

$$\tilde{A} = \tilde{t}_A A_1 + (1-\tilde{t}_A)X = (\tilde{x},\tilde{y})^t, \;\; 0 \leq \tilde{t}_A \leq 1,$$

$$\bar{A} = \bar{t}_A A_1 + (1-\bar{t}_A)X = (\bar{x},\bar{y})^t, \;\; 0 \leq \bar{t}_A \leq 1.$$

The above relationships are also true if we replace $\tilde{A}(\bar{A})$ by $\tilde{M}(\bar{M})$, $\tilde{t}_A(\bar{t}_A)$ by $\tilde{t}_M(\bar{t}_M)$ respectively $(0 \leq \tilde{t}_M, \; \bar{t}_M \leq 1)$.

Denote $\tilde{A}^{\perp}$ and $\tilde{M}^{\perp}$ be the orthogonal projection of $\tilde{A}$ and $\tilde{M}$ onto $\overline{DE}$, respectively. By Lemma 2.1 in [52], we have the following lemma.

Lemma 2.3.2. *There exist constant $h_0 > 0$ such that for all $0 \leq h \leq h_0$ and any $T \in \mathcal{T}_h^i$ and point $\tilde{A} \in \Gamma \cap T$,*

$$\|\tilde{A} - \tilde{A}^{\perp}\|_{0,T} \lesssim h^2, \tag{2.3.3}$$

$$\|\bar{\boldsymbol{n}} - \boldsymbol{n}\|_{0,T} \lesssim h. \tag{2.3.4}$$

For simplicity, in the rest of this paper, we will drop X from $\boldsymbol{\phi}_i(X)$ without danger of causing confusion. Using the notation $\bar{l}_i$ $(i=1,\cdots,6)$ in Lemma 2.3.1, the following lemma holds.

Lemma 2.3.3. *Given a two-dimension vector $\boldsymbol{q}$ and matrix $\boldsymbol{N}$, points $X \in T^{*,-}$, $\overline{X} \in \overline{DE}$, there exists a function $\boldsymbol{v} \in \boldsymbol{U}_h^i(T)$ such that $\boldsymbol{v}(X) = \boldsymbol{q}$,*

$$\nabla \boldsymbol{v}(X) = \boldsymbol{N} = \begin{pmatrix} N_{11} & N_{12} \\ N_{21} & N_{22} \end{pmatrix},$$

$$-\boldsymbol{N}\sum_{i=1}^{3}(\boldsymbol{\phi}_i(A_i - X) + \boldsymbol{\phi}_{i+3}(M_i - X)) = (\boldsymbol{N_0} - \boldsymbol{N})(\boldsymbol{\phi}_1(A_1 - \overline{X}) + \boldsymbol{\phi}_4(M_1 - \overline{X})),$$

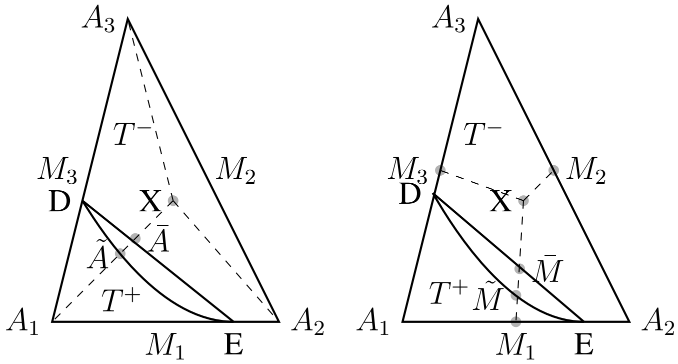

Figure 2-4 The skeleton of interface elements

where

$$N_l = (N_{11}, N_{21} + N_{22}, N_{22})^t, \ \ \bar{L}_f = (\bar{l}_1, \bar{l}_2, \bar{l}_3)^t, \ \ \bar{L}_b = (\bar{l}_4, \bar{l}_5, \bar{l}_6)^t,$$

$$\boldsymbol{N_0} = \begin{pmatrix} \frac{\bar{n}_1}{\bar{n}_2}\bar{L}_f \cdot N_l & \bar{L}_f \cdot N_l \\ \frac{\bar{n}_1}{\bar{n}_2}\bar{L}_b \cdot N_l & \bar{L}_b \cdot N_l \end{pmatrix}.$$

Proof. Let

$$\boldsymbol{v}(Y) = \begin{cases} \boldsymbol{v}^-(Y), & \text{if } Y \in T^-, \\ \boldsymbol{v}^+(Y), & \text{if } Y \in T^+ \end{cases}$$

be a function in $S_h^i(T)$. Since $\boldsymbol{v}(Y)$ is piecewise linear, $\boldsymbol{v}(X) = \boldsymbol{q}$ and $\nabla\boldsymbol{v}(X) = \boldsymbol{N}$ uniquely determine $\boldsymbol{v}^-(Y)$. Furthermore, $\boldsymbol{v}^+(Y)$ can be uniquely determined by interface conditions. Because $\boldsymbol{v}^-(Y)$ is linear, we obtain

$$\boldsymbol{v}(A_i) = \boldsymbol{v}^-(A_i) = \boldsymbol{q} + \boldsymbol{N}(A_i - X), \qquad i = 2, 3, \tag{2.3.5}$$

$$\boldsymbol{v}(M_i) = \boldsymbol{v}^-(M_i) = \boldsymbol{q} + \boldsymbol{N}(M_i - X), \qquad i = 2, 3. \tag{2.3.6}$$

Moreover, by (2.3.1),

$$\begin{aligned} \boldsymbol{v}(A_1) = \boldsymbol{v}^+(A_1) &= \boldsymbol{v}^+(\overline{X}) + \nabla\boldsymbol{v}^+(\overline{X})(A_1 - \overline{X}) \\ &= \boldsymbol{v}^-(\overline{X}) + \nabla\boldsymbol{v}^+(\overline{X})(A_1 - \overline{X}) \end{aligned}$$

$$= \boldsymbol{q} + \boldsymbol{N}(\overline{X} - X) + \boldsymbol{N_0}(A_1 - \overline{X}). \tag{2.3.7}$$

Similarly,

$$\boldsymbol{v}(M_1) = \boldsymbol{q} + \boldsymbol{N}(\overline{X} - X) + \boldsymbol{N_0}(M_1 - \overline{X}). \tag{2.3.8}$$

It follows from (2.3.5)−(2.3.8) and Lemma 2.2.2 that

$$\begin{aligned}
\boldsymbol{v}(X) =& I_{h,T}\boldsymbol{v}(X) = \sum_{i=1}^{3}(\boldsymbol{\phi}_i \boldsymbol{v}(A_i) + \boldsymbol{\phi}_{i+3}\boldsymbol{v}(M_i)) \\
=& \boldsymbol{q} + \boldsymbol{N}\sum_{i=1}^{3}(\boldsymbol{\phi}_i(A_i - X) + \boldsymbol{\phi}_{i+3}(M_i - X)) \\
&+ (\boldsymbol{N} - \boldsymbol{N_0})\boldsymbol{\phi}_1(\overline{X} - A_1) + (\boldsymbol{N} - \boldsymbol{N_0})\boldsymbol{\phi}_4(\overline{X} - M_1).
\end{aligned}$$

The desired result then follows. □

Let $\mathcal{A}_i = tA_i + (1-t)X$ and $\mathcal{M}_i = tM_i + (1-t)X$, $i = 1, 2, 3$, we derive that

Lemma 2.3.4. *For any $\boldsymbol{u} \in \widetilde{\boldsymbol{C}}^2(T)$, $X \in T^{*,-}$ and $\overline{X} \in \overline{DE}$, it holds*

$$\begin{aligned}
I_{h,T}\boldsymbol{u}(X) - \boldsymbol{u}(X) = &\sum_{i=2}^{3}(\boldsymbol{\phi}_i I_i + \boldsymbol{\phi}_{i+3} I_{i+3}) + \boldsymbol{\phi}_1(I_1^+ + I_1^-) \\
&+ \boldsymbol{\phi}_4(I_4^+ + I_4^-) + [\nabla \boldsymbol{u}(\tilde{A})]\boldsymbol{\phi}_1(A_1 - \tilde{A}) + [\nabla \boldsymbol{u}(\tilde{M})]\boldsymbol{\phi}_4(M_1 - \tilde{M}) \\
&+ \left(\nabla \boldsymbol{u}^+(\overline{X}) - \nabla \boldsymbol{u}(X)\right)(\boldsymbol{\phi}_1(\overline{X} - A_1) + \boldsymbol{\phi}_4(\overline{X} - M_1)),
\end{aligned}$$

where

$$I_1^- = \int_0^{\tilde{t}_A}(1-t)\frac{d^2}{dt^2}\boldsymbol{u}(\mathcal{A}_1)dt, \quad I_1^+ = \int_{\tilde{t}_A}^{1}(1-t)\frac{d^2}{dt^2}\boldsymbol{u}(\mathcal{A}_1)dt;$$

$$I_4^- = \int_0^{\tilde{t}_M}(1-t)\frac{d^2}{dt^2}\boldsymbol{u}(\mathcal{M}_1)dt, \quad I_4^+ = \int_{\tilde{t}_M}^{1}(1-t)\frac{d^2}{dt^2}\boldsymbol{u}(\mathcal{M}_1)dt;$$

$$I_i = \int_0^{1}(1-t)\frac{d^2}{dt^2}\boldsymbol{u}(\mathcal{A}_i)dt, \quad i = 2, 3;$$

$$I_i = \int_0^1 (1-t)\frac{d^2}{dt^2}\boldsymbol{u}(\mathcal{M}_{i-3})dt, \ \ i = 5, 6.$$

Proof. For $i = 2, 3$, it is obvious that

$$\boldsymbol{u}(A_i) = \boldsymbol{u}(X) + \int_0^1 \frac{d}{dt}\boldsymbol{u}(\mathcal{A}_i)dt = \boldsymbol{u}(X) + \nabla\boldsymbol{u}(X)(A_i - X) + I_i \tag{2.3.9}$$

$$\boldsymbol{u}(M_i) = \boldsymbol{u}(X) + \int_0^1 \frac{d}{dt}\boldsymbol{u}(\mathcal{M}_i)dt = \boldsymbol{u}(X) + \nabla\boldsymbol{u}(X)(M_i - X) + I_{i+3}. \tag{2.3.10}$$

For $i = 1$, some manipulation yields

$$\begin{aligned}
\boldsymbol{u}(A_1) =& \boldsymbol{u}(X) + \int_0^1 \frac{d}{dt}\boldsymbol{u}(\mathcal{A}_1)dt \\
=& \boldsymbol{u}(X) + \int_0^{\tilde{t}_A} \frac{d}{dt}\boldsymbol{u}(\mathcal{A}_1)dt + \int_{\tilde{t}_A}^1 \frac{d}{dt}\boldsymbol{u}(\mathcal{A}_1)dt \\
=& \boldsymbol{u}(X) + (\nabla\boldsymbol{u}^+(\tilde{A}) - \nabla\boldsymbol{u}^-(\tilde{A}))(A_1 - X)(1 - \tilde{t}_A) + I_1^+ \\
&+ \nabla\boldsymbol{u}(X)(A_1 - X) + I_1^-,
\end{aligned} \tag{2.3.11}$$

$$\begin{aligned}
\boldsymbol{u}(M_1) =& \boldsymbol{u}(X) + (\nabla\boldsymbol{u}^+(\tilde{M}) - \nabla\boldsymbol{u}^-(\tilde{M}))(M_1 - X)(1 - \tilde{t}_M) + I_4^- \\
&+ \nabla\boldsymbol{u}(X)(M_1 - X) + I_4^+.
\end{aligned} \tag{2.3.12}$$

Combining(2.3.9)$-$(2.3.12), the following equality holds:

$$\begin{aligned}
I_{h,T}\boldsymbol{u}(X) =& \sum_{i=1}^{3}(\boldsymbol{\phi}_i\boldsymbol{u}(A_i) + \boldsymbol{\phi}_{i+3}\boldsymbol{u}(M_i)) \\
=& \boldsymbol{u}(X)\sum_{i=1}^{3}\boldsymbol{\phi}_i + \nabla\boldsymbol{u}(X)\sum_{i=1}^{3}(\boldsymbol{\phi}_i(A_i - X) + \boldsymbol{\phi}_{i+3}(M_i - X)) \\
&+ \sum_{i=2,3,5,6}\boldsymbol{\phi}_i I_i + \boldsymbol{\phi}_1(X)(I_1^+ + I_1^-) + \boldsymbol{\phi}_4(I_4^+ + I_4^-)
\end{aligned}$$

$$+ [\nabla \boldsymbol{u}(\tilde{A})]\boldsymbol{\phi}_1(A_1 - \tilde{A}) + [\nabla \boldsymbol{u}(\tilde{M})]\boldsymbol{\phi}_4(M_1 - \tilde{M}). \tag{2.3.13}$$

By Lemma 2.3.3, we obtain

$$\begin{aligned}\boldsymbol{u}(X) =& \boldsymbol{u}(X)\sum_{i=1}^{6}\boldsymbol{\phi}_i + \nabla \boldsymbol{u}(X)\sum_{i=1}^{3}(\boldsymbol{\phi}_i(A_i - X) + \boldsymbol{\phi}_{i+3}(M_i - X)) \\ &+ \left(\nabla \boldsymbol{u}(X) - \nabla \boldsymbol{u}^+(\overline{X})\right)(\boldsymbol{\phi}_1(\overline{X} - A_1) + \boldsymbol{\phi}_4(\overline{X} - M_1)).\end{aligned} \tag{2.3.14}$$

Subtracting (2.3.14) from (2.3.13), the proof is completed. □

Theorem 2.3.1. *For any $T \in \mathcal{T}_h^i$, it holds*

$$\|I_{h,T}\boldsymbol{u} - \boldsymbol{u}\|_{0,T^{*,-}} \lesssim h^2 \|\boldsymbol{u}\|_{2,T}, \ \forall \boldsymbol{u} \in \tilde{\boldsymbol{H}}^2(T). \tag{2.3.15}$$

Proof. Since $\widetilde{\boldsymbol{C}}^2(T)$ is dense in $\tilde{\boldsymbol{H}}^2(T)$ for any $T \in \mathcal{T}_h^i$, we only need to show (2.3.15) for any $\boldsymbol{u} \in \widetilde{\boldsymbol{C}}^2(T)$. According to Lemma 2.3.4, the righthand side of (2.3.4) can be estimated term by term. Let $\xi = tx_{A_2} + (1-t)x$, $\eta = ty_{A_2} + (1-t)y$, $A_2 = (x_{A_2}, y_{A_2})$. Using the notation in Lemma 2.3.4, we first estimate $\boldsymbol{\phi}_2 I_2$.

$$\begin{aligned}|I_2|^2 =& \left|\int_0^1 (1-t)\frac{d^2}{dt^2}\boldsymbol{u}(\mathcal{A}_2)dt\right|^2 \lesssim \Big(\int_0^1 (1-t)\big(\boldsymbol{u}_{xx}(\xi,\eta)(x_{A_2} - x)^2 \\ &+ 2\boldsymbol{u}_{xy}(\xi,\eta)(x_{A_2} - x)(y_{A_2} - y) + \boldsymbol{u}_{yy}(\xi,\eta)(y_{A_2} - y)^2\big)dt\Big)^2 \\ &\lesssim h^4 \int_0^1 (1-t)^2 \left(\boldsymbol{u}_{xx}^2(\xi,\eta) + \boldsymbol{u}_{xy}^2(\xi,\eta) + \boldsymbol{u}_{yy}^2(\xi,\eta)\right) dt.\end{aligned} \tag{2.3.16}$$

Combining (2.3.16) with Lemma 2.2.2, we deduce

$$\|\boldsymbol{\phi}_2 I_2\|_{0,T^{*,-}}^2 \lesssim h^4 \|\boldsymbol{u}\|_{2,T^-}^2.$$

By similar tedious computations, the same results for the $\boldsymbol{\phi}_i I_i$ $(i = 3, 5, 6)$ and $\boldsymbol{\phi}_i I_i^s$ $(i = 1, 4, \ s = +, -)$ can be obtained.

Taking $\overline{X} = \tilde{A}^{\perp}$, the fourth and fifth terms on the righthand side of (2.3.4) can be written as

$$
\begin{aligned}
&[\nabla \boldsymbol{u}(\tilde{A})]\boldsymbol{\phi}_1(A_1-\tilde{A}) + \big(\nabla \boldsymbol{u}^+(\overline{X}) - \nabla \boldsymbol{u}(X)\big)\,\boldsymbol{\phi}_1(\overline{X}-A_1)\\
&= [\nabla \boldsymbol{u}(\tilde{A})]\boldsymbol{\phi}_1(A_1-\tilde{A}) + (\nabla \boldsymbol{u}^+(\tilde{A}^\perp) - \nabla \boldsymbol{u}^-(\tilde{A}^\perp))\boldsymbol{\phi}_1(\tilde{A}^\perp - A_1)\\
&\quad + (\nabla \boldsymbol{u}^-(\tilde{A}^\perp) - \nabla \boldsymbol{u}(X))\boldsymbol{\phi}_1(\tilde{A}^\perp - A_1)\\
&= ([\nabla \boldsymbol{u}(\tilde{A})] - [\nabla \boldsymbol{u}(\tilde{A}^\perp)])\boldsymbol{\phi}_1(A_1-\tilde{A}) + [\nabla \boldsymbol{u}(\tilde{A}^\perp)]\boldsymbol{\phi}_1(\tilde{A}^\perp-\tilde{A})\\
&\quad + (\nabla \boldsymbol{u}^-(\tilde{A}^\perp) - \nabla \boldsymbol{u}(X))\boldsymbol{\phi}_1(\tilde{A}^\perp - A_1).
\end{aligned}
\tag{2.3.17}
$$

Now we expand $[\nabla \boldsymbol{u}(\tilde{A}^\perp)]$ at the point X. Actually, for $i = 1,\ 2$,

$$
\begin{aligned}
\frac{\partial u_i^-(\tilde{A}^\perp)}{\partial x} &= \frac{\partial u_i(X)}{\partial x} + \int_0^1 \frac{d}{dt}\frac{\partial}{\partial x} u_i(t\tilde{A}^\perp + (1-t)X)dt\\
&= \frac{\partial u_i(X)}{\partial x} + \int_0^1 (1-t)(u_{ixx}(\xi,\eta)(\tilde{x}^\perp - x) + u_{ixy}(\xi,\eta)(\tilde{y}^\perp - y))dt\\
&= \frac{\partial u_i(X)}{\partial x} + f_{xi}(\tilde{x}^\perp, \tilde{y}^\perp),\\
\frac{\partial u_i^-(\tilde{A}^\perp)}{\partial y} &= \frac{\partial u_i(X)}{\partial y} + \int_0^1 \frac{d}{dt}\frac{\partial}{\partial y} u_i(t\tilde{A}^\perp + (1-t)X)dt\\
&= \frac{\partial u_i(X)}{\partial y} + \int_0^1 (1-t)(u_{iyx}(\xi,\eta)(\tilde{x}^\perp - x) + u_{iyy}(\xi,\eta)(\tilde{y}^\perp - y))dt\\
&= \frac{\partial u_i(X)}{\partial y} + f_{yi}(\tilde{x}^\perp, \tilde{y}^\perp)
\end{aligned}
$$

with $\xi = t\tilde{x}^\perp + (1-t)x$, $\eta = t\tilde{y}^\perp + (1-t)y$, $\tilde{A}^\perp = (\tilde{x}^\perp, \tilde{y}^\perp)$. By using the notation l_i and $\bar{l}_i$ $(i = 1, \cdots, 6)$ and inserting $\frac{\partial u_i^-(\tilde{A}^\perp)}{\partial x}$ and $\frac{\partial u_i^-(\tilde{A}^\perp)}{\partial y}$ $(i = 1,\ 2)$ into $[\nabla \boldsymbol{u}(\tilde{A}^\perp)]$, we derive the desired Taylor expansion at the point X.

$$
[\nabla \boldsymbol{u}(\tilde{A}^\perp)] = \begin{pmatrix} \bar{G}_{11}(\tilde{A}^\perp) & \bar{G}_{12}(\tilde{A}^\perp) \\ \bar{G}_{21}(\tilde{A}^\perp) & \bar{G}_{22}(\tilde{A}^\perp) \end{pmatrix} = \begin{pmatrix} \bar{G}_{11}(X) & \bar{G}_{12}(X) \\ \bar{G}_{21}(X) & \bar{G}_{22}(X) \end{pmatrix}
$$

$$
+\begin{pmatrix} \left(\frac{\bar{n}_1}{\bar{n}_2}\overline{L}_f-(1,0,0)\right)\cdot F(\tilde{x}^\perp,\tilde{y}^\perp) & \overline{L}_f\cdot L_u-f_{y1}(\tilde{x}^\perp,\tilde{y}^\perp) \\ \frac{\bar{n}_1}{\bar{n}_2}\overline{L}_b\cdot L_u-f_{x2}(\tilde{x}^\perp,\tilde{y}^\perp) & \left(\overline{L}_b-(0,0,1)\right)\cdot F(\tilde{x}^\perp,\tilde{y}^\perp) \end{pmatrix},
$$

where

$$
\bar{G}_{11}=(\frac{\bar{n}_1}{\bar{n}_2}\overline{L}_f-(1,0,0))\cdot L_u,\ \ \bar{G}_{22}=\left(\overline{L}_b-(0,0,1)\right)\cdot L_u,
$$

$$
\bar{G}_{12}=\overline{L}_f\cdot L_u-\frac{\partial u_1^-}{\partial y},\ \ \bar{G}_{21}=\frac{\bar{n}_1}{\bar{n}_2}\overline{L}_b\cdot L_u-\frac{\partial u_2^-}{\partial x},
$$

$$
F(\tilde{x}^\perp,\tilde{y}^\perp)=\left(f_{x1}(\tilde{x}^\perp,\tilde{y}^\perp),f_{y1}(\tilde{x}^\perp,\tilde{y}^\perp)+f_{x2}(\tilde{x}^\perp,\tilde{y}^\perp),f_{y2}(\tilde{x}^\perp,\tilde{y}^\perp)\right)^t.
$$

Similarly,

$$
[\nabla\boldsymbol{u}(\tilde{A})]=\begin{pmatrix} G_{11}(\tilde{A}) & G_{12}(\tilde{A}) \\ G_{21}(\tilde{A}) & G_{22}(\tilde{A}) \end{pmatrix}=\begin{pmatrix} G_{11}(X) & G_{12}(X) \\ G_{21}(X) & G_{22}(X) \end{pmatrix}
$$

$$
+\begin{pmatrix} \left(\frac{n_1}{n_2}L_f-(1,0,0)\right)\cdot F(\tilde{x},\tilde{y}) & L_f\cdot L_u-f_{y1}(\tilde{x},\tilde{y}) \\ \frac{n_1}{n_2}L_b\cdot L_u-f_{x2}(\tilde{x},\tilde{y}) & (L_b-(0,0,1))\cdot F(\tilde{x},\tilde{y}) \end{pmatrix},
$$

where

$$
F(\tilde{x},\tilde{y})=(f_{x1}(\tilde{x},\tilde{y}),f_{y1}(\tilde{x},\tilde{y})+f_{x2}(\tilde{x},\tilde{y}),f_{y2}(\tilde{x},\tilde{y}))^t.
$$

Let $\bar{C}=\max\{|\frac{\bar{n}_1}{\bar{n}_2}\bar{l}_1-1|,\ |\bar{l}_2-1|,\ |\frac{\bar{n}_1}{\bar{n}_2}\bar{l}_5-1|,\ |\bar{l}_6-1|,\ |\frac{\bar{n}_1}{\bar{n}_2}\bar{l}_i|,\ |\bar{l}_i|,\ i=1,\cdots,6\}$. From (2.2.1) and Lemma 2.3.1, by tedious calculations, the following estimates hold:

$$
\|([\nabla\boldsymbol{u}(\tilde{A})]-[\nabla\boldsymbol{u}(\tilde{A}^\perp)])\boldsymbol{\phi}_1(A_1-\tilde{A})\|_{0,T^{*,-}}\lesssim h^2\|\boldsymbol{u}\|_{2,T^{*,-}}, \tag{2.3.18}
$$

$$
\|[\nabla\boldsymbol{u}(\tilde{A}^\perp)]\boldsymbol{\phi}_1(\tilde{A}^\perp-\tilde{A})\|_{0,T^{*,-}}\lesssim h^2\|\boldsymbol{u}\|_{2,T^{*,-}}, \tag{2.3.19}
$$

$$
\|(\nabla\boldsymbol{u}^-(\tilde{A}^\perp)-\nabla\boldsymbol{u}(X))\boldsymbol{\phi}_1(\tilde{A}^\perp-A_1)\|_{0,T^{*,-}}\lesssim h^2\|\boldsymbol{u}\|_{2,T^{*,-}}. \tag{2.3.20}
$$

Combining with (2.3.18)−(2.3.20),

$$
\|[\nabla\boldsymbol{u}(\tilde{A})]\boldsymbol{\phi}_1(A_1-\tilde{A})+(\nabla\boldsymbol{u}^+(\tilde{A}^\perp)-\nabla\boldsymbol{u}(X))\boldsymbol{\phi}_1(\overline{X}-A_1)\|_{0,T^{*,-}}\lesssim h^2\|\boldsymbol{u}\|_{2,T^{*,-}}.
$$

Taking $\overline{X}=\tilde{M}^{\perp}$, the last two terms on the righthand side of (2.3.4) can be estimated by the same argument,

$$\|[\nabla \boldsymbol{u}(\tilde{M})]\boldsymbol{\phi}_4(M_1-\tilde{M})+(\nabla \boldsymbol{u}^+(\tilde{M}^{\perp})-\nabla \boldsymbol{u}(X))\boldsymbol{\phi}_4(\overline{X}-M_1)\|_{0,T^{*,-}}\lesssim h^2\|\boldsymbol{u}\|_{2,T^{*,-}}.$$

Thus we get the conclusion. □

Let $\overline{\mathcal{X}}=t\overline{X}+(1-t)X$, $u_x=\frac{\partial \boldsymbol{u}_i}{\partial x}$, $u_{ixx}=\frac{\partial^2 u_i}{\partial x^2}$, $u_{ixy}=\frac{\partial^2 u_i}{\partial y\partial x}$, $i=1,2$. Now, by using the notations $\bar{l}_i$ $(i=1,\cdots,6)$, we turn to estimate H^1 norm of $I_{h,T}\boldsymbol{u}(X)-\boldsymbol{u}(X)$ on $T^{*,-}$.

Lemma 2.3.5. *For any $\boldsymbol{u}\in\widetilde{\boldsymbol{C}}^2(T)$, $\overline{X}\in\overline{DE}$ and $X\in T^{*,-}$, we have the following result for $s=x,\ y$,*

$$\begin{aligned}\frac{\partial}{\partial s}\left(I_{h,T}\boldsymbol{u}(X)-\boldsymbol{u}(X)\right)=&[\nabla \boldsymbol{u}(\tilde{A})]\frac{\partial \boldsymbol{\phi}_1}{\partial s}(A_1-\tilde{A})+[\nabla \boldsymbol{u}(\tilde{M})]\frac{\partial \boldsymbol{\phi}_4}{\partial s}(M_1-\tilde{M})\\&-(\nabla \boldsymbol{u}^+(\overline{X})-\nabla \boldsymbol{u}(X))\frac{\partial \boldsymbol{\phi}_1}{\partial s}(A_1-\overline{X})+\sum_{i=1}^{6}\frac{\partial \boldsymbol{\phi}_i}{\partial s}I_i\\&-(\nabla \boldsymbol{u}^+(\overline{X})-\nabla \boldsymbol{u}(X))\frac{\partial \boldsymbol{\phi}_4(X)}{\partial s}(M_1-\overline{X})\\&+Q_0\boldsymbol{\phi}_1(A_1-\overline{X})+Q_0\boldsymbol{\phi}_4(M_1-\overline{X}),\end{aligned}$$

where

$$\boldsymbol{Q_0}=\begin{pmatrix}\frac{\bar{n}_1}{\bar{n}_2}\overline{L}_f\cdot Q_l & \overline{L}_f\cdot Q_l\\ \frac{\bar{n}_1}{\bar{n}_2}\overline{L}_b\cdot Q_l & \overline{L}_b\cdot Q_l\end{pmatrix},$$

$$Q_l=\left(\int_0^1\frac{d}{dt}u_{1xx}(\overline{\mathcal{X}})dt,\int_0^1\frac{d}{dt}u_{1xy}(\overline{\mathcal{X}})dt+\int_0^1\frac{d}{dt}u_{2xx}(\overline{\mathcal{X}})dt,\int_0^1\frac{d}{dt}u_{2xy}(\overline{\mathcal{X}})dt\right)^t.$$

Proof. We only give a proof for the case $s=x$. The other case can be carried out similarly. According to (2.3.4), let $I_1=I_1^-+I_1^+$ and $I_4=I_4^-+I_4^+$. Then

$$\frac{\partial}{\partial x}(I_{h,T}\boldsymbol{u}(X)-\boldsymbol{u}(X))=\sum_{i=1}^{6}\left(\boldsymbol{\phi}_i(X)\frac{\partial I_i}{\partial x}+\frac{\partial \boldsymbol{\phi}_i}{\partial x}I_i\right)$$

$$+\frac{\partial}{\partial x}\Big([\nabla \boldsymbol{u}(\tilde{A})]\boldsymbol{\phi}_1(A_1-\tilde{A})+[\nabla \boldsymbol{u}(\tilde{M})]\boldsymbol{\phi}_4(M_1-\tilde{M})\Big)$$

$$-\frac{\partial}{\partial x}\left((\nabla \boldsymbol{u}^+(\overline{X})-\nabla \boldsymbol{u}(X))(\boldsymbol{\phi}_1(A_1-\overline{X})-\boldsymbol{\phi}_4(M_1-\overline{X}))\right). \quad (2.3.21)$$

From (2.3.9), we deduce

$$-\frac{\partial I_i}{\partial x}=\frac{\partial \boldsymbol{u}(X)}{\partial x}+\begin{pmatrix} u_{1xx}(X)(x_{A_i}-x)+u_{1xy}(X)(y_{A_i}-y)-\partial u_{1x}(X) \\ u_{2xx}(X)(x_{A_i}-x)+u_{2xy}(X)(y_{A_i}-y)-\partial u_{2x}(X)\end{pmatrix}$$

$$=\begin{pmatrix} u_{1xx}(X)(x_{A_i}-x)+u_{1xy}(X)(y_{A_i}-y) \\ u_{2xx}(X)(x_{A_i}-x)+u_{2xy}(X)(y_{A_i}-y)\end{pmatrix}, \quad (2.3.22)$$

where $i=2,3$. By similar calculations and $(2.3.10)$, for $i=5,6$,

$$-\frac{\partial I_i}{\partial x}=\frac{\partial \boldsymbol{u}(X)}{\partial x}+\begin{pmatrix} u_{1xx}(X)(x_{M_{i-3}}-x)+u_{1xy}(X)(y_{M_{i-3}}-y)-\partial u_{1x}(X) \\ u_{2xx}(X)(x_{M_{i-3}}-x)+u_{2xy}(X)(y_{M_{i-3}}-y)-\partial u_{2x}(X)\end{pmatrix}$$

$$=\begin{pmatrix} u_{1xx}(X)(x_{M_{i-3}}-x)+u_{1xy}(X)(y_{M_{i-3}}-y) \\ u_{2xx}(X)(x_{M_{i-3}}-x)+u_{2xy}(X)(y_{M_{i-3}}-y)\end{pmatrix}. \quad (2.3.23)$$

Moreover, according to the expansions (2.3.11) and (2.3.12), we get

$$-\frac{\partial I_1}{\partial x}=\begin{pmatrix} u_{1xx}(X) & u_{1xy}(X) \\ u_{2xx}(X) & u_{2xy}(X)\end{pmatrix}\begin{pmatrix} x_{A_1}-x \\ y_{A_1}-y\end{pmatrix}+\frac{\partial}{\partial x}\Big([\nabla \boldsymbol{u}(\tilde{A})](A_1-\tilde{A})\Big), \quad (2.3.24)$$

$$-\frac{\partial I_4}{\partial x}=\begin{pmatrix} u_{1xx}(X) & u_{1xy}(X) \\ u_{2xx}(X) & u_{2xy}(X)\end{pmatrix}\begin{pmatrix} x_{A_1}-x \\ y_{A_1}-y\end{pmatrix}+\frac{\partial}{\partial x}\Big([\nabla \boldsymbol{u}(\tilde{M})](M_1-\tilde{M})\Big). \quad (2.3.25)$$

Combining with (2.3.22)-$(2.3.35)$,

$$-\sum_{i=1}^{6}\frac{\partial I_i}{\partial x}\boldsymbol{\phi}_i=\boldsymbol{\phi}_1\frac{\partial}{\partial x}\Big([\nabla \boldsymbol{u}(\tilde{A})](A_1-\tilde{A})\Big)+\boldsymbol{\phi}_4\frac{\partial}{\partial x}\Big([\nabla \boldsymbol{u}(\tilde{M})](M_1-\tilde{M})\Big)$$

$$+\sum_{i=1}^{3}(\boldsymbol{\phi}_i(X)\boldsymbol{N}_2(A_i-X)+\boldsymbol{\phi}_{i+3}\boldsymbol{N}_2(M_i-X)), \tag{2.3.26}$$

where

$$\boldsymbol{N}_2=\begin{pmatrix} N_{11} & N_{12}\\ N_{21} & N_{22}\end{pmatrix}=\begin{pmatrix} u_{1xx}(X) & u_{1xy}(X)\\ u_{2xx}(X) & u_{2xy}(X)\end{pmatrix}.$$

Then, by Lemma 2.3.3, there exists $\boldsymbol{v}\in\boldsymbol{U}_h^i(T)$ be such that $\nabla\boldsymbol{v}(X)=\boldsymbol{N}_2$ and

$$\begin{aligned}&-\sum_{i=1}^{3}(\boldsymbol{\phi}_i(X)N(A_i-X)+\boldsymbol{\phi}_{i+3}(X)N(M_i-X))\\ =&(\boldsymbol{N_0}-\boldsymbol{N}_2)(\boldsymbol{\phi}_1(X)(A_1-\overline{X})+\boldsymbol{\phi}_4(X)(M_1-\overline{X})).\end{aligned} \tag{2.3.27}$$

Substituting (2.3.27) into (2.3.26), we obtain

$$\begin{aligned}\sum_{i=1}^{6}\frac{\partial I_i}{\partial x}\boldsymbol{\phi}_i=&(\boldsymbol{N_0}-\boldsymbol{N}_2)(\boldsymbol{\phi}_1(A_1-\overline{X})+\boldsymbol{\phi}_4(M_1-\overline{X}))\\ &-\boldsymbol{\phi}_1\frac{\partial}{\partial x}([\nabla\boldsymbol{u}(\tilde{A})](A_1-\tilde{A}))-\boldsymbol{\phi}_4\frac{\partial}{\partial x}([\nabla\boldsymbol{u}(\tilde{M})](M_1-\tilde{M})).\end{aligned} \tag{2.3.28}$$

Finally, inserting (2.3.28) into (2.3.21), the desired result can be deduced. □

Proceeding as in the proof of Theorem 4.1, using Lemma 4.5, we have the following thoerem.

Theorem 2.3.2. *For any $T\in\mathcal{T}_h^i$, and any $\boldsymbol{u}\in\tilde{\boldsymbol{H}}^2(T)$,*

$$\|\partial_s(I_{h,T}\boldsymbol{u}-\boldsymbol{u})\|_{0,T^{*,-}}\lesssim h\|\boldsymbol{u}\|_{2,T},\qquad s=x,y.$$

Arguing as Theorem 2.3.1 and Theorem 2.3.2, we have similar result on $T^{*,+}$.

Theorem 2.3.3. *For any $T\in\mathcal{T}_h^i$ and $\boldsymbol{u}\in\tilde{\boldsymbol{H}}^2(T)$,*

$$\|I_{h,T}\boldsymbol{u}-\boldsymbol{u}\|_{0,T^{*,+}}\lesssim h^2\|\boldsymbol{u}\|_{2,T},$$

$$\|\partial_s(I_{h,T}\boldsymbol{u}-\boldsymbol{u})\|_{0,T^{*,+}}\lesssim h\|\boldsymbol{u}\|_{2,T},\qquad s=x,y.$$

By the same argument in the proof of Theorem 3.5 in [52], the following result holds.

Theorem 2.3.4. *For any* $\boldsymbol{u} \in \tilde{\boldsymbol{H}}^2(T)$ *and* $p > 1$*, it holds*

$$\|I_{h,T}\boldsymbol{u} - \boldsymbol{u}\|_{0,T^*} \lesssim h^2\|\boldsymbol{u}\|_{2,T} + Ch^{5/2-3/p}\|\boldsymbol{u}\|_{1,p,T^*},$$

$$\|\partial_s(I_{h,T}\boldsymbol{u} - \boldsymbol{u})\|_{0,T^*} \lesssim h\|\boldsymbol{u}\|_{2,T} + Ch^{3/2-3/p}\|\boldsymbol{u}\|_{1,p,T^*}, \qquad s = x,\ y,$$

where $T \in \mathcal{T}_h^i$.

Finally, combining Theorem 2.3.1-Theorem 2.3.4, arguing as Theorem 3.7 in [52], we can deduce our main result.

Theorem 2.3.5. *For any* $\boldsymbol{u} \in \tilde{\boldsymbol{H}}^2(T)$ *and* $h > 0$ *small enough,*

$$\|I_h\boldsymbol{u} - \boldsymbol{u}\|_{0,\Omega} \lesssim h^2\|\boldsymbol{u}\|_{\widetilde{H}^2(\Omega)},$$

$$\|\partial_s(I_h\boldsymbol{u} - \boldsymbol{u})\|_{0,\Omega} \lesssim h\|\boldsymbol{u}\|_{\widetilde{H}^2(\Omega)}, \qquad s = x,\ y.$$

2.4 The approximation capability for another P_1/CR IFEM

In this part, we will give the approximation capability for another P_1/CR IFE method, which has been proposed in [59]. For completeness, we descript it simply. The local basis functions are chosen to satisfy the following conditions

$$\boldsymbol{\psi}_{j,T}^E(A_i) = (\delta_{i,j}, 0)^t, \qquad j = 1, 2, 3; \tag{2.4.1}$$

$$\frac{1}{|e_i|}\int_{e_i} \boldsymbol{\psi}_{j,T}^E ds = (0, \delta_{j-3,i})^t, \qquad j = 4, 5, 6, \tag{2.4.2}$$

where A_i and e_i $(i = 1, 2, 3)$ are the vertices and the edges of T respectively.

We can determine the piecewise linear basis function $\hat{\boldsymbol{\phi}}_j^E$ $(j = 1, \cdots, 6)$ by (2.1.2)-(2.1.5) with replacing the (2.1.3) by the integral average values on the edges of $\hat{T}$,

$$\frac{1}{|\hat{e}_i|}\int_{\hat{e}_i} \hat{\phi}_{2,j} ds = \delta_{i,j-3}, \qquad i = 1, 2, 3. \tag{2.4.3}$$

The unisolvent property of this method has be proved in [59]. Define the local basis functions $\boldsymbol{\phi}_j^E$ on the element T as $\boldsymbol{\phi}_{j,T}$, the local P_1/CR IFE space $S_h^i(T)$ is given by $S_h^i(T) = \text{Span}\{\boldsymbol{\phi}_{j,T}^E : j = 1, \cdots, 6\}$.

The global P_1/CR IFE space can be expressed as

$$\begin{aligned} S_h(\Omega) = \big\{&\boldsymbol{v}_h = (v_{1h}, v_{2h})^t \in \boldsymbol{L}^2(\Omega) : \boldsymbol{v}_h|_T \in S_h^\alpha(T),\ \alpha = i, n,\ \forall T \in \mathcal{T}_h; \\ &v_{1h}|_{T_1}(A_j) = v_{1h}|_{T_2}(A_j),\ j = 1, 2,\ \text{and} \int_{\overline{A_1A_2}} v_{2h}|_{T_1} ds = \int_{\overline{A_1A_2}} v_{2h}|_{T_2} ds, \\ &\forall T_1 \cap T_2 = \overline{A_1A_2}\big\}. \end{aligned}$$

The discrete problem is

$$a_h(\boldsymbol{u}_h, \boldsymbol{v}_h) = (\boldsymbol{f}, \boldsymbol{v}_h), \quad \forall \boldsymbol{v}_h \in S_{h,0}(\Omega), \tag{2.4.4}$$

where

$$\begin{aligned} S_{h,0}(\Omega) = \big\{&\boldsymbol{v}_h = (v_{1,h}, v_{2,h})^t \in S_h(\Omega),\ \text{if } \partial T \cap \partial\Omega = \overline{A_1A_2},\ v_{1,h}|(A_i) = g_1(A_i), \\ &i = 1, 2,\ \text{and} \int_{\overline{A_1A_2}} v_{2,h} ds = \int_{\overline{A_1A_2}} v_{2,h} ds = 0,\ T \in \mathcal{T}_h\big\}. \end{aligned}$$

Define a local interpolation operator $I_{h,T}^E : \tilde{\boldsymbol{H}}^2(T) \to S_h(T)$ as

$$I_{h,T}^E \boldsymbol{u} = \begin{cases} \sum_{j=1}^6 c_j \boldsymbol{\psi}_{j,T}^E, & \text{if } T \text{ is a non-interface element,} \\ \sum_{j=1}^6 c_j \boldsymbol{\phi}_{j,T}^E, & \text{if } T \text{ is an interface element,} \end{cases}$$

where

$$c_i = u_1(A_i)\ \ i = 1, 2, 3, \quad c_j = \frac{1}{|e_{j-3}|} \int_{e_{j-3}} u_2 ds\ \ j = 4, 5, 6.$$

The global IFE interpolation operator $I_h^E : \tilde{\boldsymbol{H}}^2(\Omega) \to S_h(\Omega)$ is denoted by

$$I_h^E \boldsymbol{u}|_T = I_{h,T}^E \boldsymbol{u}, \qquad \forall T \in \mathcal{T}_h.$$

At first, we give an error bound for IFE basis function $\phi_{i,T}^E$.

Lemma 2.4.1. *For any $T \in \mathcal{T}_h^i$,*

$$\left\|\phi_{i,T}^E\right\|_{0,T} + h\left|\phi_{i,T}^E\right|_{1,T} \lesssim h, \quad i = 1, \cdots, 6. \tag{2.4.5}$$

Proof. According to Theorem 2.4 in [52] and Theorem 3.2 in [72], the estimate holds

$$\left\|\phi_{i,T}^E\right\|_{0,T}^2 = \int_T (\phi_{i,T}^E(x,y))^2 dxdy \le \left\|\phi_{i,T}^E\right\|_{0,\infty,T}^2 \int_T 1 dxdy \lesssim h^2. \tag{2.4.6}$$

Similarly,

$$\left|\phi_{i,T}^E\right|_{1,T}^2 = \int_T \nabla\phi_{i,T}^E(x,y)\cdot\nabla\phi_{i,T}^E(x,y)dxdy \le \left|\phi_{i,T}^E\right|_{1,\infty,T}^2 \int_T 1 dxdy \lesssim 1. \tag{2.4.7}$$

Combining (2.4.6) with (2.4.7), the desired result is obtained. □

Then we estimate the interpolation error $\boldsymbol{u} - I_{h,T}^E\boldsymbol{u}$.

Theorem 2.4.1. *For any $T \in \mathcal{T}_h^i$, it holds*

$$\left\|I_{h,T}^E\boldsymbol{u} - \boldsymbol{u}\right\|_{0,T} + h\left|I_{h,T}^E\boldsymbol{u} - \boldsymbol{u}\right|_{1,T} \lesssim h^2\|\boldsymbol{u}\|_{2,T}, \quad \forall \boldsymbol{u} \in \tilde{\boldsymbol{H}}^2(T). \tag{2.4.8}$$

Proof. By triangular inequality,

$$|I_{h,T}^E\boldsymbol{u} - \boldsymbol{u}|_{k,T} \le |I_{h,T}^E\boldsymbol{u} - I_{h,T}\boldsymbol{u}|_{k,T} + |I_{h,T}\boldsymbol{u} - \boldsymbol{u}|_{k,T}, \quad k = 0, 1, \tag{2.4.9}$$

where the notation $|\cdot|_{0,T}$ means the L^2 norm on T. The estimate of the term $|I_{h,T}\boldsymbol{u} - \boldsymbol{u}|_{k,T}$ can be obtained by Theorem 2.3.4. Hence, we only need to bound $|I_{h,T}^E\boldsymbol{u} - I_{h,T}\boldsymbol{u}|_{k,T}$. At first,

$$\begin{aligned} & I_{h,T}^E\boldsymbol{u}(X) - I_{h,T}\boldsymbol{u}(X) \\ & = \sum_{i=1}^{3} \boldsymbol{u}(A_i)(\boldsymbol{\phi}_i^E - \boldsymbol{\phi}_i) + \sum_{i=4}^{6} \boldsymbol{\phi}_{i-3}^E \bar{\boldsymbol{u}}_{i-3}(X) - \sum_{i=4}^{6} \boldsymbol{\phi}_i \boldsymbol{u}(M_{i-3}) \end{aligned}$$

$$= \sum_{i=1}^{3} \big(\boldsymbol{u}(A_i)(\boldsymbol{\phi}_i^E - \boldsymbol{\phi}_i) + \bar{\boldsymbol{u}}_i(X)(\boldsymbol{\phi}_{i+3}^E - \boldsymbol{\phi}_{i+3}) + (\bar{\boldsymbol{u}}_i(X) - \boldsymbol{u}(M_i)\boldsymbol{\phi}_{i+3} \big), \tag{2.4.10}$$

where

$$\bar{\boldsymbol{u}}_i(X) = \frac{1}{|e_i|} \int_{e_i} \boldsymbol{u}(X) ds, \ \ i = 1, 2, 3.$$

Then, we note that

$$\boldsymbol{\phi}_1^E = \boldsymbol{\phi}_1 = (a_1^-,\ 0)^t, \ \ \boldsymbol{\phi}_2^E = \boldsymbol{\phi}_2 = (a_1^+ + b_1^+,\ 0)^t \tag{2.4.11}$$

$$\boldsymbol{\phi}_3^E = \boldsymbol{\phi}_3 = (a_1^+ + c_1^+,\ 0)^t, \ \ \boldsymbol{\phi}_4^E = (0,\ a_2^+ + \frac{1}{2} b_2^+)^t, \ \ \boldsymbol{\phi}_4 = (0,\ f_1)^t, \tag{2.4.12}$$

$$\boldsymbol{\phi}_5^E = (0,\ a_2^+ + \frac{1}{2} b_2^+ + \frac{1}{2} c_2^+)^t, \ \ \boldsymbol{\phi}_5 = (0,\ a_2^+ + \frac{1}{2} b_2^+ + \frac{1}{2} c_2^+)^t, \tag{2.4.13}$$

$$\boldsymbol{\phi}_6^E = (0,\ a_2^- + \frac{1}{2} c_2^-)^t, \ \ \boldsymbol{\phi}_6 = (0,\ f_2)^t, \tag{2.4.14}$$

where

$$f_1 = a_2^- d + \frac{1}{2} b_2^- d^2 + a_2^+ (1-d) + \frac{1}{2} b_2^+ (1-d^2),$$

$$f_2 = a_2^- e + \frac{1}{2} c_2^- e^2 + a_2^+ (1-e) + \frac{1}{2} c_2^+ (1-e^2).$$

Inserting (2.4.11)-(2.4.15) into (2.4.10) and integrating on T, we obtain

$$\begin{aligned} &\| I_{h,T}^E \boldsymbol{u}(X) - I_{h,T} \boldsymbol{u}(X) \|_{k,T} \\ &= \| \sum_{i=4}^{6} \big[\bar{\boldsymbol{u}}_{i-3}(X) \left(\phi_i^E - \phi_i \right) + (\bar{\boldsymbol{u}}_{i-3}(X) - \boldsymbol{u}(M_{i-3}))\phi_i \big] \|_{k,T} \\ &= \| I_1 + I_2 \|_{k,T}. \end{aligned} \tag{2.4.15}$$

Moreover, from Cacuchy-Schwarz inequality and Lemma 2.4.1,

$$\| I_1 \|_{k,T} \leq \sum_{i=4}^{6} \frac{1}{|e_{i-3}|^{1/2}} \| \boldsymbol{u} \|_{0,e_{i-3}} \| \phi_i^E - \phi_i \|_{k,T}$$

$$
\begin{aligned}
&\lesssim h^{1-k}\sum_{i=4}^{6}\frac{1}{|e_{i-3}|^{1/2}}(h^{-1/2}\|\boldsymbol{u}\|_{0,T}+h^{1/2}|\boldsymbol{u}|_{1,T})\\
&\lesssim h^{-k}\|\boldsymbol{u}\|_{0,T}+h^{1-k}|\boldsymbol{u}|_{1,T}. \qquad (2.4.16)
\end{aligned}
$$

By Taylor expansion, we deduce

$$
\begin{aligned}
\|I_2\|_{k,T} &\lesssim \sum_{i=1}^{3}\frac{1}{|e_i|}\int_{e_i}|\nabla\boldsymbol{u}(X)(X-M_i)|ds\\
&\lesssim h\sum_{i=1}^{3}\frac{1}{|e_i|^{1/2}}\|\nabla\boldsymbol{u}(X)\|_{0,e_i}\\
&\lesssim h\sum_{i=1}^{3}\frac{1}{|e_i|^{1/2}}(h^{-1/2}\|\nabla\boldsymbol{u}\|_{0,T}+h^{1/2}|\nabla\boldsymbol{u}|_{1,T})\\
&\lesssim \|\boldsymbol{u}\|_{1,T}+h|\boldsymbol{u}|_{2,T}. \qquad (2.4.17)
\end{aligned}
$$

Combining (2.4.16) with (2.4.17),

$$
|I_{h,T}^{E}\boldsymbol{u}-I_{h,T}\boldsymbol{u}|_{k,T}\lesssim (h^{-k}h^2\|\boldsymbol{u}\|_{2,T}+h^{1-k}h\|\boldsymbol{u}\|_{2,T})\lesssim h^{2-k}\|\boldsymbol{u}\|_{2,T}. \qquad (2.4.18)
$$

The proof is completed. □

Summing over all the elements, the following estimate holds.

Theorem 2.4.2. *For any $\boldsymbol{u}\in\tilde{\boldsymbol{H}}^2(\Omega)$,*

$$
\|I_{h,T}^{E}\boldsymbol{u}-\boldsymbol{u}\|_{0,\Omega}+h|I_{h,T}^{E}\boldsymbol{u}-\boldsymbol{u}|_{1,\Omega}\lesssim h^2\|\boldsymbol{u}\|_{\widetilde{H}^2(\Omega)}. \qquad (2.4.19)
$$

2.5 The trace inequality for IFE functions

In this section, we extend the trace inequality to IFE functions in $S_h^i(T)$ for $T\in\mathcal{T}_h^i$. The same result in $\boldsymbol{U}_h^i(T)$ can be also obtained as follow.

Lemma 2.5.1. *For any linear IFE function $\boldsymbol{v} \in S_h^i(T)$ in the interface element T, it holds*

$$\|(b_1^-, c_1^-, b_2^-, c_2^-)\| \lesssim \|(b_1^+, c_1^+, b_2^+, c_2^+)\|, \tag{2.5.1}$$

where $\|\cdot\|$ is a Euclidean norm.

Proof. We only prove the right inequality in (2.5.1), the left one can be derived similarly. Using the interface conditions, we obtain

$$M^-(a_1^-, b_1^-, c_1^-, a_2^-, b_2^-, c_2^-)^t = M^+(a_1^+, b_1^+, c_1^+, a_2^+, b_2^+, c_2^+),$$

where

$$M^s = \begin{pmatrix} 1 & 0 & e & 0 & 0 & 0 \\ 1 & d & 0 & 0 & 0 & 0 \\ 0 & 0 & 0 & 1 & 0 & e \\ 0 & 0 & 0 & 1 & d & 0 \\ 0 & (\lambda^s + 2\mu^s)e & \mu^s d & 0 & \mu^s d & \lambda^s e \\ 0 & \lambda^s d & \mu^s e & 0 & \mu^s e & (\lambda^s + 2\mu^s)d \end{pmatrix}, \; s = +, -.$$

By tedious calculation, since $(d, e) \neq (0, 0)$, we have $\det(M^s) \neq 0$. Let $\rho^s = 2\mu^s + \lambda^s$, $\eta^s = \rho^s d^2 - \lambda^s e^2$, $\xi^s = \rho^s e^2 - \lambda^s d^2$ $(s = +,\ -)$ and $H = \rho^+(d^3 + e^3 + 2e^2 d) + \lambda^+ de(e - d)$, $f_{\lambda\mu} = \frac{\mu^-}{\mu^+ H}$, then

$$b_1^+ = g_{11}b_1^- + g_{12}c_1^- + g_{13}b_2^- + g_{14}c_2^-,\ \ b_2^+ = g_{21}b_1^- + g_{22}c_1^- + g_{23}b_2^- + g_{24}c_2^-, \tag{2.5.2}$$

$$c_1^+ = g_{31}b_1^- + g_{32}c_1^- + g_{33}b_2^- + g_{34}c_2^-,\ \ c_2^+ = g_{41}b_1^- + g_{42}c_1^- + g_{43}b_2^- + g_{44}c_2^-, \tag{2.5.3}$$

where

$$g_{11} = \frac{d\eta^+ + e\eta^- + 2\rho^- de^2}{H} + 2f_{\lambda\mu}\lambda^+ de^2,$$

$$g_{12} = g_{13} = e\eta^+(f_{\lambda\mu} - \frac{1}{H}),\ g_{14} = e\frac{\eta^+ - \eta^- + 2\lambda^- ed}{H} - 2f_{\lambda\mu}\lambda^+ de^2,$$

$$g_{21} = \frac{d\xi^+ - \rho^- e(e+d) + \lambda^- d(d^2+2e^2)}{H} + \lambda^+ e(\frac{\lambda^-(ed-d-e)}{\mu^+ H} - 2f_{\lambda\mu} ed),$$

$$g_{23} = \frac{\rho^+ d(d^2+3e^2) + \lambda^+ de^2 + \mu^-(2e^3+d^2e-d-de)}{H} + f_{\lambda\mu}\lambda^+(2e^3-d^2-de),$$

$$g_{24} = \frac{d^3(\rho^- - \rho^+) + de^2(2\rho^- - 3\rho^+) - \lambda^+ de^2 - \lambda^- e(d+e)}{H}$$

$$+ \lambda^+ e(2f_{\lambda\mu} ed - \frac{\lambda^-(ed-d-e)}{\mu^+ H}),$$

$$g_{22} = \frac{-e\xi^+ + \mu^-(2e^3+d^2e-d-de)}{H} + f_{\lambda\mu}\lambda^+(2e^3-d^2-de),$$

$$g_{31} = d\frac{-\xi^+ - 4de(\lambda^+ + \mu^+) + \rho^- e(e+2d) - \lambda^- ed(4+d)}{H} + 2f_{\lambda\mu}\lambda^+ d^2 e,$$

$$g_{32} = e\frac{\xi^+ + 4de(\lambda^+ + \mu^+)}{H} + f_{\lambda\mu}\eta^+ d, \quad g_{33} = d\eta^+(f_{\lambda\mu} - \frac{1}{H}),$$

$$g_{34} = d\frac{\eta^+ - \eta^- + 2\lambda^- ed}{H} - 2f_{\lambda\mu}\lambda^+ d^2 e,$$

$$g_{41} = d\frac{\xi^+ - 2\mu^- e^2 + \lambda^-(e^2+d^2)}{H} - 2f_{\lambda\mu}\lambda^+ de^2,$$

$$g_{42} = g_{43} = e\xi^+(f_{\lambda\mu} - \frac{1}{H}),$$

$$g_{44} = \frac{e\xi^+ + 2\mu^- de^2 + \rho^- d(e^2+d^2)}{H} + 2f_{\lambda\mu}\lambda^+ de^2.$$

Therefore, there exists a constant C that depends on λ^s and μ^s $(s=+,-)$ but is independ of $d,\ e$, such that

$$|g_{ij}| \le C,\ \ 1 \le i,\ j \le 4. \tag{2.5.4}$$

Combining (2.5.4) with (2.5.2) and (2.5.3), the proof is completed. □

Lemma 2.5.2. *For an arbitrary linear IFE function $\boldsymbol{v}$, we have*

$$\|\mu\boldsymbol{\epsilon}(\boldsymbol{v})\cdot\mathbf{n}\|_{0,e} \lesssim h^{1/2}|T|^{-1/2}\|\mu\boldsymbol{\epsilon}(\boldsymbol{v})\|_{0,T}, \tag{2.5.5}$$

$$\|\lambda(\nabla\cdot\boldsymbol{v})I\cdot\mathbf{n}\|_{0,e} \lesssim h^{1/2}|T|^{-1/2}\|\mu\boldsymbol{\epsilon}(\boldsymbol{v})\|_{0,T}, \tag{2.5.6}$$

where $T\in\mathcal{T}_h^i$ and $e\in\varepsilon_h^i$.

Proof. Without loss of generality, we consider a triangle in Fig.2-2. Assume that $|T^+|\geq\frac{1}{2}|T|$ and $e=e^-\cup e^+$, where $e^-=\overline{EA_3}$ and $e^+=\overline{A_1E}$. By direct calculations, on e^+, we deduce that

$$\|\mu^+\boldsymbol{\epsilon}(\boldsymbol{v})\|_{0,e^+}^2=(\mu^+)^2\left\|\begin{pmatrix} b_1^+ & \frac{1}{2}(c_1^++b_2^+)\\ \frac{1}{2}(c_1^++b_2^+) & c_2^+\end{pmatrix}\right\|_{0,e^+}^2$$

$$\leq(\mu^+)^2\frac{|e^+|}{|T^+|}\left\|\begin{pmatrix} b_1^+ & \frac{1}{2}(c_1^++b_2^+)\\ \frac{1}{2}(c_1^++b_2^+) & c_2^+\end{pmatrix}\right\|_{0,T^+}^2\lesssim\frac{|e^+|}{|T|}\|\mu\boldsymbol{\epsilon}(\boldsymbol{v})\|_{0,T}^2. \tag{2.5.7}$$

On e^-, by (2.5.1), we have

$$\|\mu^-\boldsymbol{\epsilon}(\boldsymbol{v})\|_{0,e^-}^2=(\mu^-)^2\left\|\begin{pmatrix} b_1^- & \frac{1}{2}(c_1^-+b_2^-)\\ \frac{1}{2}(c_1^-+b_2^-) & c_2^-\end{pmatrix}\right\|_{0,e^-}^2$$

$$\lesssim(\mu^-)^2\frac{|e^-|}{|T^+|}\left\|\begin{pmatrix} b_1^+ & \frac{1}{2}(c_1^++b_2^+)\\ \frac{1}{2}(c_1^++b_2^+) & c_2^+\end{pmatrix}\right\|_{0,T^+}^2\lesssim\frac{|e^-|}{|T^+|}\|\mu\boldsymbol{\epsilon}(\boldsymbol{v})\|_{0,T}^2. \tag{2.5.8}$$

Combining (2.5.7), (2.5.8) with $|T^+|\geq\frac{1}{2}|T|$,

$$\|\mu\boldsymbol{\epsilon}(\boldsymbol{v})\cdot\boldsymbol{n}\|_{0,e}\lesssim h^{1/2}|T|^{-1/2}\|\mu\boldsymbol{\epsilon}(\boldsymbol{v})\|_{0,T}.$$

Similarly, the following result is obtained

$$\|\lambda(\nabla\cdot\boldsymbol{v})I\cdot\boldsymbol{n}\|_{0,e}\lesssim h^{1/2}|T|^{-1/2}\|\mu\boldsymbol{\epsilon}(\boldsymbol{v})\|_{0,T}.$$

The proof is completed. □

Now, we have the trace inequality.

Lemma 2.5.3. *For any linear IFE function $\boldsymbol{v} \in S_h(\Omega)$, the following inequality holds*

$$\sum_{e\in\varepsilon_h^i} (h\{\boldsymbol{n}\cdot\boldsymbol{\sigma}(\boldsymbol{v})\}, \{\boldsymbol{n}\cdot\boldsymbol{\epsilon}(\boldsymbol{v})\})_e \lesssim \sum_{T\in\mathcal{T}_h^i} (\boldsymbol{\sigma}(\boldsymbol{v}), \boldsymbol{\epsilon}(\boldsymbol{v}))_T,$$

where $e \in \varepsilon_h^i$ and $T \in \mathcal{T}_h^i$.

Proof. For any interface edge $e = T_1 \cap T_2$, we first note

$$\begin{aligned}(h\boldsymbol{n}\cdot\boldsymbol{\sigma}(\boldsymbol{v}), \boldsymbol{n}\cdot\boldsymbol{\epsilon}(\boldsymbol{v}))_e &= h\left(\boldsymbol{n}\cdot(2\mu\boldsymbol{\epsilon}(\boldsymbol{v}) + \lambda(\nabla\cdot\boldsymbol{v})I), \boldsymbol{n}\cdot\boldsymbol{\epsilon}(\boldsymbol{v})\right)_e \\ &= h\|\lambda(\nabla\cdot\boldsymbol{v})I\cdot\boldsymbol{n}\|_{0,e}^2 + 2h\|\mu\boldsymbol{\epsilon}(\boldsymbol{v})\cdot\boldsymbol{n}\|_{0,e}^2. \qquad (2.5.9)\end{aligned}$$

Combining (2.5.9) with Lemma 2.5.2,

$$\begin{aligned}&(h\{\boldsymbol{n}\cdot\boldsymbol{\sigma}(\boldsymbol{v})\}, \{\boldsymbol{n}\cdot\boldsymbol{\epsilon}(\boldsymbol{v})\})_e \\ &\le \frac{1}{2}\left((h\boldsymbol{n}\cdot\boldsymbol{\sigma}(\boldsymbol{v})|_{T_1}, \boldsymbol{n}\cdot\boldsymbol{\epsilon}(\boldsymbol{v})|_{T_1})_e + (h\boldsymbol{n}\cdot\boldsymbol{\sigma}(\boldsymbol{v})|_{T_2}, \boldsymbol{n}\cdot\boldsymbol{\epsilon}(\boldsymbol{v})|_{T_2})_e\right) \\ &\lesssim \|\mu\boldsymbol{\epsilon}(\boldsymbol{v})\cdot\boldsymbol{n}\|_{0,T_1}^2 + \|\mu\boldsymbol{\epsilon}(\boldsymbol{v})\cdot\boldsymbol{n}\|_{0,T_2}^2 \\ &\lesssim (\boldsymbol{\sigma}(\boldsymbol{v}), \boldsymbol{\epsilon}(\boldsymbol{v}))_{T_1} + (\boldsymbol{\sigma}(\boldsymbol{v}), \boldsymbol{\epsilon}(\boldsymbol{v}))_{T_2}.\end{aligned}$$

Summing over all edges $e \in \varepsilon_h^i$, the proof is completed. □

2.6 The finite element error analysis

We start by proving the coercivity of the bilinear form $a_h(\boldsymbol{u}_h, \boldsymbol{v}_h)$ in the IFE space with respect to the following energy norm

$$\|\boldsymbol{v}_h\|_h = \left(\sum_{T\in\mathcal{T}_h} \big(\boldsymbol{\sigma}(\boldsymbol{v}_h), \boldsymbol{\epsilon}(\boldsymbol{v}_h)\big)_T + \sum_{e\in\varepsilon_h^i} h^{-1}((\mu+\lambda)[\boldsymbol{v}_h], [\boldsymbol{v}_h])_e\right)^{\frac{1}{2}}. \qquad (2.6.1)$$

Theorem 2.6.1. *There exists a constant $\kappa > 0$ such that*

$$\kappa\|\boldsymbol{v}_h\|_h^2 \le a_h(\boldsymbol{v}_h, \boldsymbol{v}_h) \quad \forall \boldsymbol{v}_h \in S_{h,0}(\Omega). \tag{2.6.2}$$

Proof. First, we note

$$\boldsymbol{\epsilon} = \frac{1}{2\mu}(\boldsymbol{\sigma} - \frac{\lambda}{2\mu+2\lambda} tr\boldsymbol{\sigma} I) = \frac{1}{2\mu}\boldsymbol{\sigma}^D + \frac{1}{4(\mu+\lambda)} tr\boldsymbol{\sigma} I,$$

where $\boldsymbol{\sigma}^D = \boldsymbol{\sigma} - (tr\boldsymbol{\sigma} I)/2$. Furthermore,

$$\boldsymbol{\sigma} : \boldsymbol{\epsilon} = \frac{1}{2\mu}\boldsymbol{\sigma}^D : \boldsymbol{\sigma}^D + \frac{1}{4(\mu+\lambda)}(tr\boldsymbol{\sigma})^2,$$

$$\boldsymbol{\sigma} : \boldsymbol{\sigma} = \boldsymbol{\sigma}^D : \boldsymbol{\sigma}^D + \frac{1}{2}(tr\boldsymbol{\sigma})^2,$$

so that $\boldsymbol{\sigma} : \boldsymbol{\sigma} = 2(\mu+\lambda)\boldsymbol{\sigma} : \boldsymbol{\epsilon}$. Thus

$$\frac{1}{2}\|\frac{1}{\sqrt{\mu+\lambda}}\boldsymbol{n}\cdot\boldsymbol{\sigma}(\boldsymbol{v}_h)\|_{0,e}^2 \le (\boldsymbol{n}\cdot\boldsymbol{\sigma}(\boldsymbol{v}_h), \boldsymbol{n}\cdot\boldsymbol{\epsilon}(\boldsymbol{v}_h))_e. \tag{2.6.3}$$

For each $e \in \varepsilon_h^i$, using (2.6.3) and Cauchy-Schwarz inequality, there exists a constant $\delta > 0$ such that

$$\begin{aligned}
2(\boldsymbol{n}\cdot\boldsymbol{\sigma}(\boldsymbol{v}_h), [\boldsymbol{v}_h])_e &\le 2\|\boldsymbol{n}\cdot\boldsymbol{\sigma}(\boldsymbol{v}_h)\|_{0,e}\|[\boldsymbol{v}_h]\|_{0,e} \\
&\le \delta h\|\frac{1}{\sqrt{\mu+\lambda}}\boldsymbol{n}\cdot\boldsymbol{\sigma}(\boldsymbol{v}_h)\|_{0,e}^2 + \frac{4}{\delta h}\|\sqrt{\mu+\lambda}[\boldsymbol{v}_h]\|_{0,e}^2 \\
&\le 2\delta h\left(\boldsymbol{n}\cdot\boldsymbol{\sigma}(\boldsymbol{v}_h), \boldsymbol{n}\cdot\boldsymbol{\epsilon}(\boldsymbol{v}_h)\right)_e + \frac{4}{\delta h}\|\sqrt{\mu+\lambda}[\boldsymbol{v}_h]\|_{0,e}^2.
\end{aligned} \tag{2.6.4}$$

Combining (2.6.4) with Lemma 2.5.3, we have

$$2\sum_{e\in\varepsilon_h^i}(\{\boldsymbol{n}\cdot\boldsymbol{\sigma}(\boldsymbol{v}_h)\}, [\boldsymbol{v}_h])_e \le \sum_{e\in\varepsilon_h^i} 2\delta h\left(\boldsymbol{n}\cdot\boldsymbol{\sigma}(\boldsymbol{v}_h), \boldsymbol{n}\cdot\boldsymbol{\epsilon}(\boldsymbol{v}_h)\right)_e + \sum_{e\in\varepsilon_h^i}\frac{4}{\delta h}\|\sqrt{\mu+\lambda}[\boldsymbol{v}_h]\|_{0,e}^2$$

$$\leq \sum_{T\in\mathcal{T}_h^i} C\delta\left(\boldsymbol{\sigma}(\boldsymbol{v}_h),\boldsymbol{\epsilon}(\boldsymbol{v}_h)\right)_e + \sum_{e\in\varepsilon_h^i}\frac{4}{\delta h}((\mu+\lambda)[\boldsymbol{v}_h],[\boldsymbol{v}_h])_e.$$

Finally,

$$\begin{aligned}
a_h(\boldsymbol{v}_h,\boldsymbol{v}_h) &= \sum_{T\in\mathcal{T}_h}\big(\boldsymbol{\sigma}(\boldsymbol{v}_h),\boldsymbol{\epsilon}(\boldsymbol{v}_h)\big)_T - 2\sum_{e\in\varepsilon_h^i}\big(\{\boldsymbol{\sigma}(\boldsymbol{v}_h)\cdot\boldsymbol{n}\},[\boldsymbol{v}_h]\big)_e \\
&\quad + \sum_{e\in\varepsilon_h^i} h^{-1}((\mu+\lambda)[\boldsymbol{v}_h],[\boldsymbol{v}_h])_e \\
&\geq \sum_{T\in\mathcal{T}_h}\big(\boldsymbol{\sigma}(\boldsymbol{v}_h),\boldsymbol{\epsilon}(\boldsymbol{v}_h)\big)_T - 2\sum_{T\in\mathcal{T}_h^i} C\delta\left(\boldsymbol{\sigma}(\boldsymbol{v}_h),\boldsymbol{\epsilon}(\boldsymbol{v}_h)\right)_e \\
&\quad - 2\sum_{e\in\varepsilon_h^i}\frac{4}{\delta h}((\mu+\lambda)[\boldsymbol{v}_h],[\boldsymbol{v}_h])_e + \sum_{e\in\varepsilon_h^i} h^{-1}((\mu+\lambda)[\boldsymbol{v}_h],[\boldsymbol{v}_h])_e.
\end{aligned}$$

Therefore, there exists κ such that $a_h(\boldsymbol{v}_h,\boldsymbol{v}_h)\geq\kappa\|\boldsymbol{v}_h\|_h^2$ by choosing a proper δ. □

Lemma 2.6.1. *For any* $\boldsymbol{u}\in\tilde{\boldsymbol{H}}^2(\Omega)$,

$$\|\boldsymbol{u}-I_h\boldsymbol{u}\|_h \lesssim h\|\boldsymbol{u}\|_{\widetilde{H}^2(\Omega)}. \tag{2.6.5}$$

Proof. Taking (2.6.1) into consideration, we derive

$$\begin{aligned}
\|\boldsymbol{u}-I_h\boldsymbol{u}\|_h^2 &= \sum_{T\in\mathcal{T}_h}\big(\boldsymbol{\sigma}(\boldsymbol{u}-I_h\boldsymbol{u}),\boldsymbol{\epsilon}(\boldsymbol{u}-I_h\boldsymbol{u})\big)_T \\
&\quad + \sum_{e\in\varepsilon_h^i} h^{-1}(\mu+\lambda)([\boldsymbol{u}-I_h\boldsymbol{u}],[\boldsymbol{u}-I_h\boldsymbol{u}])_e,
\end{aligned}\tag{2.6.6}$$

According to Lemma 2.5.3,

$$\sum_{T\in\mathcal{T}_h}\big(\boldsymbol{\sigma}(\boldsymbol{u}-I_h\boldsymbol{u}),\boldsymbol{\epsilon}(\boldsymbol{u}-I_h\boldsymbol{u})\big)_T \lesssim h^2\|\boldsymbol{u}\|^2_{\widetilde{H}^2(\Omega)}. \tag{2.6.7}$$

Therefore, we only need to estimate the last term in (2.6.6). By the standard trace inequality,

$$\begin{aligned}\|[\boldsymbol{u}-I_h\boldsymbol{u}]\|_{0,e}^2 &\leq (\|(\boldsymbol{u}-I_h\boldsymbol{u})|_{T_1}\|_{0,e}+\|(\boldsymbol{u}-I_h\boldsymbol{u})|_{T_2}\|_{0,e})^2\\ &\lesssim \sum_{i=1}^{2}|e||T_i|^{-1}(\|(\boldsymbol{u}-I_h\boldsymbol{u})\|_{0,T_i}+h\|\nabla(\boldsymbol{u}-I_h\boldsymbol{u})\|_{0,T_i})^2\\ &\lesssim \sum_{i=1}^{2}|e|(h\|\boldsymbol{u}\|_{\widetilde{H}^2(T_i)})^2. \end{aligned}\tag{2.6.8}$$

Combining (2.6.6), (2.6.7) with (2.6.8), we deduce the desired result. □

Theorem 2.6.2. *Let* $\boldsymbol{u}\in\tilde{\boldsymbol{H}}^2(\Omega)$ *and* $\boldsymbol{u}_h\in S_h(\Omega)$ *are the solutions of* (2.0.5) *and* (2.4.4)*, respectively. The inequality holds*

$$\|\boldsymbol{u}-\boldsymbol{u}_h\|_h\lesssim h\|\boldsymbol{u}\|_{\widetilde{H}^2(\Omega)}.\tag{2.6.9}$$

Proof. As needed, we quote the following second Strang lemma for the IFE solution,

$$\|\boldsymbol{u}-\boldsymbol{u}_h\|_h\lesssim \inf_{\forall\boldsymbol{v}_h\in S_{h,0}(\Omega)}\|\boldsymbol{u}-\boldsymbol{v}_h\|_h+\sup_{\forall\boldsymbol{w}_h\in S_{h,0}(\Omega)}\frac{|a_h(\boldsymbol{u},\boldsymbol{w}_h)-(\boldsymbol{f},\boldsymbol{w}_h)|}{\|\boldsymbol{w}_h\|_h}.\tag{2.6.10}$$

Consider the last term in (2.6.10), by Cauchy-Schwarz inequality and the standard trace theorem, we deduce that

$$\begin{aligned}&|a_h(\boldsymbol{u},\boldsymbol{w}_h)-(\boldsymbol{f},\boldsymbol{w}_h)|=\Big|\sum_{e\in\varepsilon_h^n}(\{\boldsymbol{n}\cdot\boldsymbol{\sigma}(\boldsymbol{u})\},[\boldsymbol{w}_h])_e\Big|\\ &\lesssim\Big|\sum_{e\in\varepsilon_h^n}(\boldsymbol{n}\cdot\boldsymbol{\sigma}(\boldsymbol{u})-\overline{\boldsymbol{n}\cdot\boldsymbol{\sigma}(\boldsymbol{u})},[\boldsymbol{w}_h])_e\Big|\lesssim h\|\boldsymbol{u}\|_{\widetilde{H}^2(\Omega)}\|\boldsymbol{w}_h\|_h.\end{aligned}\tag{2.6.11}$$

Furthermore, by Lemma (2.6.1),

$$\inf_{\forall\boldsymbol{v}_h\in S_{h,0}(\Omega)}\|\boldsymbol{u}-\boldsymbol{v}_h\|_h\lesssim h\|\boldsymbol{u}\|_{\widetilde{H}^2(\Omega)}.\tag{2.6.12}$$

Combining (2.6.12) with (2.6.10) and (2.6.11), the proof is completed. □

2.7 Numerical examples

We will give several numerical examples to show the performance of our partially penalized P_1/CR IFE method. Let $\Omega=(-1,1)\times(-1,1)$, we denote the approximation error of the IFE interpolation by $\boldsymbol{u}-\boldsymbol{I}_h\boldsymbol{u}$ and the IFE solution error by $\boldsymbol{u}-\boldsymbol{u}_h$, which are measured in L^2 and the energy norm.

2.7.1 Numerical examples with circle domains

Example 1. The domain Ω is divided into subdomains $\Omega^+=\{(x,y): r^2=x^2+y^2>r_0^2\}$ and $\Omega^-=\{(x,y): x^2+y^2<r_0^2\}$. The interface curve Γ is a circle with radius $r_0=\frac{\pi}{8}$. The exact solution is ($\alpha_1=5$ and $\alpha_2=7$)

$$\boldsymbol{u}(x,y))=\begin{pmatrix}u_1(x,y)\\u_2(x,y)\end{pmatrix}=\begin{cases}\begin{pmatrix}u_1^-(x,y)\\u_2^-(x,y)\end{pmatrix}=\begin{pmatrix}\frac{1}{\lambda^-}r^{\alpha_1}\\\frac{1}{\lambda^-}r^{\alpha_2}\end{pmatrix} & \text{in } \Omega^-,\\ \begin{pmatrix}u_1^+(x,y)\\u_2^+(x,y)\end{pmatrix}=\begin{pmatrix}\frac{1}{\lambda^+}r^{\alpha_1}+\left(\frac{1}{\lambda^-}-\frac{1}{\lambda^+}\right)r_0^{\alpha_1}\\\frac{1}{\lambda^+}r^{\alpha_2}+\left(\frac{1}{\lambda^-}-\frac{1}{\lambda^+}\right)r_0^{\alpha_2}\end{pmatrix} & \text{in } \Omega^+.\end{cases}$$

Table 2-1 The interpolation errors and the IFE solution errors with $\lambda^+=5$, $\lambda^-=1$, $\mu^+=10$, $\mu^-=2$.

$\frac{1}{h}$	$\Vert\boldsymbol{u}-\boldsymbol{I}_h\boldsymbol{u}\Vert_{L^2}$	order	$\Vert\boldsymbol{u}-\boldsymbol{I}_h\boldsymbol{u}\Vert_h$	order
16	1.25e-002		7.21e-001	
32	3.15e-003	1.994	3.64e-001	0.990
64	7.88e-004	1.998	1.82e-001	0.998
128	1.97e-004	1.999	9.13e-002	0.999
$\frac{1}{h}$	$\Vert\boldsymbol{u}-\boldsymbol{u}_h\Vert_{L^2}$	order	$\Vert\boldsymbol{u}-\boldsymbol{u}_h\Vert_h$	order
16	1.97e-002		8.74e-001	
32	3.31e-003	1.989	4.42e-001	0.989
64	8.36e-004	1.994	2.22e-001	0.997
128	2.11e-004	1.997	1.11e-001	0.999

Table 2-2 The interpolation errors and the IFE solution errors with $\lambda^+ = 100$, $\lambda^- = 1$, $\mu^+ = 200$, $\mu^- = 2$.

$\frac{1}{h}$	$\|\boldsymbol{u} - \boldsymbol{I}_h\boldsymbol{u}\|_{L^2}$	order	$\|\boldsymbol{u} - \boldsymbol{I}_h\boldsymbol{u}\|_h$	order
16	6.26e-002		3.85e-000	
32	1.57e-002	1.994	1.95e-000	0.986
64	3.93e-003	1.998	9.77e-001	0.998
128	9.84e-004	2.000	4.90e-001	0.999
$\frac{1}{h}$	$\|\boldsymbol{u} - \boldsymbol{u}_h\|_{L^2}$	order	$\|\boldsymbol{u} - \boldsymbol{u}_h\|_h$	order
16	7.83e-002		4.28e-000	
32	2.01e-002	1.969	2.19e-000	0.965
64	5.09e-003	1.989	1.11e-000	0.988
128	1.28e-003	1.997	5.56e-001	0.997

Table 2-3 The interpolation errors and the IFE solution errors with $\lambda^+ = 20000$, $\lambda^- = 10000$, $\mu^+ = 20$, $\mu^- = 10$.

$\frac{1}{h}$	$\|\boldsymbol{u} - \boldsymbol{I}_h\boldsymbol{u}\|_{L^2}$	order	$\|\boldsymbol{u} - \boldsymbol{I}_h\boldsymbol{u}\|_h$	order
16	3.13e-006		1.84e-004	
32	7.86e-007	1.994	9.29e-005	0.989
64	1.97e-007	1.998	4.67e-005	0.997
128	4.92e-008	2.000	2.34e-005	0.999
$\frac{1}{h}$	$\|\boldsymbol{u} - \boldsymbol{u}_h\|_{L^2}$	order	$\|\boldsymbol{u} - \boldsymbol{u}_h\|_h$	order
16	7.13e-004		3.18e-002	
32	1.89e-004	1.920	1.62e-002	0.971
64	4.81e-005	1.971	8.16e-003	0.991
128	1.21e-005	1.991	4.09e-003	0.997

In the first two tables, two different coefficient configurations are considered, small jump case $(\lambda^+, \lambda^-) = (5, 1)$, $(\mu^+, \mu^-) = (10, 2)$, and moderate jumps $(\lambda^+, \lambda^-) = (100, 1)$, $(\mu^+, \mu^-) = (200, 2)$. The Poisson ratios in two subdomains are $\nu^{\pm} = \frac{1}{6}$ so that the material is compressible. The IFE interpolation error and the IFE solution error are optimal in L^2 norm and the energy norm.

In Table 2-3, we set $(\lambda^+, \lambda^-) = (20000, 10000)$, $(\mu^+, \mu^-) = (20, 10)$ and the Poisson ratios are $\nu^+ = \nu^- \approx 0.4995$, which is corresponding to nearly incompressible case. The IFE interpolation error and the IFE solution error are also optimal. Moreover, we can observe that no locking phenomenon happens although the material is nearly incompressible.

2.7.2 Numerical examples with straight line

Table 2-4 The interpolation errors and the IFE solution errors with $x_0 = 1 - \frac{\pi}{300}$, $\lambda^+ = 2$, $\lambda^- = 1$, $\mu^+ = 3$, $\mu^- = 2$, $\nu^+ = 0.2$.

$\frac{1}{h}$	$\|\boldsymbol{u} - \boldsymbol{I}_h\boldsymbol{u}\|_{L^2}$	order	$\|\boldsymbol{u} - \boldsymbol{I}_h\boldsymbol{u}\|_h$	order
16	2.18e-003	1.988	1.74e-001	0.993
32	5.44e-004	1.998	8.73e-002	0.998
64	1.36e-004	2.002	4.38e-002	1.000
128	3.38e-005	2.007	2.19e-002	1.000
$\frac{1}{h}$	$\|\boldsymbol{u} - \boldsymbol{u}_h\|_{L^2}$	order	$\|\boldsymbol{u} - \boldsymbol{u}_h\|_h$	order
16	5.25e-003	1.916	2.09e-001	0.970
32	1.34e-003	1.974	1.05e-001	0.991
64	3.38e-004	1.984	5.28e-002	0.995
128	8.51e-005	1.990	2.65e-002	0.997

Example 2. The interface curve Γ is a vertical straight line $x = x_0$ that separates Ω into subdomains $\Omega^+ = \{(x,y)^t : x > x_0\}$ and $\Omega^- = \{(x,y)^t : x < x_0\}$. The exact solution is given by

$$\boldsymbol{u}(x,y) = \begin{cases} \begin{pmatrix} u_1^-(x,y) \\ u_2^-(x,y) \end{pmatrix} = \begin{pmatrix} \frac{1}{\lambda^- + 2\mu^-}(x - x_0)\cos(2xy) \\ \frac{1}{\mu^-}(x - x_0)\cos(2xy) \end{pmatrix} & \text{in } \Omega^-, \\ \begin{pmatrix} u_1^+(x,y) \\ u_2^+(x,y) \end{pmatrix} = \begin{pmatrix} \frac{1}{\lambda^+ + 2\mu^+}(x - x_0)\cos((x + x_0)y) \\ \frac{1}{\mu^+}(x - x_0)\cos((x + x_0)y) \end{pmatrix} & \text{in } \Omega^+. \end{cases}$$

Table 2-5 The interpolation errors and the IFE solution errors with $x_0 = 1 - \frac{\pi}{250}$, $\lambda^+ = 2000$, $\lambda^- = 1000$, $\mu^+ = 3$, $\mu^- = 1$, $\nu^+ \approx 0.4995$, $\nu^- \approx 0.4993$.

$\frac{1}{h}$	$\|\boldsymbol{u} - \boldsymbol{I}_h\boldsymbol{u}\|_{L^2}$	order	$\|\boldsymbol{u} - \boldsymbol{I}_h\boldsymbol{u}\|_h$	order
32	7.60e-004		1.65e-001	
64	1.88e-004	2.013	8.28e-002	0.998
128	4.69e-005	2.007	4.15e-002	0.999
$\frac{1}{h}$	$\|\boldsymbol{u} - \boldsymbol{u}_h\|_{L^2}$	order	$\|\boldsymbol{u} - \boldsymbol{u}_h\|_h$	order
32	6.07e-003		2.96e-001	
64	1.51e-003	2.012	1.50e-001	0.989
128	3.82e-004	1.999	7.51e-002	0.997

Table 2-6 The interpolation errors and the IFE solution errors with $x_0 = 0$ and $x_0 = \frac{e}{5}$. $\lambda^+ = 2$, $\lambda^- = 1$, $\mu^+ = 3$, $\mu^- = 2$.

Interface	$\frac{1}{h}$	$\|\boldsymbol{u} - \boldsymbol{I}_h\boldsymbol{u}\|_{L^2}$	order	$\|\boldsymbol{u} - \boldsymbol{I}_h\boldsymbol{u}\|_h$	order
$x_0 = 0$	32	3.43e-004		6.23e-002	
	64	8.59e-005	1.999	3.12e-002	0.999
	128	2.15e-005	2.000	1.56e-002	1.000
$x_0 = \frac{e}{5}$	32	4.30e-004		7.76e-002	
	64	1.17e-004	2.006	3.89e-002	0.999
	128	2.91e-005	2.005	1.95e-002	1.001
Interface	$\frac{1}{h}$	$\|\boldsymbol{u} - \boldsymbol{u}_h\|_{L^2}$	order	$\|\boldsymbol{u} - \boldsymbol{u}_h\|_h$	order
$x_0 = 0$	32	8.37e-004		9.67e-002	
	64	2.12e-004	1.990	4.86e-002	0.996
	128	5.33e-005	1.997	2.43e-002	0.999
$x_0 = \frac{e}{5}$	32	1.81e-003		1.88e-001	
	64	4.55e-004	1.998	9.32e-002	1.013
	128	1.15e-004	1.995	4.68e-002	0.998

In Tables 2-4 and 2-5, we set the interface $x_0 = -1 + \frac{\pi}{300}$ near the left boundary, $(\mu^+, \mu^-) = (3, 2)$, $(\lambda^+, \lambda^-) = (2, 1)$, and $x_0 = 1 - \frac{\pi}{250}$ near the right boundary, $(\mu^+, \mu^-) = (3, 1)$, $(\lambda^+, \lambda^-) = (2000, 1000)$, respectively. In Table 2-6, let $(\lambda^+, \lambda^-) = (2, 1)$, $(\mu^+, \mu^-) = (3, 2)$ and $(\nu^+, \nu^-) = (\frac{1}{5}, \frac{1}{6})$. The interface location varies from $x_0 = 0$ to $x_0 = \frac{e}{5}$. As can be seen, Convergence rates in L^2 norm and the energy norm confirm our error analysis.

2.7.3 Numerical examples with elliptic domain

Example 3. Ω is separated by an ellipse interface curve Γ into subdomains $\Omega^+ = \{(x, y)^t : x^2 + 4y^2 > r_0^2\}$ and $\Omega^- = \{(x, y)^t : x^2 + 4y^2 < r_0^2\}$. Let $r_0 = 0.2$, the exact solution is

$$\boldsymbol{u}(x, y)) = \begin{pmatrix} u_1(x, y) \\ u_2(x, y) \end{pmatrix} = \begin{cases} \begin{pmatrix} u_1^-(x, y) \\ u_2^-(x, y) \end{pmatrix} = \begin{pmatrix} \frac{1}{\lambda^- + 2\mu^-}\left(x^2 + 4y^2 - r_0^2\right) \\ \frac{1}{\mu^-}\left(x^2 + 4y^2 - r_0^2\right) \end{pmatrix} & \text{in } \Omega^-, \\ \begin{pmatrix} u_1^+(x, y) \\ u_2^+(x, y) \end{pmatrix} = \begin{pmatrix} \frac{1}{\lambda^+ + 2\mu^+}\left(x^2 + 4y^2 - r_0^2\right) \\ \frac{1}{\mu^+}\left(x^2 + 4y^2 - r_0^2\right) \end{pmatrix} & \text{in } \Omega^+. \end{cases}$$

Table 2-7 The interpolation errors and the IFE solution errors with $\lambda^+ = 100$, $\lambda^- = 1$, $\mu^+ = 200$, $\mu^- = 2$.

$\frac{1}{h}$	$\lVert\boldsymbol{u} - \boldsymbol{I}_h\boldsymbol{u}\rVert_{L^2}$	order	$\lVert\boldsymbol{u} - \boldsymbol{I}_h\boldsymbol{u}\rVert_h$	order
16	5.81e-003	2.014	2.95e-001	1.002
32	1.49e-003	1.960	1.49e-001	0.985
64	4.23e-004	1.818	7.68e-002	0.963
128	1.04e-004	2.029	3.85e-002	1.000

$\frac{1}{h}$	$\lVert\boldsymbol{u} - \boldsymbol{u}_h\rVert_{L^2}$	order	$\lVert\boldsymbol{u} - \boldsymbol{u}_h\rVert_h$	order
16	1.54e-002	1.948	5.48e-001	0.968
32	3.96e-003	1.963	2.77e-001	0.987
64	9.95e-004	2.001	1.39e-001	1.003
128	2.55e-004	1.972	6.98e-002	0.994

Table 2-7 presents the numerical results for the case $(\lambda^+, \lambda^-) = (100, 1)$, $(\mu^+, \mu^-) = (200, 2)$. We text nearly incompressible case in Table 2-8, where $(\lambda^+, \lambda^-) = (20000, 10000)$, $(\mu^+, \mu^-) = (20, 10)$, the Poisson ratios in subdomains are $\nu^+ = \nu^- \approx 0.4995$. The numerical results indicate that the convergence orders of the P_1/CR IFE method in L^2 norm and the energy norm are optimal, no matter the material is compressible or almost incompressible.

Table 2-8 The interpolation errors and the IFE solution errors with $\lambda^+ = 20000$, $\lambda^- = 10000$, $\mu^+ = 20$, $\mu^- = 10$.

$\frac{1}{h}$	$\|\boldsymbol{u} - \boldsymbol{I}_h\boldsymbol{u}\|_{L^2}$	order	$\|\boldsymbol{u} - \boldsymbol{I}_h\boldsymbol{u}\|_h$	order
16	5.02e-004	1.993	2.67e-002	1.000
32	1.27e-004	1.983	1.34e-002	0.992
64	3.17e-005	2.001	6.73e-003	0.999
128	8.24e-006	1.943	3.41e-003	0.985
$\frac{1}{h}$	$\|\boldsymbol{u} - \boldsymbol{u}_h\|_{L^2}$	order	$\|\boldsymbol{u} - \boldsymbol{u}_h\|_h$	order
16	6.99e-001	1.918	4.63e-000	0.970
32	1.79e-001	1.967	2.35e-000	0.984
64	4.54e-002	1.986	1.18e-000	0.993
128	1.15e-002	1.990	5.90e-001	0.995

In conclusion, we have developed a partially penalized IFE method for solving elasticity interface problems on triangular Cartesian meshes. The IFE basis functions are constructed according to the interface conditions. We prove that the P_1/CR IFE space has the optimal approximation capability. Moreover, the optimal error estimate of the IFE solution is derived. Finally, the numerical results confirm the rate of convergence is optimal in L^2 norm and the energy norm.

Chapter 3 A nonconforming enriched finite element methods for elasticity interface problems

We still consider the elasticity interface problem $(2.0.1)-(2.0.4)$. Let the pressure variable $p=-\lambda\mathrm{tr}(\boldsymbol{\epsilon}(\boldsymbol{u}))$, the elasticity interface problem in the mixed formulation can be written as

$$\begin{aligned} -\nabla\cdot(2\mu\boldsymbol{\epsilon}(\boldsymbol{u})-p\boldsymbol{I})=\boldsymbol{f} &\quad \text{in } \Omega^+\cup\Omega^-,\\ [\boldsymbol{u}]=\boldsymbol{0},\ [(2\mu\boldsymbol{\epsilon}(\boldsymbol{u})-p\boldsymbol{I})\boldsymbol{n}]=\boldsymbol{g} &\quad \text{on } \Gamma,\\ \boldsymbol{u}=\boldsymbol{0} &\quad \text{on } \partial\Omega. \end{aligned} \tag{3.0.1}$$

The Lamé parameters μ and λ are positive and discontinuous across the interface Γ, i.e.,

$$\begin{cases} \mu=\mu_i \\ \lambda=\lambda_i \end{cases} \text{in } \Omega_i,$$

where $\mu_i,\lambda_i\in W^{1,\infty}(\Omega_i)$, $i=1,2$.

An enriched finite element space based on the nonconforming P_1 finite element space is proposed for the velocity space and the extended P_0 finite element space is proposed for the pressure space. The main advantage of our method is that the new approximation space is independent of jump conditions. To overcome the difficult of the estimate of consistent error, we apply the super penalty method, which is proposed by Babuška and Zlǎmal in [9] and applied in [5, 19]. We can obtain the optimal convergence of finite element error by only adding the super penalty terms on the edges of interface elements.

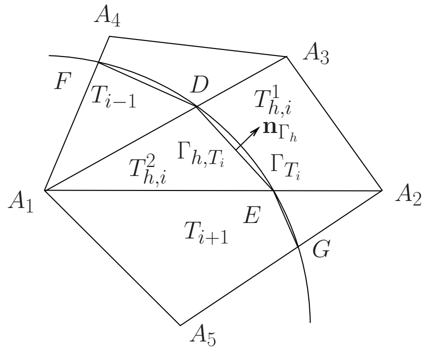

Figure 3-1 Three elements cut by the interface.

3.1 The nonconforming enriched finite element spaces

Define $\boldsymbol{U} = \boldsymbol{H}_0^1(\Omega)$ and $M = L_0^2(\Omega) = \{q \in L^2(\Omega) |\ \int_\Omega q dx = 0\}$. The space $\boldsymbol{U} \times M$ is equipped with the norm

$$\|(\boldsymbol{v}, q)\|_{\boldsymbol{U}\times M} = (|\boldsymbol{v}|_{H^1(\Omega)}^2 + \|q\|_{L^2(\Omega)}^2)^{1/2},\ \forall(\boldsymbol{v}, q) \in \boldsymbol{U} \times M.$$

Let $\boldsymbol{V}_h$ be the P_1-nonconforming FE space and $Q_h = \{q_h \in L_0^2(\Omega); q_h|_T \in P_0(T), \forall T \in \mathcal{T}_h\}$ be the piecewise constant space. For any triangle T^s which is intersected with the interface Γ (see Fig. 3-1), we construct a piecewise linear function

$$\psi_i = \begin{cases} a_i^+ x + b_i^+ y + c_i^+ & (x, y) \in T_{h,i}^+, \\ a_i^- x + b_i^- y + c_i^- & (x, y) \in T_{h,i}^- \end{cases}$$

determined by the following conditions

$$\begin{cases} \psi_i(A_j) = 0,\ \ 1 \le j \le 3, \\ [\psi_i(D)] = [\psi_i(E)] = 0, \\ [\dfrac{\partial \psi_i}{\partial \bar{\boldsymbol{n}}}] = 1. \end{cases}$$

As the technique developed in [65], let $\bar{\psi}_i$ be a piecewise continuous linear function in the three sub-triangles determined by the values at the points A_1, A_2, A_3, D and E

(see Fig. 3-2), i.e.,

$$\begin{cases} \bar{\psi}_i(A_j) = 0, \ \ 1 \le j \le 3, \\ \bar{\psi}_i(D) = (\psi_i(D) + \psi_{i-1}(D))/2, \\ \bar{\psi}_i(E) = (\psi_i(E) + \psi_{i+1}(E))/2. \end{cases}$$

We set the enrichment function $\bar{\psi}$ as

$$\bar{\psi}|_{T_i} = \begin{cases} \bar{\psi}_i & \text{if } T_i \in \mathcal{T}_h^i, \\ 0 & \text{if } T_i \notin \mathcal{T}_h^i. \end{cases}$$

With the desired function $\bar{\psi}$, we define a special space of shape functions by

$$\boldsymbol{\mathcal{P}}_1(T) = \{\boldsymbol{v}_h = \boldsymbol{z}_h \bar{\psi}|_T; \ \boldsymbol{z}_h \in \boldsymbol{P}_1(T)\}$$

for all $T \in \mathcal{T}_h$. The enrichment space can be defined as

$$\boldsymbol{V}_h^I = \{\boldsymbol{v}_h \in \boldsymbol{L}^2(\Omega); \ \boldsymbol{v}_h|_T \in \boldsymbol{\mathcal{P}}_1(T), \ [\boldsymbol{v}_h]|_{m_e} = 0, \ \forall e \in \varepsilon_h\},$$

where m_e is the midpoint of e. Notice that $\bar{\psi}$ vanishes if $T \notin \mathcal{T}_h^i$, the support of the functions in $\boldsymbol{V}_h^I$ is in Ω_h^I, the neighbourhood domain of the interface. Now we define the enriched finite element spaces for the displacement and pressure as follows

$$\begin{aligned} &\boldsymbol{U}_h = \boldsymbol{V}_h \oplus \boldsymbol{V}_h^I, \\ &M_h = \{q_h \in L_0^2(\Omega); \ q_h = q_h^+ \chi^+ + q_h^- \chi^-, \ q_h^+, q_h^- \in Q_h\}, \end{aligned}$$

where χ_i represents the characteristic function, i.e.,

$$\chi^s = \begin{cases} 1, & (x, y) \in \Omega^s, \\ 0, & (x, y) \in \Omega \backslash \Omega^s. \end{cases}$$

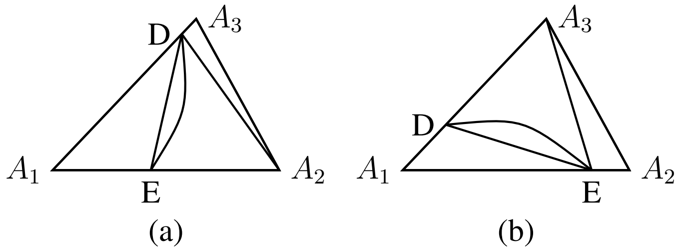

Figure 3-2 The sub-triangulation of an interface element $\triangle A_1A_2A_3$. (a) The case of $\frac{|A_1E|}{|A_1A_2|} \leq \frac{|A_1D|}{|A_1A_3|}$. (b) The case of $\frac{|A_1E|}{|A_1A_2|} \geq \frac{|A_1D|}{|A_1A_3|}$.

Observe that $\boldsymbol{V}_h \times Q_h \subset \boldsymbol{U}_h \times M_h$, therefore $\boldsymbol{U}_h \times M_h$ can be viewed as an enriched space of $\boldsymbol{V}_h \times Q_h$.

Let $Q_h(\Omega^s_{h,F})$ be the P_0 finite element space defined on $\Omega^s_{h,F}$, i.e.,

$$Q_h(\Omega^s_{h,F}) = \{p_h \in L^2(\Omega^s_{h,F}); p_h|_T \in P_0(T),\ \forall T \subset \Omega^s_{h,F}\},\ \ s = +, -.$$

A given function $p_h \in M_h$ uniquely determines a pair $(p_h^-, p_h^+) \in Q_h(\Omega^-_{h,E}) \times Q_h(\Omega^+_{h,E})$ such that

$$p_h^s = p_h,\ \ s = +, -.$$

The continuous variational problem for (3.0.1) reads as follows: find $(\boldsymbol{u}, p) \in \boldsymbol{U} \times M$ such that

$$\begin{cases} a(\boldsymbol{u}, \boldsymbol{v}) - b(\boldsymbol{v}, p) = f(\boldsymbol{v}) \ \ \forall \boldsymbol{v} \in \boldsymbol{U}, \\ b(\boldsymbol{u}, q) + c(p, q) = 0 \qquad \forall q \in M, \end{cases} \tag{3.1.1}$$

where

$$a(\boldsymbol{u}, \boldsymbol{v}) = (\mu\boldsymbol{\epsilon}(\boldsymbol{u}), \boldsymbol{\epsilon}(\boldsymbol{v})),\ \ b(\boldsymbol{v}, q) = (\nabla\cdot\boldsymbol{v}, q),$$

$$\langle \boldsymbol{g}, \boldsymbol{v}\rangle_\Gamma = \int_\Gamma \boldsymbol{g} \cdot \boldsymbol{v} ds,\ \ c(p, q) = (\tfrac{1}{\lambda}p, q),\ \ f(\boldsymbol{v}) = (\boldsymbol{f}, \boldsymbol{v}) + \langle \boldsymbol{g}, \boldsymbol{v}\rangle_\Gamma.$$

Define

$$A((\boldsymbol{u}, p), (\boldsymbol{v}, q)) = a(\boldsymbol{u}, \boldsymbol{v}) - b(\boldsymbol{v}, p) + b(\boldsymbol{u}, q) + c(p, q),$$

$$F((\boldsymbol{v},q)) = f(\boldsymbol{v}).$$

The problem (3.1.1) equals: find $(\boldsymbol{u},p) \in \boldsymbol{U} \times M$ such that

$$A((\boldsymbol{u},p),(\boldsymbol{v},q)) = F((\boldsymbol{v},q)) \;\; \forall(\boldsymbol{v},q) \in \boldsymbol{U} \times M. \tag{3.1.2}$$

In order to extend the definition of bilinear forms $a(\cdot,\cdot)$ and $b(\cdot,\cdot)$ to $(\boldsymbol{U}+\boldsymbol{U}_h)\times(\boldsymbol{U}+\boldsymbol{U}_h)$ and $(\boldsymbol{U}+\boldsymbol{U}_h)\times M$ respectively, we rewrite the definitions of $a(\cdot,\cdot)$ and $b(\cdot,\cdot)$ as

$$a(\boldsymbol{u},\boldsymbol{v}) = (\mu\boldsymbol{\epsilon}_h(\boldsymbol{u}),\boldsymbol{\epsilon}_h(\boldsymbol{v})),$$

$$b(\boldsymbol{v},q) = (\nabla_h\cdot\boldsymbol{v},q),$$

where $(\nabla_h\boldsymbol{v})|_T = \nabla(\boldsymbol{v}|_T)$ and $(\nabla_h\cdot\boldsymbol{v})|_T = \nabla\cdot(\boldsymbol{v}|_T)$ are the discrete gradient and divergence operators for all $T \in \mathcal{T}_h$. Similarly, $\boldsymbol{\epsilon}_h(\boldsymbol{v})|_T = \boldsymbol{\epsilon}(\boldsymbol{v}|_T)$.

The discrete variational problem is: find $(\boldsymbol{u}_h,p_h) \in \boldsymbol{U}_h \times M_h$ such that

$$\begin{cases} a_h(\boldsymbol{u}_h,\boldsymbol{v}_h) - b_h(\boldsymbol{v}_h,p_h) = f(\boldsymbol{v}_h) \quad \forall\boldsymbol{v}_h \in \boldsymbol{U}_h, \\ b_h(\boldsymbol{u}_h,q_h) + c(p_h,q_h) + \gamma j_h(p_h,q_h) = 0 \quad \forall q_h \in M_h, \end{cases} \tag{3.1.3}$$

where

$$a_h(\boldsymbol{u}_h,\boldsymbol{v}_h) = \sum_{T\in\mathcal{T}_h}(\mu\boldsymbol{\epsilon}_h(\boldsymbol{u}),\boldsymbol{\epsilon}_h(\boldsymbol{v}))_T + h^{-1}\sum_{e\in\varepsilon_h^n}\mu\langle[\boldsymbol{u}_h],[\boldsymbol{v}_h]\rangle_e + h^{-2}\sum_{e\in\varepsilon_h^i}\mu\langle[\boldsymbol{u}_h],[\boldsymbol{v}_h]\rangle_e,$$

$$b_h(\boldsymbol{v}_h,q_h) = \sum_{T\in\mathcal{T}_h}(\nabla\cdot\boldsymbol{v}_h,q_h)_T$$

and the stabilization term (see [39]) is defined as

$$j_h(p_h,q_h) = \sum_{i=1}^{2} j^s(p_h^s,q_h^s) = \sum_{s=+,-}\sum_{e\in\varepsilon_h^i} h\langle[p_h^s],[q_h^s]\rangle_e. \tag{3.1.4}$$

Furthermore, we define

$$A_h((\boldsymbol{u}_h, p_h), (\boldsymbol{v}_h, q_h)) = a_h(\boldsymbol{u}_h, \boldsymbol{v}_h) - b_h(\boldsymbol{v}_h, p_h) + b_h(\boldsymbol{u}_h, q_h) + c(p_h, q_h) + \gamma j_h(p_h, q_h).$$

The problem (3.1.3) equals: find $(\boldsymbol{u}_h, p_h) \in \boldsymbol{U}_h \times M_h$ such that

$$A_h((\boldsymbol{u}_h, p_h), (\boldsymbol{v}_h, q_h)) = F((\boldsymbol{v}_h, q_h)) \ \ \forall (\boldsymbol{v}_h, q_h) \in \boldsymbol{U}_h \times M_h. \tag{3.1.5}$$

3.2 Stability analysis

Define norms for the spaces $\boldsymbol{U}_h$, M_h and $\boldsymbol{U}_h \times M_h$

$$\|\boldsymbol{v}_h\|_h = a_h^{\frac{1}{2}}(\boldsymbol{v}_h, \boldsymbol{v}_h), \ \ \forall \boldsymbol{v}_h \in \boldsymbol{U}_h, \tag{3.2.1}$$

$$\|q_h\|_{0,h} = (\|q_{h,1}\|^2_{L^2(\Omega^-_{h,E})} + \|q_{h,2}\|^2_{L^2(\Omega^+_{h,E})})^{1/2}, \ \ \forall q_h \in M_h, \tag{3.2.2}$$

$$\|(\boldsymbol{v}_h, q_h)\|_H = (\|\boldsymbol{v}_h\|^2_h + \|q_h\|^2_{0,h})^{1/2}, \ \ \forall (\boldsymbol{u}_h, p_h) \in \boldsymbol{U}_h \times M_h. \tag{3.2.3}$$

Lemma 3.2.1. *For any $\mathbf{v}_h \in \boldsymbol{U}_h$, there exists a constant C_μ such that*

$$a_h(\boldsymbol{v}_h, \boldsymbol{v}_h) \geq C_\mu \|\boldsymbol{v}_h\|^2_h. \tag{3.2.4}$$

Proof. It is equal to prove $\|\boldsymbol{v}_h\|_{\boldsymbol{U}_h}$ is a norm. By Korn's inequality for piecewise H^1 vector fields (see [15]), the inequality holds,

$$\|\nabla_h \boldsymbol{v}_h\|_{L^2(\Omega)} \lesssim \|\boldsymbol{\epsilon}_h(\boldsymbol{v}_h)\|_{L^2(\Omega)} + \big|\sum_{T\in\mathcal{T}_h} \int_T \nabla \times \boldsymbol{v}_h dx\big|. \tag{3.2.5}$$

Furthermore,

$$\begin{aligned}
\big|\sum_{T\in\mathcal{T}_h} \int_T \nabla \times \boldsymbol{v}_h dx\big| &= \big|\sum_{T\in\mathcal{T}_h} \int_{\partial T} \boldsymbol{v}_h \cdot \boldsymbol{\tau} dx\big| = \big|\sum_{e\in\varepsilon_h} \int_e [\boldsymbol{v}_h] \cdot \boldsymbol{\tau} dx\big| \\
&\lesssim \sum_{e\in\varepsilon_h} h^{\frac{1}{2}} \|[\boldsymbol{v}_h]\|_{L^2(e)} \lesssim \Big(\sum_{e\in\varepsilon_h} \|[\boldsymbol{v}_h]\|^2_{L^2(e)}\Big)^{\frac{1}{2}} \Big(\sum_{e\in\varepsilon_h} h\Big)^{\frac{1}{2}}
\end{aligned}$$

$$
\begin{aligned}
&\lesssim \Big(h^{-1}\sum_{e\in\varepsilon_h^i\cup\varepsilon_h^n}\|[\boldsymbol{v}_h]\|^2_{L^2(e)}\Big)^{\frac{1}{2}} \\
&\lesssim \Big(h^{-1}\sum_{e\in\varepsilon_h^n}\|[\boldsymbol{v}_h]\|^2_{L^2(e)}\Big)^{\frac{1}{2}} + \Big(h^{-1}\sum_{e\in\varepsilon_h^i}\|[\boldsymbol{v}_h]\|^2_{L^2(e)}\Big)^{\frac{1}{2}}, \qquad (3.2.6)
\end{aligned}
$$

where we use

$$
\sum_{e\in\varepsilon_h} 1 = O(h^{-2}), \qquad \int_e [\boldsymbol{v}_h]\cdot\boldsymbol{\tau}dx = 0
$$

for any $e \in \partial\Omega$. Then, combining (3.2.5) with (3.2.6), we obtain

$$
\|\nabla_h \boldsymbol{v}_h\|_{L^2(\Omega)} \lesssim \|\boldsymbol{v}_h\|_h.
$$

The proof is completed. □

Moveover, we can show the continuity of the bilinear form $a_h(\cdot,\cdot)$.

Theorem 3.2.1. *For any $(\boldsymbol{v}_h, q_h), (\boldsymbol{\omega}_h, \lambda_h) \in \boldsymbol{U}_h \times M_h$, there exits a constant C_μ which only depends on μ, such that*

$$
A_h((\boldsymbol{v}_h, q_h), (\boldsymbol{\omega}_h, \lambda_h)) \le C_\mu \|(\boldsymbol{v}_h, q_h)\|_H \|(\boldsymbol{\omega}_h, \lambda_h)\|_H. \qquad (3.2.7)
$$

Similarly, for any $(\boldsymbol{v}, q), (\boldsymbol{\omega}, \lambda) \in (\boldsymbol{U} + \boldsymbol{U}_h) \times M$, it holds that

$$
A((\boldsymbol{v}, q), (\boldsymbol{\omega}, \lambda)) \le C_\mu \|(\boldsymbol{v}, q)\|_H \|(\boldsymbol{\omega}, \lambda)\|_H. \qquad (3.2.8)
$$

Proof. By Cauchy-Schwarz inequality and the trace inequality, we can deduce that

$$
\begin{aligned}
j_h(q_h, \lambda_h) &= h\sum_{i=1}^{2}\sum_{e\in\mathcal{F}_i}\langle [q_{h,i}], [\lambda_{h,i}]\rangle_e \lesssim h\sum_{i=1}^{2}\sum_{e\in\mathcal{F}_i}\|[q_{h,i}]\|_{L^2(e)}\|[\lambda_{h,i}]\|_{L^2(e)} \\
&\lesssim \sum_{i=1}^{2}\sum_{e\in\mathcal{F}_i}\Big(\sum_{k=1}^{2}\|q_{h,i}\|^2_{L^2(T_{e,k})}\Big)^{1/2}\Big(\sum_{k=1}^{2}\|\lambda_{h,i}\|^2_{L^2(T_{e,k})}\Big)^{1/2} \qquad (3.2.9) \\
&\lesssim \|q_h\|_{M_h}\|\lambda_h\|_{M_h}.
\end{aligned}
$$

Then, using Cauchy-Schwarz inequality again,

$$
\begin{aligned}
&A_h((\boldsymbol{v}_h, q_h), (\boldsymbol{\omega}_h, \lambda_h)) \\
&= a_h(\boldsymbol{v}_h, \boldsymbol{\omega}_h) - b_h(\boldsymbol{\omega}_h, q_h) + b_h(\boldsymbol{v}_h, \lambda_h) + c(q_h, \lambda_h) + \gamma j_h(q_h, \lambda_h) \\
&\lesssim C_\mu \|\boldsymbol{v}_h\|_{\boldsymbol{U}_h} \|\boldsymbol{\omega}_h\|_{\boldsymbol{U}_h} + \|q_h\|_{M_h} \|\boldsymbol{\omega}_h\|_{\boldsymbol{U}_h} + \|\lambda_h\|_{M_h} \|\boldsymbol{v}_h\|_{\boldsymbol{U}_h} + \|q_h\|_{M_h} \|\lambda_h\|_{M_h} \\
&\leq C_\mu \|(\boldsymbol{v}_h, q_h)\|_{\boldsymbol{U}_h \times M_h} \|(\boldsymbol{\omega}_h, \lambda_h)\|_{\boldsymbol{U}_h \times M_h}.
\end{aligned}
\tag{3.2.10}
$$

The above inequality uses the assumption that λ_i $(i = 1, 2)$ has a positive lower bound. Thus, (3.2.7) is proved. (3.2.8) can be obtained by using the same argument. □

Define a piecewise constant

$$
\lambda_0 = \begin{cases} |\Omega^-|^{-1} & \text{in } \Omega^-, \\ -|\Omega^+|^{-1} & \text{in } \Omega^+. \end{cases}
$$

One can easily verifies that $\lambda_0 \in M_h$. Let $M_0 = span\{\lambda_0\}$ be a one-dimensional subspace of M_h. Then the pressure space M_h can be decomposed as

$$
M_h = M_0 \oplus M_0^\perp,
$$

where $M_0^\perp$ is the orthogonal complement of M_0. It is easy to prove that

$$
M_0^\perp = \{q_h \in M_h; \int_{\Omega^-} q_h dx = \int_{\Omega^+} q_h dx = 0\}.
$$

Denote the nonconforming P_1-P_0 element space pair on $\Omega_{h,i}^-$ by $\boldsymbol{V}_h(\Omega_{h,F}^s) \times Q_{h,0}(\Omega_{h,F}^s)$, where $(s = +, -)$

$$
\begin{aligned}
&\boldsymbol{V}_h(\Omega_{h,F}^s) = \{\boldsymbol{w}_h \in (L^2(\Omega_{h,F}^s))^2; \boldsymbol{w}_h|_T \in P_1(T), \int_e [\boldsymbol{w}_h] ds = 0\}, \\
&Q_{h,0}(\Omega_{h,F}^s) = Q_h(\Omega_{h,F}^s) \cap L_0^2(\Omega_{h,F}^s).
\end{aligned}
$$

Then, we can obtain the LBB inf-sup property.

Lemma 3.2.2. *There exists a function $\boldsymbol{z}_h \in \boldsymbol{V}_h(\Omega^s_{h,F})$ such that*

$$\inf_{\boldsymbol{z}_h\in\boldsymbol{V}_h(\Omega^s_{h,F})} \frac{(\nabla_h\cdot\boldsymbol{z}_h, q_h)_{\Omega^s_{h,F}}}{\|\nabla_h\boldsymbol{z}_h\|_{L^2(\Omega^s_{h,F})}} \geq C_\Omega\|q_h\|_{L^2(\Omega^s_{h,F})}, \quad \forall q_h \in Q_{h,0}(\Omega^s_{h,F}). \tag{3.2.11}$$

Proof. For any given $q \in Q_{h,0}(\Omega^s_{h,F})$, we first extend q on the domain Ω, such that

$$\bar{q} = \begin{cases} q, & \Omega^s_{h,F}, \\ 0, & \Omega/\Omega^s_{h,F}. \end{cases}$$

We can see $\bar{q} \in Q_{h,0}(\Omega)$. Then, there exists a unique $w \in H^2(\Omega)$ satisfying

$$\begin{cases} -\Delta w = \bar{q}, & in\ \Omega, \\ \dfrac{\partial w}{\partial n} = 0, & on\ \partial\Omega \end{cases}$$

with $\int_\Omega w dx = 0$. Moveover, by lemma in [17], there exists a $\boldsymbol{v} \in \boldsymbol{H}^1_0(\Omega)$, such that $\nabla\cdot\boldsymbol{v} = \bar{q}$.

Let $\Pi^{CR} : \boldsymbol{H}^2(\Omega)\cap\boldsymbol{H}^1_0(\Omega) \to \boldsymbol{V}_h$ be the standard CR element interpolation operator, and P_h be the L^2 projection operator. Since the operator $\nabla\cdot : \boldsymbol{V}_h \mapsto Q_h$ is surjection, we derive that

$$div(\boldsymbol{v}_h) = P_h(div\boldsymbol{v}) = P_h\bar{q} = \bar{q}, \tag{3.2.12}$$

where $\boldsymbol{v}_h = \Pi^{CR}\boldsymbol{v}$. Combining (3.2.12), the elliptic regularity with the stability of Π^{CR} operator, we can deduce

$$|\boldsymbol{v}_h|_{\Omega^s_{h,F}}|_{1,\Omega^s_{h,F}} \lesssim |\boldsymbol{v}_h|_{1,\Omega} \lesssim |\boldsymbol{v}|_{1,\Omega} = |w|_{2,\Omega} \leq C_\Omega\|\bar{q}\|_{0,\Omega} = C_\Omega\|q\|_{0,\Omega^s_{h,F}}. \tag{3.2.13}$$

Finally, from (3.2.12) and (3.2.13),

$$\frac{(\nabla_h\cdot\boldsymbol{v}_h, q_h)_{\Omega^s_{h,F}}}{\|\nabla_h\boldsymbol{v}_h\|_{L^2(\Omega^s_{h,F})}} \geq \frac{1}{C_\Omega}\|q_h\|_{L^2(\Omega^s_{h,F})}, \quad \forall q_h \in Q_{h,0}(\Omega^s_{h,F}).$$

The proof is completed. □

Now we derive a discrete inf-sup result for the bilinear form $A_h(\cdot,\cdot)$ w.r.t. the space $\boldsymbol{U}_h \times M_h$. The analysis is along the lines as in [39, 48].

Lemma 3.2.3. *For any $q_0 \in M_0$, if h is sufficiently small, there exists a function $\boldsymbol{w}_h \in V_h$ such that*

$$
\begin{aligned}
b(\boldsymbol{w}_h, q_0) &\gtrsim \|q_0\|_{0,h}^2, \\
\|\boldsymbol{w}_h\|_h &\lesssim \|q_0\|_{0,h}.
\end{aligned}
\tag{3.2.14}
$$

Proof. Since M_0 is the one-dimensional subspace of M_h, it is sufficient to prove (3.2.14) holds for the piecewise constant function λ_0. Let

$$
\lambda_h = P_h\lambda_0 - |\Omega|^{-1}\int_\Omega P_h\lambda_0 dx,
$$

where P_h is the L^2 projection operator from M_0 to Q_h. We can easily verify that $\lambda_h \in Q_h$. By direct calculation,

$$
\begin{aligned}
\|\lambda_0 - \lambda_h\|_{L^2(\Omega)} &= \|\lambda_0 - P_h\lambda_0 + |\Omega|^{-1}\int_\Omega (P_h\lambda_0 - \lambda_0)dx\|_{L^2(\Omega)} \\
&\lesssim \|\lambda_0 - P_h\lambda_0\|_{L^2(\Omega)} = \|\lambda_0 - P_h\lambda_0\|_{L^2(\Omega_h^I)} \\
&\lesssim \|\lambda_0\|_{L^\infty(\Omega_h^I)}|\Omega_h^I|^{1/2} \lesssim h^{1/2}.
\end{aligned}
\tag{3.2.15}
$$

Note that $\|\lambda_0\|_{L^2(\Omega)} = O(1)$, by the triangle inequality, we conclude that $\|\lambda_h\|_{L^2(\Omega)} = O(1)$. If h is sufficiently small, we also derive that $\|\lambda_0\|_{0,h} = O(1)$. Since the finite element pair $\boldsymbol{V}_h \times Q_h$ is inf-sup stable, there exists a function $\boldsymbol{w}_h \in \boldsymbol{V}_h$ such that

$$
\begin{aligned}
b_h(\boldsymbol{w}_h, \lambda_h) = (\nabla_h\cdot\boldsymbol{w}_h, \lambda_h) &\gtrsim \|\lambda_h\|_{L^2(\Omega)}^2, \\
\|\boldsymbol{w}_h\|_h &\lesssim \|\lambda_h\|_{L^2(\Omega)}.
\end{aligned}
$$

From (3.2.15), we deduce

$$
\|\boldsymbol{w}_h\|_h \lesssim \|\lambda_h\|_{L^2(\Omega)} \lesssim \|\lambda_0\|_{L^2(\Omega)} + \|\lambda_h - \lambda_0\|_{L^2(\Omega)} \lesssim \|\lambda_0\|_{L^2(\Omega)} + h^{1/2},
$$

and

$$\begin{aligned} b(\boldsymbol{w}_h, \lambda_0) &= b(\boldsymbol{w}_h, \lambda_h) + b(\boldsymbol{w}_h, \lambda_0 - \lambda_h) \\ &\gtrsim \|\lambda_h\|_{L^2(\Omega)}^2 - \sum_{T\in\mathcal{T}_h} (\mathrm{div}\boldsymbol{w}_h, \lambda_h - \lambda_0)_T \\ &\gtrsim \|\lambda_h\|_{L^2(\Omega)}^2 - h^{1/2}\|\boldsymbol{w}_h\|_h \gtrsim 1 - h^{1/2}. \end{aligned} \tag{3.2.16}$$

Using the fact $\|\lambda_0\|_{0,h} = O(1)$, we obtain

$$b(\boldsymbol{w}_h, \lambda_0) \gtrsim \|\lambda_0\|_{0,h}^2, \qquad \|\boldsymbol{w}_h\|_h \lesssim \|\lambda_0\|_{0,h},$$

which completes the proof. □

The following lemma shows the reason why we add the stabilization term.

Lemma 3.2.4. *For any $q_h^s \in Q_h(\Omega_{h,E}^s)$, we have*

$$\|q_{h,i}\|_{L^2(\Omega_{h,E}^s)}^2 \lesssim \|q_{h,i}\|_{L^2(\Omega_{h,F}^s)}^2 + j_i(q_h^s, q_h^s),\ s = +, -. \tag{3.2.17}$$

Proof. Note that

$$\|q_h^s\|_{L^2(\Omega_{h,E}^s)}^2 = \|q_h^s\|_{L^2(\Omega_{h,F}^s)}^2 + \sum_{T\in\mathcal{T}_h^I} \|q_h^s\|_{L^2(T)}^2.$$

For any $T_0 \in \mathcal{T}_h^i$, there exists a sequence $\{T_j\}_{j=1}^k$ with edges $e_j = \bar{T}_j \cap \bar{T}_{j-1}, j = 1, \cdots, k$, and $T_k \in \Omega_{h,F}^s$, we have the relation

$$q_h^s|_{T_0} = q_h^s|_{T_k} + \sum_{j=1}^k [q_h^s]|_{e_j}.$$

Since $\mathcal{T}_h$ is a regular and quasi-uniform triangulation of Ω, it yields

$$\|q_h^s\|_{L^2(T_0)}^2 \lesssim \|q_h^s\|_{L^2(T_k)}^2 + \sum_{j=1}^k h\|[q_h^s]\|_{L^2(e_j)}^2 = \|q_h^s\|_{L^2(T_k)}^2 + j^s(q_h^s, q_h^s).$$

Summing over $T_0 = T \in \mathcal{T}_h^i$ and using a finite overlap argument, we have

$$\sum_{T\in\mathcal{T}_h^i} \|q_h^s\|_{L^2(T)}^2 \lesssim \|q_h^s\|_{L^2(\Omega_{h,F}^s)}^2 + j^s(q_h^s, q_h^s),$$

which completes the proof. □

Lemma 3.2.5. *For any $q_0^\perp \in M_0^\perp$, if h is sufficiently small, there exists a function $\boldsymbol{z}_h \in \boldsymbol{V}_h$ such that*

$$\begin{aligned} b(\boldsymbol{z}_h, q_0^\perp) &\gtrsim \|q_0^\perp\|_{0,h}^2 - C_1 j_h(q_0^\perp, q_0^\perp), \\ \|\boldsymbol{z}_h\|_h &\lesssim \|q_0^\perp\|_{0,h}, \end{aligned} \tag{3.2.18}$$

where C_1 is a positive constant independent of h and the location of interface relative to the mesh.

Proof. Let $q^s = q_0^\perp - \alpha^s$, where $\alpha^s = |\Omega_{h,F}^s|^{-1}\int_{\Omega_{h,F}^s} q_0^\perp dx$. We can derive $\int_{\Omega_{h,F}^s} q^s dx = 0$ and

$$\begin{aligned} \|\alpha^s\|_{L^2(\Omega_{h,E}^s)} &= |\Omega_{h,E}^s|^{1/2}|\Omega_{h,F}^s|^{-1}|\int_{\Omega_{h,F}^s} q_0^\perp dxdy| \lesssim |\int_{\Omega_{h,F}^s} q_0^\perp dxdy| \\ &= |\int_{\Omega^s\setminus\Omega_{h,F}^s} q_0^\perp dxdy| \lesssim h^{1/2}\|q_0^\perp\|_{L^2(\Omega^s\setminus\Omega_{h,F}^s)} \\ &\lesssim h^{1/2}\|q_0^\perp\|_{L^2(\Omega_{h,E}^s)}. \end{aligned} \tag{3.2.19}$$

By Lemma 3.2.2, there exists $\boldsymbol{z}_{h,i} \in \boldsymbol{V}_h$ that corresponds to q_i $(i = 1, 2)$ that satisfies

$$\begin{aligned} (\nabla_h\cdot\boldsymbol{z}_{h,i}|_{\Omega_{h,i}^-}, q_i)_{L^2(\Omega_{h,i}^-)} &\gtrsim \|q_i\|_{L^2(\Omega_{h,i}^-)}^2, \\ \|\nabla_h\boldsymbol{z}_{h,i}\|_{L^2(\Omega)} &\lesssim \|q_i\|_{L^2(\Omega_{h,i}^-)}. \end{aligned} \tag{3.2.20}$$

Using Lemma 3.2.4, we obtain

$$\|q^s\|_{L^2(\Omega_{h,E}^s)}^2 \lesssim \|q^s\|_{L^2(\Omega_{h,F}^s)}^2 + j^s(q^s, q^s). \tag{3.2.21}$$

Form (3.2.19), the following inequality holds

$$\|q^s\|^2_{L^2(\Omega^s_{h,E})} \gtrsim \|q_0^\perp\|^2_{L^2(\Omega^s_{h,E})} - \|\alpha^s\|^2_{L^2(\Omega^s_{h,E})} \geq \|q_0^\perp\|^2_{L^2(\Omega^s_{h,E})}(1 - Ch). \tag{3.2.22}$$

By (3.1.4),

$$j^s(q^s, q^s) = j^s(q_0^\perp - \alpha^s, q_0^\perp - \alpha^s) = j^s(q_0^\perp, q_0^\perp). \tag{3.2.23}$$

Let $\boldsymbol{z}_h = \boldsymbol{z}_h^+ + \boldsymbol{z}_h^-$, combining with (3.2.20)-(3.2.23), if h is sufficiently small, we deduce that

$$\begin{aligned} b(\boldsymbol{z}_h, q_0^\perp) &= (\nabla_h \cdot \boldsymbol{z}_h^-, q_0^\perp)_{\Omega^-_{h,F}} + (\nabla_h \cdot \boldsymbol{z}_h^+, q_0^\perp)_{\Omega^+_{h,F}} \gtrsim \|q^-\|^2_{L^2(\Omega^-_{h,F})} + \|q^+\|^2_{L^2(\Omega^+_{h,F})} \\ &\gtrsim \|q^-\|^2_{L^2(\Omega^+_{h,E})} - C_1 j^-(q^-, q^-) + \|q^+\|^2_{L^2(\Omega^-_{h,E})} - C_1 j^+(q^+, q^+) \\ &\gtrsim \|q_0^\perp\|^2_{0,h} - C_1 j_h(q_0^\perp, q_0^\perp). \end{aligned}$$

By the triangle inequality,

$$\|q^s\|_{L^2(\Omega^s_{h,F})} \leq \|q_0^\perp\|_{L^2(\Omega^s_{h,F})} + \|\alpha^s\|_{L^2(\Omega^s_{h,F})} \lesssim \|q_0^\perp\|_{L^2(\Omega^s_{h,F})}. \tag{3.2.24}$$

Moreover,

$$\begin{aligned} \|\boldsymbol{z}_h\|^2_{\boldsymbol{U}_h} &= a_h(\boldsymbol{z}_h, \boldsymbol{z}_h) = \|\nabla_h \boldsymbol{z}_h^+ + \nabla_h \boldsymbol{z}_h^-\|^2_{L^2(\Omega)} \\ &\lesssim \|q_1\|^2_{L^2(\Omega^+_{h,F})} + \|q_2\|^2_{L^2(\Omega^-_{h,F})} \lesssim \|q_0^\perp\|^2_{L^2(\Omega^+_{h,F})} + \|q_0^\perp\|^2_{L^2(\Omega^-_{h,F})} \leq \|q_0^\perp\|^2_{0,h}, \end{aligned}$$

where we use the fact $\int_e [\boldsymbol{z}_h] ds = 0$ for any $e \in \varepsilon_h$. The proof is completed. □

Lemma 3.2.6. *For sufficiently small h and any $q_h \in M_h$, there exists a function $\boldsymbol{v}_h \in \boldsymbol{U}_h$ such that*

$$\begin{aligned} b(\boldsymbol{v}_h, q_h) &\gtrsim \|q_h\|^2_{0,h} - C_2 j_h(q_h, q_h), \\ \|\boldsymbol{v}_h\|_h &\lesssim \|q_h\|_{0,h}, \end{aligned} \tag{3.2.25}$$

where C_2 is a positive constant independent of h and the location of interface relative to the mesh.

Proof. For any $q_h \in M_h$, we have the following orthogonal decomposition

$$q_h = q_0 + q_0^{\perp},$$

where $q_0 \in M_0$, $q_0^{\perp} \in M_0^{\perp}$. Let $\boldsymbol{w}_h$ and $\boldsymbol{z}_h$ be such that Lemma 3.2.3 and Lemma 3.2.5 are satisfied respectively. Define $\boldsymbol{v}_h = \boldsymbol{w}_h + \alpha \boldsymbol{z}_h$, where $\alpha > 0$ is a constant. By Lemma 3.2.2 and Lemma 3.2.5, we note that

$$\begin{aligned} b(\boldsymbol{z}_h, q_0) &= \int_{\Omega} \nabla \cdot (\boldsymbol{z}_h^- + \boldsymbol{z}_h^+) q_0 dx = \int_{\Omega_{h,F}^-} q^- q_0 dx + \int_{\Omega_{h,F}^+} q^+ q_0 dx \\ &= \int_{\Omega_{h,F}^-} (q_0^{\perp} - \alpha_1) q_0 dx + \int_{\Omega_{h,F}^+} (q_0^{\perp} - \alpha_2) q_0 dx = 0. \end{aligned} \tag{3.2.26}$$

Thus, combining Lemma 3.2.3 with Lemma 3.2.5,

$$\begin{aligned} b(\boldsymbol{v}_h, q_h) &= b(\boldsymbol{w}_h, q_0) + b(\boldsymbol{w}_h, q_0^{\perp}) + \alpha b(\boldsymbol{z}_h, q_0^{\perp}) + \alpha b(\boldsymbol{z}_h, q_0^{\perp}) \\ &\gtrsim \|q_0\|_{0,h}^2 - C\|q_0\|_{0,h}\|q_0^{\perp}\|_{0,h} + \alpha\|q_0^{\perp}\|_{0,h}^2 - \alpha C_1 j_h(q_0^{\perp}, q_0^{\perp}) \\ &= \frac{1}{2}(\|q_0\|_{0,h} - C\|q_0^{\perp}\|_{0,h})^2 + \frac{1}{2}\|q_0\|_{0,h}^2 + (\alpha - \frac{C^2}{2})\|q_0^{\perp}\|_{0,h}^2 \\ &\quad - \alpha C_1 j_h(q_0^{\perp}, q_0^{\perp}). \end{aligned}$$

Taking $\alpha = \frac{1+C^2}{2}$, the following result holds

$$b(\boldsymbol{v}_h, q_h) \gtrsim \|q_h\|_{0,h}^2 - C_2 j_h(q_0^{\perp}, q_0^{\perp}),$$

where $C_2 = \frac{(1+C^2)C_1}{2}$. Finally, we conclude that

$$\|\boldsymbol{v}_h\|_{\boldsymbol{U}_h} \le \|\boldsymbol{w}_h\|_h + \alpha\|\boldsymbol{z}_h\|_h \lesssim \|q_0\|_{0,h} + \|q_0^{\perp}\|_{0,h} \lesssim \|q_h\|_{0,h},$$

which completes the proof. □

Theorem 3.2.2. *If h is sufficient small, for any $(\boldsymbol{v}_h, q_h) \in \boldsymbol{U}_h \times M_h$, there exists a positive constant C_μ independent of h and the location of interface relative to the* *mesh such that*

$$\sup_{(\boldsymbol{\omega}_h,\lambda_h)\in \boldsymbol{U}_h\times M_h} \frac{A_h((\boldsymbol{v}_h,q_h),(\boldsymbol{\omega}_h,\lambda_h))}{\|(\boldsymbol{\omega}_h,\lambda_h)\|_H} \geq C_\mu \|(\boldsymbol{v}_h,q_h)\|_H. \tag{3.2.27}$$

Proof. Given $q_h \in M_h$, by Lemma 3.2.6, there exists a function $\boldsymbol{z}_h \in \boldsymbol{V}_h$ such that

$$b(\boldsymbol{z}_h,q_h) \gtrsim \|q_h\|_{M_h}^2 - C_2 j_h(q_h,q_h), \quad \|\boldsymbol{z}_h\|_{\boldsymbol{U}_h} \leq C\|q_h\|_{M_h}.$$

Let $\boldsymbol{\omega}_h = \boldsymbol{v}_h - \alpha \boldsymbol{z}_h$, $\lambda_h = q_h$, where $\alpha > 0$ is a constant. By the Cauchy-Schwarz inequality and above inequalities, we derive

$$\begin{aligned}
A_h((\boldsymbol{v}_h,q_h),(\boldsymbol{\omega}_h,\lambda_h)) &= a(\boldsymbol{v}_h,\boldsymbol{v}_h) - \alpha a(\boldsymbol{v}_h,\boldsymbol{z}_h) + \alpha b(\boldsymbol{z}_h,q_h) + \gamma j_h(q_h,q_h) \\
&\geq \mu_{min}\|\boldsymbol{v}_h\|_{\boldsymbol{U}_h}^2 - \alpha C \mu_{max}\|\boldsymbol{v}_h\|_{\boldsymbol{U}_h}\|q_h\|_{M_h} \\
&\quad + \alpha\|q_h\|_{M_h}^2 + (\gamma - \alpha C_2) j_h(q_h,q_h) \\
&\geq \frac{1}{2}\mu_{min}(\|\boldsymbol{v}_h\|_{\boldsymbol{U}_h} - \frac{\alpha C \mu_{max}}{\mu_{min}}\|q_h\|_{M_h})^2 + \frac{1}{2}\mu_{min}\|v_h\|_{\boldsymbol{U}_h}^2 \\
&\quad + (\alpha - \frac{\alpha^2 C^2 \mu_{max}^2}{2\mu_{min}})\|q_h\|_{M_h}^2 + (\gamma - \alpha C_2) j_h(q_h,q_h),
\end{aligned}$$

where $\mu_{max} = \max\limits_{x\in\Omega}\mu(x)$, $\mu_{min} = \min\limits_{x\in\Omega}\mu(x)$. Taking $\alpha = \frac{\mu_{min}}{C^2\mu_{max}^2}$ and $\gamma \geq \alpha C_2$, with suitable $C_\mu > 0$, we have

$$A_h((\boldsymbol{v}_h,q_h),(\boldsymbol{\omega}_h,\lambda_h)) \geq C_\mu \|(\boldsymbol{v}_h,q_h)\|_{\boldsymbol{U}_h\times M_h}^2.$$

Combining with

$$\begin{aligned}
\|(\boldsymbol{\omega}_h,\lambda_h)\|_{\boldsymbol{U}_h\times M_h} &\lesssim \|\boldsymbol{v}_h\|_{\boldsymbol{U}_h} + \alpha\|\boldsymbol{z}_h\|_{\boldsymbol{U}_h} + \|q_h\|_{M_h} \\
&\leq \|\boldsymbol{v}_h\|_{\boldsymbol{U}_h} + \frac{\mu_{min}}{C\mu_{max}^2}\|q_h\|_{M_h} + \|q_h\|_{M_h} \leq C_\mu\|(\boldsymbol{v}_h,q_h)\|_{\boldsymbol{U}_h\times M_h},
\end{aligned}$$

the desired result then follows. □

3.3 Error analysis

Define an interpolation operator $\mathbf{\Pi}_h : \tilde{\boldsymbol{H}}^2(\Omega_1 \cup \Omega_2) \to \boldsymbol{U}_h$ by

$$\mathbf{\Pi}_h \boldsymbol{v} = \pi_h \boldsymbol{v} + (\sqcap_h \boldsymbol{\omega})\bar{\psi},$$

where π_h is the nodal interpolation operator and $\sqcap_h$ is the Ćlement interpolation operator. For the pressure space, as the result in [39], we choose extension operators $E_k^s : H^k(\Omega^s) \to H^k(\Omega)$ such that $(E_1^s q)|_{\Omega^s} = q$ and

$$\|E_k^s w\|_{k,\Omega} \leq C\|w\|_{k,\Omega^s}, \ \ \forall w \in H^k(\Omega^s), \ s = +, -.$$

Let C_h be the local projection on the piecewise constants. Define

$$C_h q \doteq \begin{cases} C_h^- q^- & \text{in } \Omega^-, \\ C_h^+ q^+ & \text{in } \Omega^+, \end{cases}$$

where $C_h^s q_s \doteq (C_h E_1^s q^s)|_{\Omega^s}$, $s = +, -$. Then, the following interpolation error estimates holds.

Theorem 3.3.1. *For any* $(\boldsymbol{v}, q) \in \tilde{\boldsymbol{H}}^2(\Omega_1 \cup \Omega_2) \times H^1(\Omega_1 \cup \Omega_2)$*, it holds that*

$$\|(\boldsymbol{v} - \mathbf{\Pi}_h \boldsymbol{v}, q - C_h q)\|_H \lesssim h(\|\boldsymbol{v}\|_{\tilde{\boldsymbol{H}}^2(\Omega_1\cup\Omega_2)} + \|q\|_{H^1(\Omega_1\cup\Omega_2)}).$$

Based on Theorem 3.2.2, the finite element error estimate can be derived.

Theorem 3.3.2. *The problem* (3.1.5) *has a unique solution pair* $(\boldsymbol{u_h}, p_h) \in \boldsymbol{U}_h \times M_h$*. Furthermore, assume that the solution pair of the problem* (3.1.2) $(\boldsymbol{u}, p)$ *belongs to* $\tilde{\boldsymbol{H}}^2(\Omega_1 \cup \Omega_2) \times H^1(\Omega_1 \cup \Omega_2)$*, there exists a constant* $C_\mu > 0$ *such that*

$$\|(\boldsymbol{u} - \boldsymbol{u}_h, p - p_h)\|_H \leq C_\mu h(\|\boldsymbol{u}\|_{\tilde{\boldsymbol{H}}^2(\Omega_1\cup\Omega_2)} + \|p\|_{H^1(\Omega_1\cup\Omega_2)}). \tag{3.3.1}$$

Proof. From Theorem 3.2.2, we conclude that the problem (3.1.5) has a unique solution pair $(\boldsymbol{u_h}, p_h) \in \boldsymbol{U}_h \times M_h$. By the triangle inequality, it holds

$$\|(\boldsymbol{u} - \boldsymbol{u}_h, p - p_h)\|_H \lesssim \|(\boldsymbol{u} - \mathbf{\Pi}_h \boldsymbol{u}, p - C_h p)\|_H + \|(\mathbf{\Pi}_h \boldsymbol{u} - \boldsymbol{u}_h, C_h p - p_h)\|_H.$$

Using Theorem 3.3.1,

$$\|(\boldsymbol{v}-\boldsymbol{\Pi}_h\boldsymbol{v}, p-C_hp)\|_H \lesssim h(\|\boldsymbol{v}\|_{\tilde{\boldsymbol{H}}^2(\Omega_1\cup\Omega_2)}+\|p\|_{H^1(\Omega_1\cup\Omega_2)}). \tag{3.3.2}$$

According to Green's formula,

$$\begin{aligned} F((\boldsymbol{v}_h,q_h)) =& a_h(\boldsymbol{u},\boldsymbol{v}_h)-b_h(\boldsymbol{v}_h,p)+b_h(\boldsymbol{u},q_h)+c(p_h,q_h)\\ &-\sum_{e\in\varepsilon_h}\langle\{(2\mu\epsilon(\boldsymbol{u})-p\boldsymbol{I})\boldsymbol{n}\},[\boldsymbol{v}_h]\rangle_e+\gamma j_h(p_h,q_h)\\ =& A_h((\boldsymbol{u},p),(\boldsymbol{v}_h,q_h))-E((\boldsymbol{u},p),(\boldsymbol{v}_h,q_h)), \end{aligned}$$

where

$$E((\boldsymbol{u},p),(\boldsymbol{v}_h,q_h))=\sum_{e\in\varepsilon_h}\langle\{(2\mu\epsilon(\boldsymbol{u})-p\boldsymbol{I})\boldsymbol{n}\},[\boldsymbol{v}_h]\rangle_e-\gamma j_h(C_hp,q_h). \tag{3.3.3}$$

According to Theorem 3.2.2, we derive

$$\begin{aligned} &\|(\boldsymbol{I}_h\boldsymbol{u}-\boldsymbol{u}_h, C_hp-p_h)\|_H\\ &\le\frac{1}{C_\mu}\sup_{(\boldsymbol{v}_h,q_h)\in\boldsymbol{U}_h\times M_h}\frac{A_h((\boldsymbol{\Pi}_h\boldsymbol{u}-\boldsymbol{u}_h,C_hp-p_h),(\boldsymbol{v}_h,q_h))}{\|(\boldsymbol{v}_h,q_h)\|_H}\\ &=\frac{1}{C_\mu}\sup_{(\boldsymbol{v}_h,q_h)\in\boldsymbol{U}_h\times M_h}\frac{A_h((\boldsymbol{I}_h\boldsymbol{u},C_hp),(\boldsymbol{v}_h,q_h))-F((\boldsymbol{v}_h,q_h))}{\|(\boldsymbol{v}_h,q_h)\|_H}\\ &=\frac{1}{C_\mu}\sup_{(\boldsymbol{v}_h,q_h)\in\boldsymbol{U}_h\times M_h}\frac{A((\boldsymbol{I}_h\boldsymbol{u}-\boldsymbol{u},C_hp-p),(\boldsymbol{v}_h,q_h))+E((\boldsymbol{u},p),(\boldsymbol{v}_h,q_h))}{\|(\boldsymbol{v}_h,q_h)\|_H}. \end{aligned} \tag{3.3.4}$$

In the following, we estimate $E((\boldsymbol{u},p),(\boldsymbol{v}_h,q_h))$. For any edge $e\in\varepsilon_h^n$, it is easy to derive that

$$\sum_{e\in\varepsilon_h^n}\langle\{(2\mu\epsilon(\boldsymbol{u})-p\boldsymbol{I})\boldsymbol{n}\},[\boldsymbol{v}_h]\rangle_e\lesssim h\|\boldsymbol{v}_h\|_{\boldsymbol{U}_h}(\|\boldsymbol{u}\|_{\tilde{\boldsymbol{H}}^2(\Omega^+\cup\Omega^-)}+\|p\|_{H^1(\Omega^+\cup\Omega^-)}). \tag{3.3.5}$$

For any $e\in\varepsilon_h^i$, denote e^s by the intersection of e and Ω^s. Extending e^s to be $\bar{e}^s$ in the

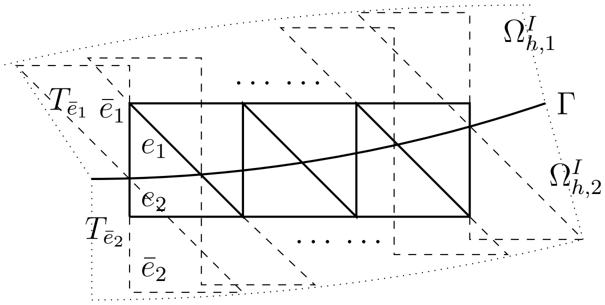

Figure 3-3 two strips $\Omega^I_{h,1}$ and $\Omega^I_{h,2}$ (dotted lines).

direction of Ω^s such that $\bar{e}^s = O(h)$ and making an auxiliary triangle $T_{\bar{e}^s}$ of length $\bar{e}^s$ $(s = -, +)$. Then, for all $e \in \varepsilon_h^i$, we can obtain two strips $\Omega_h^{I,-}$ and $\Omega_h^{I,+}$ of width $O(h)$, which contain all auxiliary triangles, as illustrated in Fig. 3-3, we note that

$$\|\boldsymbol{\sigma}\|_{L^2(e)} \lesssim \|\boldsymbol{\sigma}\|_{L^2(e^-)} + \|\boldsymbol{\sigma}\|_{L^2(e^+)} \lesssim \|\boldsymbol{\sigma}\|_{L^2(\bar{e}^-)} + \|\boldsymbol{\sigma}\|_{L^2(\bar{e}^+)}.$$

By scaling and imbedding theorem, the following estimate holds for $s = -, +$,

$$\|\boldsymbol{\sigma}\|_{L^2(\bar{e}^s)} \lesssim h^{\frac{1}{2}} \|\hat{\boldsymbol{\sigma}}\|_{L^2(\hat{\bar{e}}^s)} \lesssim h^{\frac{1}{2}} \|\hat{\boldsymbol{\sigma}}\|_{H^1(\hat{T}_{\hat{\bar{e}}^s})} \lesssim h^{-\frac{1}{2}} \|\boldsymbol{\sigma}\|_{L^2(T_{\bar{e}^s})} + h^{\frac{1}{2}} |\boldsymbol{\sigma}|_{H^1(T_{\bar{e}^s})},$$

where $\hat{T}_{\hat{\bar{e}}_s}$ is the corresponding reference triangles of $T_{\bar{e}^s}$, $\hat{\bar{e}}^s$ is the edge of $\hat{T}_{\hat{\bar{e}}^s}$. Moreover,

$$\begin{aligned} \langle \{\boldsymbol{\sigma n}\}, [\boldsymbol{v}_h] \rangle_e &\lesssim \|\boldsymbol{\sigma}\|_{L^2(e)} \|[\boldsymbol{v}_h]\|_{L^2(e)} \\ &\lesssim \sum_{i=1}^{2} \left(h^{\frac{1}{2}} \|\boldsymbol{\sigma}\|_{L^2(T_{\bar{e}^s})} + h^{\frac{3}{2}} |\boldsymbol{\sigma}|_{H^1(T_{\bar{e}^s})} \right) \left(h^{-1} \|[\boldsymbol{v}_h]\|_{L^2(e)} \right). \end{aligned} \tag{3.3.6}$$

Therefore, from (3.2.1) and (3.3.6), we deduce

$$\sum_{e \in \varepsilon_h^i} \langle \{(\boldsymbol{\sigma n}\}, [\boldsymbol{v}_h] \rangle_e \lesssim \sum_{i=1}^{2} \left(h^{\frac{1}{2}} \|\boldsymbol{\sigma}\|_{L^2(\Omega_h^{I,s})} + h^{\frac{3}{2}} |\boldsymbol{\sigma}|_{H^1(\Omega_h^{I,s})} \right) \|[\boldsymbol{v}_h]\|_h. \tag{3.3.7}$$

By Theorem 1.1 in [7],

$$\|\boldsymbol{\sigma}\|_{L^2(\Omega_h^{I,s})} \lesssim |\Omega_h^{I,s}|^{\frac{1}{2}} \|\boldsymbol{\sigma}\|_{H^1(\Omega^s)}, \quad s = -, +. \tag{3.3.8}$$

According to (3.3.6), (3.3.7) and (3.3.8), the following estimate holds,

$$\sum_{e\in\mathcal{F}_h}\langle\{(2\mu\epsilon(\boldsymbol{u})-p\boldsymbol{I})\boldsymbol{n}\},[\boldsymbol{v}_h]\rangle_e \lesssim h\|2\mu\epsilon(\boldsymbol{u})-p\boldsymbol{I}\|_{\boldsymbol{H}^1(\Omega_1\cup\Omega_2)}\|\boldsymbol{v}_h\|_{\boldsymbol{U}_h}$$
$$\lesssim h(\|\boldsymbol{u}\|_{\tilde{\boldsymbol{H}}^2(\Omega_1\cup\Omega_2)}+\|p\|_{H^1(\Omega_1\cup\Omega_2)})\|\boldsymbol{v}_h\|_{\boldsymbol{U}_h}. \tag{3.3.9}$$

For the second term on the right hand of (3.3.4), by Theorem 3.2.1, we derive

$$j_h(C_hp,q_h)\lesssim h\|p\|_{H^1(\Omega_1\cup\Omega_2)}\|q_h\|_{0,h}. \tag{3.3.10}$$

Combining (3.3.3), (3.3.4), (3.3.9) with (3.3.10),

$$\|(\boldsymbol{\Pi}_h\boldsymbol{u}-\boldsymbol{u}_h,p-p_h)\|_H$$
$$\leq C\left(\|(\boldsymbol{u}-\boldsymbol{\Pi}_h\boldsymbol{u},p-C_hp)\|_{\boldsymbol{U}\times M}+h(\|\boldsymbol{u}\|_{\tilde{\boldsymbol{H}}^2(\Omega^-\cup\Omega^+)}+\|p\|_{H^1(\Omega^-\cup\Omega^+)})\right). \tag{3.3.11}$$

Finally, by (3.3.2) and (3.3.11), the proof is completed. □

3.4 Numerical examples

We present several numerical examples to show the performance of the nonconforming enriched finite element method. The computational domain Ω is the rectangle $-1/2\leq x,y\leq 1/2$, which is divided into subdomains $\Omega_1=\{(x,y):x^2+y^2>r_0^2\}$ and $\Omega_2=\{(x,y):x^2+y^2<r_0^2\}$. The interface curve Γ is a circle centered at the origin with radius $r_0=1/4$. The exact solution is

$$\boldsymbol{u}(x,y)=\begin{cases}\begin{pmatrix}u_1^-(x,y)\\u_2^-(x,y)\end{pmatrix}=\begin{pmatrix}\frac{1}{\lambda^-}\left(x^2+y^2\right)^{\frac{\alpha_1}{2}}\\\frac{1}{\lambda^-}\left(x^2+y^2\right)^{\frac{\alpha_2}{2}}\end{pmatrix} & \text{in } \Omega^-,\\ \begin{pmatrix}u_1^+(x,y)\\u_2^+(x,y)\end{pmatrix}=\begin{pmatrix}\frac{1}{\lambda^+}\left(x^2+y^2\right)^{\frac{\alpha_1}{2}}+\left(\frac{1}{\lambda^-}-\frac{1}{\lambda^+}\right)r_0^{\alpha_1}\\\frac{1}{\lambda^+}\left(x^2+y^2\right)^{\frac{\alpha_2}{2}}+\left(\frac{1}{\lambda^-}-\frac{1}{\lambda^+}\right)r_0^{\alpha_2}\end{pmatrix} & \text{in } \Omega^+,\end{cases}$$

and

$$p = -5x(x^2+y^2)^{3/2} - 7y(x^2+y^2)^{5/2},$$

where $\alpha_1 = 5$ and $\alpha_2 = 7$.

Table 3-1 Finite element errors with $(\lambda^+, \lambda^-) = (200, 2)$, $(\mu^+, \mu^-) = (100, 1)$.

$\frac{1}{h}$	$\|\boldsymbol{u} - \boldsymbol{u}_h\|_{\boldsymbol{U}_h}$	order	$\|p - p_h\|_{0,\Omega}$	order
8	8.735e-003		4.761e-003	
16	5.248e-003	0.7351	2.472e-003	0.9454
32	2.890e-003	0.8604	1.159e-003	1.0935
64	1.586e-003	0.8663	5.640e-004	1.0433
128	8.477e-004	0.9023	2.730e-004	1.0509

In Table 1 and Table 2, we consider the jumps $(\lambda^+, \lambda^-) = (200, 2)$, $(\mu^+, \mu^-) = (100, 1)$ and $(\lambda^+, \lambda^-) = (1000, 1)$, $(\mu^+, \mu^-) = (2000, 2)$, respectively. The Poisson ratios in two subdomains are $\nu^\pm = \frac{1}{6}$ so that the material is compressible. we observe that convergence rates are optimal for the velocity in energy norm and the pressure in L^2 norm.

In Table 3, we set $(\lambda^+, \lambda^-) = (20000, 10000)$, $(\mu^+, \mu^-) = (20, 10)$ and the Poisson ratios are $\nu^+ = \nu^- \approx 0.4995$, which is corresponding to nearly incompressible case. The convergence rates are also optimal for the velocity in energy norm and the pressure in L^2 norm.

Table 3-2 Finite element errors with $(\lambda^+, \lambda^-) = (2000, 2)$, $(\mu^+, \mu^-) = (1000, 1)$.

$\frac{1}{h}$	$\|\boldsymbol{u} - \boldsymbol{u}_h\|_{\boldsymbol{U}_h}$	order	$\|p - p_h\|_{0,\Omega}$	order
8	2.788e-003		4.804e-003	
16	2.250e-003	0.3092	2.471e-003	0.9593
32	9.393e-004	1.2606	1.239e-003	0.9960
64	5.375e-004	0.8052	6.552e-004	0.9228
128	2.756e-004	0.9638	3.329e-004	0.9809

Table 3-3 Finite element errors with $(\lambda^+, \lambda^-) = (20000, 10000)$, $(\mu^+, \mu^-) = (20, 10)$.

$\frac{1}{h}$	$\|\boldsymbol{u} - \boldsymbol{u}_h\|_{\boldsymbol{U}_h}$	order	$\|p - p_h\|_{0,\Omega}$	order
8	1.254e-002		3.771e-003	
16	7.056e-003	0.8298	3.013e-003	0.3237
32	3.676e-003	0.9409	2.003e-003	0.5886
64	1.876e-003	0.9700	1.059e-003	0.9196
128	9.693e-004	0.9531	5.487e-004	0.9519

Chapter 4 The immersed finite element method for Stokes interface problems

We consider the Stokes interface problem,

$$
\begin{aligned}
-\nabla\cdot(\mu\boldsymbol{\epsilon}(\boldsymbol{u})-p\boldsymbol{I})=\boldsymbol{f} &\quad \text{in } \Omega^+\cup\Omega^-,\\
\nabla\cdot\boldsymbol{u}=0 &\quad \text{in } \Omega^+\cup\Omega^-,\\
[\![\boldsymbol{u}]\!]=\boldsymbol{0},\ [\![(\mu\boldsymbol{\epsilon}(\boldsymbol{u})-p\boldsymbol{I})\boldsymbol{n}_\Gamma]\!]=\boldsymbol{0} &\quad \text{on } \Gamma,\\
\boldsymbol{u}=\boldsymbol{0} &\quad \text{on } \partial\Omega,
\end{aligned}
\tag{4.0.1}
$$

where $\boldsymbol{f}\in\boldsymbol{L}^2(\Omega)$. The viscosity μ is discontinuous across the interface Γ, i.e.,

$$
\mu=\begin{cases}\mu_1 & \text{in } \Omega_1,\\ \mu_2 & \text{in } \Omega_2,\end{cases}
$$

where $\mu_i(>0)\in W^{1,\infty}(\Omega_i)$.

4.1 The CR immersed finite element velocity space

We first present the construction of immersed finite element space for velocity. In the non-interface element T, we apply the standard CR finite element space $\boldsymbol{U}_h^n(T)$, which is locally defined by

$$
\boldsymbol{U}_h^n(T)=\text{Span}\{\boldsymbol{\psi}_{j,T}:j=1,\cdots,6\}.
$$

The six local basis functions satisfy the following constraints

$$
\int_{e_i}\boldsymbol{\psi}_{j,T}ds=(\delta_{i,j},0)^t,\qquad i,\ j=1,\ 2,\ 3,
$$

$$\int_{e_i} \boldsymbol{\psi}_{j,T} ds = (0, \delta_{j-3,i}), \qquad i = 1,\ 2,\ 3,\ j = 4,\ 5,\ 6,$$

where e_i $(i = 1, 2, 3)$ are the edges of T.

For an interface element T, we will employ the interface conditions to construct the piecewise linear basis functions. Hence, the coupled interface condition

$$[(\mu\boldsymbol{\epsilon}(\boldsymbol{u}) - pI)\boldsymbol{n}] = \sigma\kappa\boldsymbol{n},$$

should be properly modified. We assume that σ is a constant, it follows that across the interface the shear stress is continuous, i.e.,

$$[\mu\boldsymbol{\epsilon}(\boldsymbol{u})\boldsymbol{n}] \cdot \boldsymbol{\tau} = \boldsymbol{0}, \tag{4.1.1}$$

where $\boldsymbol{\tau} = (\tau_1, \tau_2)^t$ is the unit tangent vector to Γ.

We also only describe how to construct the basis functions $\hat{\boldsymbol{\phi}}(\hat{\boldsymbol{x}})$ on $\hat{T}$. Let $\hat{\boldsymbol{\phi}}_j = (\hat{\phi}_{1,j}, \hat{\phi}_{2,j})^t$, $j = 1, \cdots, 6$, be the IFE functions on $\hat{T}$, i.e.,

$$\hat{\boldsymbol{\phi}}_j = \begin{cases} \hat{\phi}_{1,j} = \begin{pmatrix} \hat{\phi}^+_{1,j} \\ \hat{\phi}^-_{1,j} \end{pmatrix} = \begin{pmatrix} a_1^+ + b_1^+\hat{x} + c_1^+\hat{y} \\ a_1^- + b_1^-\hat{x} + c_1^-\hat{y} \end{pmatrix} & \begin{matrix} \text{if } (\hat{x},\hat{y}) \in \hat{T}^+, \\ \text{if } (\hat{x},\hat{y}) \in \hat{T}^-, \end{matrix} \\ \hat{\phi}_{2,j} = \begin{pmatrix} \hat{\phi}^+_{2,j} \\ \hat{\phi}^-_{2,j} \end{pmatrix} = \begin{pmatrix} a_2^+ + b_2^+\hat{x} + c_2^+\hat{y} \\ a_2^- + b_2^-\hat{x} + c_2^-\hat{y} \end{pmatrix} & \begin{matrix} \text{if } (\hat{x},\hat{y}) \in \hat{T}^+, \\ \text{if } (\hat{x},\hat{y}) \in \hat{T}^-, \end{matrix} \end{cases} \tag{4.1.2}$$

where a_i^s, b_i^s, c_i^s ($i = 1,\ 2$ and $s = +, -$) are undetermined coefficients. Each basis function $\hat{\boldsymbol{\phi}}_j$ is uniquely determined by following constraint conditions. The average values on the edges of $\hat{T}$ satisfy $(j = 1, \cdots, 6)$

$$\frac{1}{e_i}\int_{e_i} \hat{\phi}_{1,j} ds = \delta_{ij},\ \ i = 1,\ 2,\ 3, \tag{4.1.3}$$

$$\frac{1}{e_i}\int_{e_i} \hat{\phi}_{2,j} ds = \delta_{ij},\ \ i = 4,\ 5,\ 6. \tag{4.1.4}$$

The continuity of the velocity at the intersection points leads to

$$\hat{\phi}^+_{i,j}(\hat{D}) = \hat{\phi}^-_{i,j}(\hat{D}), \qquad \hat{\phi}^+_{i,j}(\hat{E}) = \hat{\phi}^-_{i,j}(\hat{E}), \tag{4.1.5}$$

the continuity along the interface

$$\left[-\mu\frac{\partial\hat{\phi}_{1,j}}{\partial x}\bar{n}_1+\frac{1}{2}\mu\left(\frac{\partial\hat{\phi}_{1,j}}{\partial y}+\frac{\partial\hat{\phi}_{2,j}}{\partial x}\right)(\bar{n}_1^2-\bar{n}_2^2)+\mu\frac{\partial\hat{\phi}_{2,j}}{\partial y}\bar{n}_2\right]\Big|_{\overline{\hat{D}\hat{E}}}=0, \quad (4.1.6)$$

and the extra condition

$$\nabla\cdot\boldsymbol{u}_h|_{T^s}=0,\ \ s=+,-, \quad (4.1.7)$$

where $\bar{\boldsymbol{n}}=(\bar{n}_1,\bar{n}_2)$ is the unit outer normal to the segment $\overline{DE}$ pointing from T^+ to T^-. Combining the conditions (4.1.3)-(4.1.7), we have

$$\boldsymbol{A\varphi}=\boldsymbol{b}, \quad (4.1.8)$$

where the matrix $\boldsymbol{A}$ is

$$\begin{pmatrix}
1 & \frac{1}{2} & \frac{1}{2} & 0 & 0 & 0 & 0 & 0 & 0 & 0 & 0 & 0\\
a_{21} & 0 & \frac{1-\hat{e}^2}{2} & e & 0 & \frac{\hat{e}^2}{2} & 0 & 0 & 0 & 0 & 0 & 0\\
a_{31} & \frac{1-\hat{d}^2}{2} & 0 & d & \frac{\hat{d}^2}{2} & 0 & 0 & 0 & 0 & 0 & 0 & 0\\
1 & 0 & \hat{e} & -1 & 0 & -\hat{e} & 0 & 0 & 0 & 0 & 0 & 0\\
1 & \hat{d} & 0 & -1 & -\hat{d} & 0 & 0 & 0 & 0 & 0 & 0 & 0\\
0 & 0 & 0 & 0 & 0 & 0 & 1 & \frac{1}{2} & \frac{1}{2} & 0 & 0 & 0\\
0 & 0 & 0 & 0 & 0 & 0 & a_{21} & 0 & \frac{1-\hat{e}^2}{2} & e & 0 & \frac{\hat{e}^2}{2}\\
0 & 0 & 0 & 0 & 0 & 0 & a_{21} & \frac{1-\hat{d}^2}{2} & 0 & d & \frac{\hat{d}^2}{2} & 0\\
0 & 0 & 0 & 0 & 0 & 0 & 1 & \hat{d} & 0 & -1 & -\hat{d} & 0\\
0 & 0 & 0 & 0 & 0 & 0 & 1 & 0 & \hat{e} & -1 & 0 & -\hat{e}\\
0 & a_{1,2} & \frac{\alpha\mu^+}{2} & 0 & a_{1,5} & a_{1,6} & 0 & \frac{\alpha\mu^+}{2} & a_{1,2} & 0 & a_{1,6} & a_{1,5}\\
0 & 1 & 0 & 0 & -1 & 0 & 0 & 0 & 1 & 0 & 0 & -1
\end{pmatrix},$$

$$a_{21}=1-\hat{e},\ \ a_{21}=1-\hat{d},\ \ a_{1,2}=\hat{d}\hat{e}\mu^+,\ \ a_{1,5}=-\hat{d}\hat{e}\mu^-,$$

$$a_{1,6}=-\frac{\alpha\mu^-}{2},\ \ \alpha=\hat{e}^2-\hat{d}^2,$$

and

$$\boldsymbol{\varphi}=(a_1^+,b_1^+,c_1^+,a_1^-,b_1^-,c_1^-,a_2^+,b_2^+,c_2^+,a_2^-,b_2^-,c_2^-)^t,$$

$$\boldsymbol{b} = (\delta_{j,1}, \delta_{j,2}, \delta_{j,3}, 0, 0, \delta_{j,4}, \delta_{j,5}, \delta_{j,6}, 0, 0, 0, 0)^t.$$

Through affine mapping and (4.1.2), we obtain the IFE basis functions $\boldsymbol{\phi}_j$ $(j = 1, \cdots, 6)$. For simplicity, denote the local basis functions $\boldsymbol{\phi}_j$ on the element T by $\boldsymbol{\phi}_{j,T}$. The local IFE space $\boldsymbol{U}_h^i(T)$ can be written as

$$\boldsymbol{U}_h^i(T) = \text{Span}\{\boldsymbol{\phi}_{j,T} : j = 1, \cdots, 6\}.$$

Now, we introduce the global IFE space for displacement $\boldsymbol{u}$ as follows.

$$\boldsymbol{U}_h(\Omega) \doteq \Big\{\boldsymbol{u}_h = (u_{1,h}, u_{2,h})^t \in (L^2(\Omega))^2 : \boldsymbol{u}_h\big|_T \in \boldsymbol{U}_h^\alpha(T),\ \alpha = i, n;$$
$$\int_e \boldsymbol{u}_h\big|_{T_1} = \int_e \boldsymbol{u}_h\big|_{T_2},\ e\ is\ the\ common\ edge\ of\ T_1 \cap T_2,\ \forall T_1,\ T_2 \in \mathcal{T}_h\Big\}.$$

In the rest of the chapter, we will drop Ω for $\boldsymbol{U}_h(\Omega)$ without confusion.

Theorem 4.1.1. *In any interface triangle T, the IFE function $\boldsymbol{\phi}(x, y) \in \boldsymbol{U}_h^i(T)$ can be uniquely determined by its average values on the edges of T and the jump conditions.*

Proof. We carry out the proof for $\hat{\boldsymbol{\phi}}(x, y)$. It is apparent from (4.1.8) that we only need to prove the matrix A is nonsingular. By direct calculations

$$\det(\boldsymbol{A}) = \frac{1}{32}(\hat{d}^2 + \hat{e}^2)^2 \left(\hat{d}\hat{e}\mu^+ + \mu^-(1 - \hat{d}\hat{e})\right) > 0.$$

The proof is completed. □

Define $\boldsymbol{U} = \boldsymbol{H}_0^1(\Omega)$ and

$$M = L_0^2(\Omega) = \{q \in L^2(\Omega) | \int_\Omega q dx = 0\}.$$

The space $\boldsymbol{U} \times M$ is equipped with the norm

$$\|(\boldsymbol{v}, q)\|_{\boldsymbol{U}\times M} = (|\boldsymbol{v}|^2_{H^1(\Omega)} + \|q\|^2_{L^2(\Omega)})^{1/2}\ \forall (\boldsymbol{v}, q) \in \boldsymbol{U} \times M. \tag{4.1.9}$$

The continuous variational problem for the Stokes interface problem (4.0.1) reads as follows: find $(\boldsymbol{u}, p) \in \boldsymbol{U} \times M$ such that

$$\begin{cases} a(\boldsymbol{u}, \boldsymbol{v}) - b(\boldsymbol{v}, p) = f(\boldsymbol{v}), \quad \forall \boldsymbol{v} \in \boldsymbol{U}, \\ \qquad\qquad b(\boldsymbol{u}, q) = 0, \qquad \forall q \in M, \end{cases} \tag{4.1.10}$$

where

$$a(\boldsymbol{u}, \boldsymbol{v}) = (\mu \boldsymbol{\epsilon}(\boldsymbol{u}), \boldsymbol{\epsilon}(\boldsymbol{v})),$$

$$b(\boldsymbol{v}, q) = (\nabla \cdot \boldsymbol{v}, q), \quad f(\boldsymbol{v}) = (\boldsymbol{f}, \boldsymbol{v}).$$

Let

$$A((\boldsymbol{u}, p), (\boldsymbol{v}, q)) = a(\boldsymbol{u}, \boldsymbol{v}) - b(\boldsymbol{v}, p) + b(\boldsymbol{u}, q), \quad F((\boldsymbol{v}, q)) = f(\boldsymbol{v})$$

The problem (4.1.10) equals: find $(\boldsymbol{u}, p) \in \boldsymbol{U} \times M$ such that

$$A((\boldsymbol{u}, p), (\boldsymbol{v}, q)) = F((\boldsymbol{v}, q)) \ \ \forall (\boldsymbol{v}, q) \in \boldsymbol{U} \times M. \tag{4.1.11}$$

Let $Q_h = \{q_h \in L_0^2(\Omega); q_h|_T \in P_0(T), \ \forall T \in \mathcal{T}_h\}$ be the piecewise constant space. Define

$$M_h = \{q_h \in L_0^2(\Omega); \ q_h = q_h^- \chi^- + q_h^+ \chi^+, \ q_h^+, q_h^- \in Q_h\},$$

where χ^s represents the characteristic function, i.e.,

$$\chi^s = \begin{cases} 1, & (x, y) \in \Omega^s, \\ 0, & (x, y) \in \Omega \backslash \Omega^s. \end{cases}$$

The discrete variational problem is: find $(\boldsymbol{u}_h, p_h) \in \boldsymbol{U}_h \times M_h$ such that

$$\begin{cases} a_h(\boldsymbol{u}_h, \boldsymbol{v}_h) - b_h(\boldsymbol{v}_h, p_h) = f(\boldsymbol{v}_h), \quad \forall \boldsymbol{v}_h \in \boldsymbol{U}_h, \\ b_h(\boldsymbol{u}_h, q_h) + \gamma j_h(p_h, q_h) = 0, \quad \forall q_h \in M_h, \end{cases} \tag{4.1.12}$$

where

$$a_h(\boldsymbol{u}_h,\boldsymbol{v}_h)=\sum_{T\in\mathcal{T}_h}\big(\mu\boldsymbol{\epsilon}(\boldsymbol{u}_h),\boldsymbol{\epsilon}(\boldsymbol{v}_h)\big)_T-\sum_{e\in\varepsilon_h^i}\big(\mu\{\boldsymbol{\epsilon}(\boldsymbol{u}_h)\cdot\boldsymbol{n}\},[\boldsymbol{v}_h]\big)_e$$

$$-\sum_{e\in\varepsilon_h^i}\big(\mu\{\boldsymbol{\epsilon}(\boldsymbol{v}_h)\cdot\boldsymbol{n}\},[\boldsymbol{u}_h]\big)_e+\sum_{e\in\varepsilon_h^i}h^{-1}(\mu[\boldsymbol{u}_h],[\boldsymbol{v}_h])_e,$$

$$b_h(\boldsymbol{v}_h,q_h)=\sum_{T\in\mathcal{T}_h}(\nabla\cdot\boldsymbol{v}_h,q_h)_T$$

and the stabilization term (see [39]) is defined as

$$j_h(p_h,q_h)=\sum_{i=1}^{2}j^s(p_h^s,q_h^s)=\sum_{i=1}^{2}\sum_{e\in\varepsilon_\langle^\rangle}h\langle[p_h^s],[q_h^s]\rangle_e.$$

Denote by

$$A((\boldsymbol{u}_h,p_h),(\boldsymbol{v}_h,q_h))=a(\boldsymbol{u}_h,\boldsymbol{v}_h)-b(\boldsymbol{v}_h,p_h)+b(\boldsymbol{u}_h,q_h)+\gamma j_h(p_h,q_h),$$

$$F((\boldsymbol{v}_{\boldsymbol{h}},q_h))=f(\boldsymbol{v}_h).$$

The problem (4.1.12) equals: find $(\boldsymbol{u}_h,p_h)\in\boldsymbol{U}_h\times M_h$ such that

$$A_h((\boldsymbol{u}_h,p_h),(\boldsymbol{v}_h,q_h))=F((\boldsymbol{v}_h,q_h))\ \ \forall(\boldsymbol{v}_h,q_h)\in\boldsymbol{U}_h\times M_h. \tag{4.1.13}$$

4.2 The approximation capability of the CR IFE space

For any interface triangle T, let $(s=+,-)$

$$\tilde{\boldsymbol{H}}^2(T)=\left\{\boldsymbol{u}\in[C(T)]^2,\ \boldsymbol{u}|_{T^s}\in\boldsymbol{H}^2(T^s),\ \ [\boldsymbol{\epsilon}(\boldsymbol{u})\boldsymbol{n}]=\boldsymbol{0}\text{ on }\Gamma\cap T\right\},$$

$$\tilde{\boldsymbol{C}}^2(T)=\left\{\boldsymbol{u}\in[C(T)]^2,\ \boldsymbol{u}|_{T^s}\in\boldsymbol{C}^2(T^s),\ \ [\boldsymbol{\epsilon}(\boldsymbol{u})\boldsymbol{n}]=\boldsymbol{0}\text{ on }\Gamma\cap T\right\},$$

$$\tilde{\boldsymbol{H}}^2(\Omega)=\left\{\boldsymbol{u}\in\boldsymbol{C}(\Omega),\ \boldsymbol{u}|_{\Omega^s}\in\boldsymbol{H}^2(\Omega^s),\ \ [\boldsymbol{\epsilon}(\boldsymbol{u})\boldsymbol{n}]=\boldsymbol{0}\text{ on }\Gamma\cap T\right\}.$$

Define a local interpolation operator $I_{h,T} : \tilde{\boldsymbol{H}}^2(T) \to \boldsymbol{U}_h^i(T)$ as

$$I_{h,T}\boldsymbol{u} = \begin{cases} \sum_{j=1}^{6} c_j \boldsymbol{\psi}_{j,T}, & \text{if } T \text{ is a non-interface element,} \\ \sum_{j=1}^{6} c_j \boldsymbol{\phi}_{j,T}, & \text{if } T \text{ is an interface element,} \end{cases}$$

where

$$c_j = \frac{1}{\hat{e}_j} \int_{\hat{e}_j} u_1 ds, \qquad c_{j+3} = \frac{1}{\hat{e}_j} \int_{\hat{e}_j} u_2 ds, \qquad j = 1, 2, 3.$$

For a function $\boldsymbol{u} \in \tilde{\boldsymbol{H}}^2(T)$, $T \in \mathcal{T}_h$, the global IFE interpolation operator I_h : $\tilde{\boldsymbol{H}}^2(\Omega) \to \boldsymbol{U}_h(\Omega)$ is denoted by

$$I_h\boldsymbol{u}|_T = I_{h,T}\boldsymbol{u}, \qquad \forall T \in \mathcal{T}_h.$$

In any non-interface triangle T, the error estimate of $I_h\boldsymbol{u}$ can be obtained by the standard interpolation estimate. As we mentioned in Section 2.3, in an arbitrary interface element, the error estimate for $I_{h,T}\boldsymbol{u}$ on T can be obtained by estimating over the three subsets $T^{*,-}$, $T^{*,+}$ and T^*.

We could derive the following system of linear equations by interface conditions,

$$\mathcal{M}^+\boldsymbol{Vec}(\nabla\boldsymbol{u}^+) = \mathcal{M}^-\boldsymbol{Vec}(\nabla\boldsymbol{u}^-),$$

where $\boldsymbol{Vec}$ is a vectorization map $\boldsymbol{Vec} : \mathbb{R}^{m\times n} \to \mathbb{R}^{mn\times 1}$ such that for any $A = (a_{ij})_{i=1,j=1}^{m,n}$,

$$\boldsymbol{Vec}(A) = (a_{11}, \cdots, a_{m1}, a_{12}, \cdots, a_{m2}, \cdots, a_{1n}, \cdots, a_{mn})^t$$

and

$$\mathcal{M}^i = \begin{pmatrix} -n_2 & 0 & n_1 & 0 \\ 0 & -n_2 & 0 & n_1 \\ -\mu^s n_1 n_2 & \mu^s(n_1^2 - n_2^2) & \mu^s(n_1^2 - n_2^2) & \mu^s n_1 n_2 \\ 1 & 0 & 0 & 1 \end{pmatrix}, \quad s = +, -.$$

Then, by tedious calculations, the following results hold.

Lemma 4.2.1. *Given any point $X = (x, y) \in \Gamma \cap T$, assume $\mathbf{u}(x, y)$ satisfies the interface jump conditions, then*

$$\nabla \boldsymbol{u}^+(X) = \begin{pmatrix} \frac{\partial u_1^-(X)}{\partial x} + n_1 n_2 \rho G(X) & \frac{\partial u_1^-(X)}{\partial y} + n_2^2 \rho G(X) \\ \frac{\partial u_2^-(X)}{\partial x} - n_1^2 \rho G(X) & \frac{\partial u_2^-(X)}{\partial y} - n_1 n_2 \rho G(X) \end{pmatrix} \tag{4.2.1}$$

and

$$[\nabla \boldsymbol{u}(X)] = \nabla \boldsymbol{u}^+(X) - \nabla \boldsymbol{u}^-(X) = \begin{pmatrix} n_1 n_2 \rho G(X) & n_2^2 \rho G(X) \\ -n_1^2 \rho G(X) & -n_1 n_2 \rho G(X) \end{pmatrix}, \tag{4.2.2}$$

where $\rho = \frac{\mu^- - \mu^+}{\mu^-}$,

$$G = 2n_1 n_2 \frac{\partial u_1^-}{\partial x} - (n_1^2 - n_2^2)(\frac{\partial u_1^-}{\partial y} + \frac{\partial u_2^-}{\partial x}) - 2n_1 n_2 \frac{\partial u_2^-}{\partial y}.$$

For any point $\overline{X} \in \overline{DE}$, by replacing n_i with $\bar{n}_i$ $(i = 1, 2)$, we can obtain the expressions

$$\left[\nabla \boldsymbol{u}(\overline{X})\right] = \nabla \boldsymbol{u}^+(\overline{X}) - \nabla \boldsymbol{u}^-(\overline{X}) = \begin{pmatrix} \bar{n}_1 \bar{n}_2 \rho G(\overline{X}) & \bar{n}_2^2 \rho G(\overline{X}) \\ -\bar{n}_1^2 \rho G(\overline{X}) & -\bar{n}_1 \bar{n}_2 \rho G(\overline{X}) \end{pmatrix}, \tag{4.2.3}$$

where

$$G = 2\bar{n}_1 \bar{n}_2 \frac{\partial u_1^-}{\partial x} - (\bar{n}_1^2 - \bar{n}_2^2)(\frac{\partial u_1^-}{\partial y} + \frac{\partial u_2^-}{\partial x}) - 2\bar{n}_1 \bar{n}_2 \frac{\partial u_2^-}{\partial y}.$$

Let $\tilde{P}^{\perp}$ be the orthogonal projection of $\tilde{P} \in \Gamma$ onto $\overline{DE}$ $(i = 1, 2, 3)$, respectively. As the same technique in Chapter 2, we also have following lemmas.

Lemma 4.2.2. *For any point $\tilde{P} \in \Gamma \cap T$, there exist $h_0 > 0$ such that*

$$\|\tilde{P} - \tilde{P}^{\perp}\|_{0,T} \lesssim h^2, \tag{4.2.4}$$

where $T \in \mathcal{T}_h^i$ and $0 \le h \le h_0$.

Lemma 4.2.3. *Let $X = (x, y)^t$, the functions $\boldsymbol{\phi}_j(X) \in \boldsymbol{U}_h^i(T)$ satisfy*

$$\sum_{j=1}^{6} \boldsymbol{\phi}_j(X) = I,$$

where I is a two-dimension identity matrix.

Lemma 4.2.4. *For any interface triangle $T \in \mathcal{T}_h$ and any point $X \in T$,*

$$|\boldsymbol{\phi}_j(X)| \lesssim 1, \quad \|\nabla \boldsymbol{\phi}_j(X)\|_{0,T} \lesssim h^{-1}. \tag{4.2.5}$$

Let $X \in T^{*,-}$, we assume that the line segments $\overline{P_i X}$ $(i = 2, 3)$ don't intersect with the interface Γ and $\overline{DE}$ and the line segment $\overline{P_1 X}$ meets Γ and $\overline{DE}$ at $\tilde{P}_1$ and $\bar{P}_1$, respectively. We have

$$\tilde{P} = \tilde{t}_P P_1 + (1 - \tilde{t}_P)X = (\tilde{x}, \tilde{y})^t, \ \ 0 \le \tilde{t}_P \le 1,$$

$$\bar{P} = \bar{t}_P P_1 + (1 - \bar{t}_P)X = (\bar{x}, \bar{y})^t, \ \ 0 \le \bar{t}_P \le 1.$$

Then, the following lemma holds.

Lemma 4.2.5. *Given a two-dimension vector $\boldsymbol{q}$ and matrix $\boldsymbol{N}$, points $X \in T^{*,-}$, $\overline{X} \in \overline{DE}$, there exists a function $\boldsymbol{v} \in \boldsymbol{U}_h^i(T)$ such that $\boldsymbol{v}(X) = \boldsymbol{q}$, $\nabla \boldsymbol{v}(X) = \boldsymbol{N}$, and*

$$\sum_{i=1}^{3} (\boldsymbol{\phi}_i + \boldsymbol{\phi}_{i+3}) \frac{1}{e_i} \int_{e_i} \boldsymbol{N}(P_i - X) ds(P_i) = (\boldsymbol{\phi}_1 + \boldsymbol{\phi}_4) \frac{1}{e_1} \int_{e_1} \overline{\boldsymbol{N}}(\overline{X} - P_1) ds(P_1),$$

where

$$\boldsymbol{N} = \begin{pmatrix} N_{11} & N_{12} \\ N_{21} & N_{22} \end{pmatrix}, \ \ \overline{\boldsymbol{N}} = \rho \begin{pmatrix} \bar{n}_1 \bar{n}_2 G_0 & \bar{n}_2^2 G_0 \\ -\bar{n}_1^2 G_0 & -\bar{n}_1 \bar{n}_2 G_0 \end{pmatrix}$$

and

$$G_0 = 2\bar{n}_1 \bar{n}_2 N_{11} - (\bar{n}_1^2 - \bar{n}_2^2)(N_{12} + N_{21}) - 2\bar{n}_1 \bar{n}_2 N_{22}.$$

Proof. Let

$$\boldsymbol{v}(Y) = \begin{cases} \boldsymbol{v}^-(Y), & \text{if } Y \in T^-, \\ \boldsymbol{v}^+(Y), & \text{if } Y \in T^+ \end{cases}$$

be a function in $\boldsymbol{U}_h^i(T)$. Since $\boldsymbol{v}(Y)$ is piecewise linear, $\boldsymbol{v}(X)=\boldsymbol{q}$ and $\nabla\boldsymbol{v}(X)=\boldsymbol{N}$ uniquely determine $\boldsymbol{v}^-(Y)$. Furthermore, $\boldsymbol{v}^+(Y)$ can be uniquely determined by interface conditions. Define

$$\boldsymbol{N}_0=\begin{pmatrix} N_{11}+\bar{n}_1\bar{n}_2\rho G_0 & N_{12}+\bar{n}_2^2\rho G_0 \\ N_{21}-\bar{n}_1^2\rho G_0 & N_{22}-\bar{n}_1\bar{n}_2\rho G_0 \end{pmatrix},$$

By multi-point Taylor expansion formulation, we derive

$$\boldsymbol{v}^-(P_i)=\boldsymbol{q}+\boldsymbol{N}(P_i-X),\ \ i=2,3 \tag{4.2.6}$$

and

$$\begin{aligned}\boldsymbol{v}^+(P_1)&=\boldsymbol{v}^+(\overline{X})+\nabla\boldsymbol{v}^+(\overline{X})(P_1-\overline{X})\\ &=\boldsymbol{q}+\boldsymbol{N}(\overline{X}-X)+\boldsymbol{N_0}(P_1-\overline{X})\\ &=\boldsymbol{q}+\boldsymbol{N}(P_1-X)+(\boldsymbol{N_0}-\boldsymbol{N})(P_1-\overline{X}),\end{aligned} \tag{4.2.7}$$

where P_i is an arbitrary fixed points $(i=1,2,3)$ on e_i, $X,P_2,P_3\in T^-$ and $P_1\in T^+$. Integrating (4.2.6) and (4.2.7) on each edge e_i with respect to P_i, we obtain the following multi-edge expansion for $\boldsymbol{v}(P_i)$,

$$\frac{1}{e_i}\int_{e_i}\boldsymbol{v}^-(P_i)ds(P_i)=\boldsymbol{q}+\frac{1}{e_i}\int_{e_i}\boldsymbol{N}(P_i-X)ds(P_i),\ \ i=2,3, \tag{4.2.8}$$

$$\begin{aligned}\frac{1}{e_1}\int_{e_1}\boldsymbol{v}^+(P_1)ds(P_1)=\boldsymbol{q}&+\frac{1}{e_1}\int_{e_1}\boldsymbol{N}(P_1-X)ds(P_1)\\ &+\frac{1}{e_1}\int_{e_1}(\boldsymbol{N_0}-\boldsymbol{N})(P_1-\overline{X})ds(P_1).\end{aligned} \tag{4.2.9}$$

It follows from (4.2.8)$-$(4.2.9) and Lemma 4.2.1 that

$$\boldsymbol{v}(X)=I_{h,T}\boldsymbol{v}(X)=\sum_{i=1}^{3}(\boldsymbol{\phi}_i+\boldsymbol{\phi}_{i+3})\frac{1}{e_i}\int_{e_i}\boldsymbol{v}(P_i)ds(P_1)$$

$$= \boldsymbol{q} + \sum_{i=1}^{3} (\boldsymbol{\phi}_i + \boldsymbol{\phi}_{i+3}) \frac{1}{e_i} \int_{e_i} \boldsymbol{N}(P_i - X) ds(P_i)$$

$$+ (\boldsymbol{\phi}_1 + \boldsymbol{\phi}_4) \frac{1}{e_1} \int_{e_1} (\boldsymbol{N_0} - \boldsymbol{N})(P_1 - \overline{X}) ds(P_1).$$

The desired result then follows. □

Lemma 4.2.6. *For any $\boldsymbol{u} \in \widetilde{\boldsymbol{C}}^2(T)$, $X \in T^{*,-}$ and $\overline{X} \in \overline{DE}$, it holds*

$$I_{h,T}\boldsymbol{u}(X) - \boldsymbol{u}(X) = \sum_{i=1}^{3} (\boldsymbol{\phi}_i + \boldsymbol{\phi}_{i+3}) \frac{1}{e_i} \int_{e_i} I_i ds(P_i)$$

$$+ (\boldsymbol{\phi}_1 + \boldsymbol{\phi}_4) \frac{1}{e_1} \int_{e_1} [\nabla \boldsymbol{u}(\tilde{P}_1)](P_1 - \tilde{P}_1) ds(P_1)$$

$$- (\boldsymbol{\phi}_1 + \boldsymbol{\phi}_4) \frac{1}{e_1} \int_{e_1} [\nabla \boldsymbol{u}(\overline{X})](P_1 - \overline{X}) ds(P_1), \tag{4.2.10}$$

where $I_1 = I_1^- + I_1^+$,

$$I_1^- = \int_0^{\tilde{t}_P} (1-t) \frac{d^2 \boldsymbol{u}}{dt^2} (tP_1 + (1-t)X) dt, \;\; I_1^+ = \int_{\tilde{t}_P}^1 (1-t) \frac{d^2 \boldsymbol{u}}{dt^2} (tP_1 + (1-t)X) dt$$

and

$$I_i = \int_0^1 (1-t) \frac{d^2 \boldsymbol{u}}{dt^2} (tP_i + (1-t)X) dt, \;\; i = 2, \; 3.$$

Proof. Using the similar technique in Lemma 4.2.5, for $i = 2, \; 3$, it is obvious that

$$\boldsymbol{u}(P_i) = \boldsymbol{u}(X) + \int_0^1 \frac{d\tilde{\boldsymbol{u}}(P_1)}{dt} dt = \boldsymbol{u}(X) + \nabla \boldsymbol{u}(X)(P_i - X) + I_i$$

and

$$\frac{1}{e_i} \int_{e_i} \boldsymbol{u}(P_i) ds(P_i) = \boldsymbol{u}(X) + \frac{1}{e_i} \int_{e_i} \nabla \boldsymbol{u}(X)(P_i - X) ds(P_i) + \frac{1}{e_i} \int_{e_i} I_i ds(P_i), \tag{4.2.11}$$

where $\tilde{\boldsymbol{u}}(P_i) = \boldsymbol{u}(tP_i + (1-t)X)$. For $i = 1$, some manipulation yields

$$
\begin{aligned}
\boldsymbol{u}(P_1) =&\boldsymbol{u}(X) + \int_0^1 \frac{d\tilde{\boldsymbol{u}}(P_1)}{dt}dt \\
=&\boldsymbol{u}(X) + \int_0^{\tilde{t}_P} \frac{d\tilde{\boldsymbol{u}}(P_1)}{dt}dt + \int_{\tilde{t}_P}^1 \frac{d\tilde{\boldsymbol{u}}(P_1)}{dt}dt \\
=&\boldsymbol{u}(X) + \nabla\boldsymbol{u}(X)(P_1 - X) - [\nabla\boldsymbol{u}(\tilde{P}_1)](P_1 - \tilde{P}_1) + I_1
\end{aligned}
$$

and

$$
\begin{aligned}
\frac{1}{e_1}\int_{e_1} \boldsymbol{u}(P_1)ds(P_1) = \boldsymbol{u}(X) + \frac{1}{e_i}\int_{e_1} \nabla\boldsymbol{u}(X)(P_1 - X)ds(P_1) + \frac{1}{e_1}\int_{e_1} I_1 ds(P_1) \\
+ \frac{1}{e_1}\int_{e_1} [\nabla\boldsymbol{u}(\tilde{P}_1)](P_1 - \tilde{P}_1)ds(P_1). \qquad (4.2.12)
\end{aligned}
$$

Combining(4.2.11)-(4.2.12), the following equality holds

$$
\begin{aligned}
I_{h,T}\boldsymbol{u}(X) = &\sum_{i=1}^{3}(\boldsymbol{\phi}_i + \boldsymbol{\phi}_{i+3})\frac{1}{e_i}\int_{e_i} \boldsymbol{u}(P_i)ds(P_i) \\
= &\boldsymbol{u}(X)\sum_{i=1}^{3}\boldsymbol{\phi}_i + \sum_{i=2,3}(\boldsymbol{\phi}_i + \boldsymbol{\phi}_{i+3})\frac{1}{e_i}\int_{e_i} I_i ds(P_i) \\
&+ \sum_{i=1}^{3}(\boldsymbol{\phi}_i + \boldsymbol{\phi}_{i+3})\frac{1}{e_i}\int_{e_i} \nabla\boldsymbol{u}(X)(P_i - X)ds(P_i) \\
&+ (\boldsymbol{\phi}_1 + \boldsymbol{\phi}_4)\frac{1}{e_1}\int_{e_1} ([\nabla\boldsymbol{u}(\tilde{P}_1)](P_1 - \tilde{P}_1) + I_1)ds(P_1). \qquad (4.2.13)
\end{aligned}
$$

By Lemma 4.2.5, we obtain

$$
\boldsymbol{u}(X) = \boldsymbol{u}(X)\sum_{i=1}^{3}\boldsymbol{\phi}_i + \sum_{i=1}^{3}(\boldsymbol{\phi}_i + \boldsymbol{\phi}_{i+3})\frac{1}{e_i}\int_{e_i} \nabla\boldsymbol{u}(X)(P_i - X)ds(P_i)
$$

$$+ (\boldsymbol{\phi}_1 + \boldsymbol{\phi}_4) \frac{1}{e_1} \int_{e_1} [\nabla \boldsymbol{u}(\overline{X})](P_1 - \overline{X}) ds(P_1). \tag{4.2.14}$$

Subtracting (4.2.13) from (4.2.14), the proof is completed. □

Theorem 4.2.1. *For any $T \in \mathcal{T}_h^i$ and $\boldsymbol{u} \in \tilde{\boldsymbol{H}}^2(T)$,*

$$\|\boldsymbol{u} - I_{h,T}\boldsymbol{u}\|_{0,T^{*,-}} \lesssim h^2 \|\boldsymbol{u}\|_{2,T}. \tag{4.2.15}$$

Proof. Since $\tilde{\boldsymbol{C}}^2(T)$ is dense in $\tilde{\boldsymbol{H}}^2(T)$ for any interface triangle, we only need to show (4.2.15) for any $\boldsymbol{u} \in \widetilde{\boldsymbol{C}}^2(T)$. According to Lemma 4.2.6, we estimate the righthand side of (4.2.10) term by term.

Let $\xi = tx_{P_i} + (1-t)x$, $\eta = ty_{P_i} + (1-t)y$, $P_i = (x_{P_i}, y_{P_i})$ $(i = 1, 2, 3)$. By Minkowski inequality and the same technique in [51, 57], for $i = 2, 3$, we deduce that

$$\begin{aligned}
\|\frac{1}{e_i}\int_{e_i} I_i ds(P_i)\|_{0,T^{*,-}} &= \left(\int_{T^{*,-}} \left(\frac{1}{|e_i|}\int_{e_i} I_i ds(P_i)\right)^2 d(X)\right)^{\frac{1}{2}} \\
&\leq \frac{1}{|e_i|}\int_{e_i}\left(\int_{T^{*,-}} I_i^2 d(X)\right)^{\frac{1}{2}} ds(P_i) \\
&\lesssim \frac{h^2}{|e_i|}\int_{e_i}\left(\int_{T^-}\left(\boldsymbol{u}_{xx}^2(\xi,\eta) + \boldsymbol{u}_{xy}^2(\xi,\eta) + \boldsymbol{u}_{yy}^2(\xi,\eta)\right)dX\right)^{\frac{1}{2}} ds(P_i) \\
&\lesssim \frac{h^2}{|e_i|}\int_{e_i} \|\boldsymbol{u}\|_{0,T^{*,-}} ds(P_i) \lesssim h^2 \|\boldsymbol{u}\|_{0,T^{*,-}}.
\end{aligned} \tag{4.2.16}$$

Then, according to Lemma 4.2.4, the following inequality holds

$$\|(\boldsymbol{\phi}_i + \boldsymbol{\phi}_{i+3}) I_i\|_{0,T^{*,-}} \lesssim h^2 \|\boldsymbol{u}\|_{2,T^-}, \quad i = 2,\ 3. \tag{4.2.17}$$

By similar tedious computations,

$$\|(\boldsymbol{\phi}_1 + \boldsymbol{\phi}_4) I_1^s\|_{0,T^{*,-}} \lesssim h^2 \|\boldsymbol{u}\|_{2,T^-}, \quad s = +, -. \tag{4.2.18}$$

Taking $\overline{X} = \tilde{P}^{\perp}$, for the second and third terms on the righthand side of (4.2.10), we derive

$$
\begin{aligned}
&\frac{1}{e_1}\int_{e_1}[\nabla \boldsymbol{u}(\tilde{P})](P_1-\tilde{P})ds(P_1)-\frac{1}{e_1}\int_{e_1}[\nabla \boldsymbol{u}(\overline{X})](P_1-\overline{X})ds(P_1)\\
&=\frac{1}{e_1}\int_{e_1}([\nabla \boldsymbol{u}(\tilde{P}_1)]-[\nabla \boldsymbol{u}(\tilde{P}^{\perp})])(P_1-\tilde{P})ds(P_1)+\frac{1}{e_1}\int_{e_1}[\nabla \boldsymbol{u}(\tilde{P}^{\perp})](\tilde{P}^{\perp}-\tilde{P})ds(P_1).
\end{aligned}
$$

Similarly, by Minkowski inequality,

$$
\begin{aligned}
&\|\frac{1}{e_1}\int_{e_1}([\nabla \boldsymbol{u}(\tilde{P}_1)]-[\nabla \boldsymbol{u}(\tilde{P}^{\perp})])(P_1-\tilde{P})ds(P_1)\|_{0,T^{*,-}}\\
&=\left(\int_{T^{*,-}}\left(\frac{1}{e_1}\int_{e_1}([\nabla \boldsymbol{u}(\tilde{P}_1)]-[\nabla \boldsymbol{u}(\tilde{P}^{\perp})])(P_1-\tilde{P})ds(P_1)\right)^2 d(X)\right)^{\frac{1}{2}}\\
&\leq\frac{1}{e_1}\int_{e_1}\left(\int_{T^{*,-}}\left(([\nabla \boldsymbol{u}(\tilde{P}_1)]-[\nabla \boldsymbol{u}(\tilde{P}^{\perp})])(P_1-\tilde{P})\right)^2 d(X)\right)^{\frac{1}{2}}ds(P_1). \qquad (4.2.19)
\end{aligned}
$$

Using the same technique in [51, 57], we expand $[\nabla \boldsymbol{u}(\tilde{P})]$ at the point X, for $i=1,2$,

$$
\begin{aligned}
\frac{\partial u_i^-(\tilde{P})}{\partial x}&=\frac{\partial u_i(X)}{\partial x}+\int_0^1\frac{d}{dt}\frac{\partial \tilde{u}_i(\tilde{P})}{\partial x}dt\\
&=\frac{\partial u_i(X)}{\partial x}+\int_0^1(1-t)(u_{ixx}(\xi,\eta)(\tilde{x}-x)+u_{ixy}(\xi,\eta)(\tilde{y}-y))dt\\
&=\frac{\partial u_i(X)}{\partial x}+f_{xi}(\tilde{x},\tilde{y}), \qquad (4.2.20)
\end{aligned}
$$

$$
\begin{aligned}
\frac{\partial u_i^-(\tilde{P})}{\partial y}&=\frac{\partial u_i(X)}{\partial y}+\int_0^1\frac{d}{dt}\frac{\partial \tilde{u}_i(\tilde{P})}{\partial y}dt\\
&=\frac{\partial u_i(X)}{\partial y}+\int_0^1(1-t)(u_{iyx}(\xi,\eta)(\tilde{x}-x)+u_{iyy}(\xi,\eta)(\tilde{y}-y))dt\\
&=\frac{\partial u_i(X)}{\partial y}+f_{yi}(\tilde{x},\tilde{y}) \qquad (4.2.21)
\end{aligned}
$$

with $\tilde{u}_i(\tilde{P}) = u_i(t\tilde{P} + (1-t)X)$, $\xi = t\tilde{x} + (1-t)x$, $\eta = t\tilde{y} + (1-t)y$, $\tilde{P} = (\tilde{x}, \tilde{y})$. Substituting (4.2.20) and (4.2.21) into (4.2.2), we get the desired Taylor expansion at the point X of $[\nabla \boldsymbol{u}(\tilde{P})]$,

$$\begin{aligned}
[\nabla \boldsymbol{u}(\tilde{P})] &= \rho G(\tilde{P}) \begin{pmatrix} n_1 n_2 & n_2^2 \\ -n_1^2 & -n_1 n_2 \end{pmatrix} \\
&= \rho G(X) \begin{pmatrix} n_1 n_2 & n_2^2 \\ -n_1^2 & -n_1 n_2 \end{pmatrix} + \rho J(X) \begin{pmatrix} n_1 n_2 & n_2^2 \\ -n_1^2 & -n_1 n_2 \end{pmatrix},
\end{aligned} \tag{4.2.22}$$

$$J(X) = 2n_1 n_2 f_{x1}(\tilde{P}) - (n_1^2 - n_2^2)(f_{y1}(\tilde{P}) + f_{x2}(\tilde{P}) - 2n_1 n_2 f_{y2}(\tilde{P}).$$

Let $\tilde{P}^{\perp} = (\tilde{x}^{\perp}, \tilde{y}^{\perp})$, we also obtain

$$\begin{aligned}
[\nabla \boldsymbol{u}(\tilde{P}^{\perp})] &= \rho G(\tilde{P}^{\perp}) \begin{pmatrix} \bar{n}_1 \bar{n}_2 & \bar{n}_2^2 \\ -\bar{n}_1^2 & -\bar{n}_1 \bar{n}_2 \end{pmatrix} \\
&= \rho G(X) \begin{pmatrix} \bar{n}_1 \bar{n}_2 & \bar{n}_2^2 \\ -\bar{n}_1^2 & -\bar{n}_1 \bar{n}_2 \end{pmatrix} + \rho J(X) \begin{pmatrix} \bar{n}_1 \bar{n}_2 & \bar{n}_2^2 \\ -\bar{n}_1^2 & -\bar{n}_1 \bar{n}_2 \end{pmatrix},
\end{aligned} \tag{4.2.23}$$

$$\bar{J}(X) = 2\bar{n}_1 \bar{n}_2 f_{x1}(\tilde{P}^{\perp}) - 2\bar{n}_1 \bar{n}_2 f_{y2}(\tilde{P}^{\perp}) - (\bar{n}_1^2 - \bar{n}_2^2)(f_{y1}(\tilde{P}^{\perp}) + f_{x2}(\tilde{P}^{\perp}).$$

For $i = 1, 2$,

$$f_{xi}(\tilde{P}^{\perp}) = \int_0^1 (1-t)(u_{ixx}(\xi, \eta)(\tilde{x}^{\perp} - x) + u_{ixy}(\xi, \eta)(\tilde{y}^{\perp} - y))dt,$$

$$f_{yi}(\tilde{P}^{\perp}) = \int_0^1 (1-t)(u_{iyx}(\xi, \eta)(\tilde{x}^{\perp} - x) + u_{iyy}(\xi, \eta)(\tilde{y}^{\perp} - y))dt.$$

Combining (4.2.19), (4.2.22), Lemma 4.2.2 with Lemma 4.2.4, the estimate hold

$$\|\frac{1}{e_1} \int_{e_1} ([\nabla \boldsymbol{u}(\tilde{P}_1)] - [\nabla \boldsymbol{u}(\tilde{P}^{\perp})])(P_1 - \tilde{P}) ds(P_1)\|_{0,T^{*,-}} \lesssim h^2 \|\boldsymbol{u}\|_{2,T^{*,-}}, \tag{4.2.24}$$

$$\|\frac{1}{e_1} \int_{e_1} [\nabla \boldsymbol{u}(\tilde{P}^{\perp})](\tilde{P}^{\perp} - \tilde{P}) ds(P_1)\|_{0,T^{*,-}} \lesssim h^2 \|\boldsymbol{u}\|_{2,T^{*,-}}. \tag{4.2.25}$$

From (4.2.17), (4.2.18), (4.2.24) and (4.2.25), the following result holds

$$\|\boldsymbol{u} - I_{h,T}\boldsymbol{u}\|_{0,T^{*,-}} \lesssim h^2 \|\boldsymbol{u}\|_{2,T}, \ \forall \boldsymbol{u} \in \widetilde{\boldsymbol{H}}^2(T).$$

The proof is completed. □

we next estimate H^1 norm of $\boldsymbol{u}(X) - I_{h,T}\boldsymbol{u}(X)$ on $T^{*,-}$.

Lemma 4.2.7. *For any $\boldsymbol{u} \in \widetilde{\boldsymbol{C}}^2(T)$, $\overline{X} \in \overline{DE}$ and $X \in T^{*,-}$, we have this result for $s = x,\ y$,*

$$\begin{aligned}
&\frac{\partial}{\partial x}(I_{h,T}\boldsymbol{u}(X) - \boldsymbol{u}(X)) \\
&= (\boldsymbol{\phi}_1^{'} + \boldsymbol{\phi}_4^{'}) \int_{e_1} \Big([\nabla \boldsymbol{u}(\tilde{P}_1)](P_1 - \tilde{P}_1) - [\nabla \boldsymbol{u}(\overline{X})](P_1 - \overline{X}))ds(P_1) \Big) \\
&- (\boldsymbol{\phi}_1 + \boldsymbol{\phi}_4) \frac{1}{e_1} \int_{e_1} [\nabla \boldsymbol{u}(\overline{X})]ds(P_1) + \sum_{i=1}^{3} (\boldsymbol{\phi}_i^{'} + \boldsymbol{\phi}_{i+3}^{'})\bar{I}_i.
\end{aligned} \tag{4.2.26}$$

Proof. We only give the proof for the case $s = x$. The case $s = y$ can be carried out similarly. For simplicity, let

$$\boldsymbol{\phi}_i^{'} = \frac{\partial \boldsymbol{\phi}_i(X)}{\partial x}, \quad \bar{I}_i = \frac{1}{e_i} \int_{e_i} I_i ds(P_i),\ i = 1, 2, 3.$$

According to Lemma 4.2.6, we deduce

$$\begin{aligned}
&\frac{\partial}{\partial x}(I_{h,T}\boldsymbol{u}(X) - \boldsymbol{u}(X)) \\
&= \frac{1}{e_1}(\boldsymbol{\phi}_1^{'} + \boldsymbol{\phi}_4^{'}) \int_{e_1} ([\nabla \boldsymbol{u}(\tilde{P}_1)](P_1 - \tilde{P}_1) - [\nabla \boldsymbol{u}(\overline{X})](P_1 - \overline{X}))ds(P_1) \\
&+ \frac{1}{e_1}(\boldsymbol{\phi}_1 + \boldsymbol{\phi}_4) \frac{\partial}{\partial x} \left(\int_{e_1} ([\nabla \boldsymbol{u}(\tilde{P}_1)](P_1 - \tilde{P}_1) - [\nabla \boldsymbol{u}(\overline{X})](P_1 - \overline{X}))ds(P_1) \right) \\
&+ \sum_{i=1}^{3} (\boldsymbol{\phi}_i + \boldsymbol{\phi}_{i+3}) \frac{\partial \bar{I}_i}{\partial x} + \sum_{i=1}^{3} (\boldsymbol{\phi}_i^{'} + \boldsymbol{\phi}_{i+3}^{'})\bar{I}_i.
\end{aligned} \tag{4.2.27}$$

Using (4.2.11), for $i=2,3$,

$$
\begin{aligned}
-\frac{\partial \bar{I}_i}{\partial x} &= \frac{\partial \boldsymbol{u}(X)}{\partial x} + \frac{\partial}{\partial x}\left(\frac{1}{e_i}\int_{e_i} \nabla \boldsymbol{u}(X)(P_i - X)ds(P_i)\right) \\
&= \frac{1}{e_i}\int_{e_i}\left(\frac{\partial \boldsymbol{u}(X)}{\partial x} + \frac{\partial}{\partial x}\left(\nabla \boldsymbol{u}(X)(P_i - X)\right)\right)ds(P_i) \\
&= \frac{1}{e_i}\int_{e_i} \boldsymbol{Q}(P_i - X)ds(P_i),
\end{aligned} \tag{4.2.28}
$$

where

$$
\boldsymbol{Q} = \begin{pmatrix} \frac{\partial^2 u_1(X)}{\partial x^2} & \frac{\partial^2 u_1(X)}{\partial y \partial x} \\ \frac{\partial^2 u_2(X)}{\partial x^2} & \frac{\partial^2 u_2(X)}{\partial y \partial x} \end{pmatrix}.
$$

Similarly, from (4.2.12), we derive

$$
-\frac{\partial \bar{I}_1}{\partial x} = \frac{1}{e_1}\int_{e_1} \boldsymbol{Q}(P_1 - X)ds(P_1) + \frac{\partial}{\partial x}\left(\frac{1}{e_1}\int_{e_1} [\nabla \boldsymbol{u}(\tilde{P}_1)](P_1 - \tilde{P}_1)ds(P_1)\right). \tag{4.2.29}
$$

Combining (4.2.28) with (4.2.29),

$$
\begin{aligned}
\sum_{i=1}^{3} \frac{\partial \bar{I}_i}{\partial x}(\boldsymbol{\phi}_i + \boldsymbol{\phi}_{i+3}) = &-\sum_{i=1}^{3}(\boldsymbol{\phi}_i + \boldsymbol{\phi}_{i+3})\frac{1}{e_i}\int_{e_i} \boldsymbol{Q}(P_i - X)ds(P_i) \\
&-(\boldsymbol{\phi}_1 + \boldsymbol{\phi}_4)\frac{\partial}{\partial x}\left(\frac{1}{e_1}\int_{e_1} [\nabla \boldsymbol{u}(\tilde{P}_1)](P_1 - \tilde{P}_1)ds(P_1)\right).
\end{aligned} \tag{4.2.30}
$$

By Lemma 4.2.5, there exists a function $\boldsymbol{v} \in \boldsymbol{U}_h^i(T)$ be such that $\nabla \boldsymbol{v}(X) = \boldsymbol{Q}$ and

$$
\sum_{i=1}^{3}(\boldsymbol{\phi}_i + \boldsymbol{\phi}_{i+3})\frac{1}{e_i}\int_{e_i} \boldsymbol{Q}(P_i - X)ds(P_i) = -(\boldsymbol{\phi}_1 + \boldsymbol{\phi}_4)\frac{1}{e_1}\int_{e_1} \overline{\boldsymbol{Q}}(P_1 - \overline{X})ds(P_1). \tag{4.2.31}
$$

Substituting (4.2.31) into (4.2.30), we obtain

$$
\sum_{i=1}^{3} \frac{\partial \bar{I}_i}{\partial x}(\boldsymbol{\phi}_i + \boldsymbol{\phi}_{i+3}) = (\boldsymbol{\phi}_1 + \boldsymbol{\phi}_4)\frac{1}{e_1}\int_{e_1} \overline{\boldsymbol{Q}}(P_1 - \overline{X})ds(P_1)
$$

$$-(\boldsymbol{\phi}_1+\boldsymbol{\phi}_4)\frac{1}{e_1}\int_{e_1}\frac{\partial}{\partial x}\Big([\nabla\boldsymbol{u}(\tilde{P}_1)](P_1-\tilde{P}_1)\Big)\,ds(P_1), \tag{4.2.32}$$

where

$$\overline{\boldsymbol{Q}}=\rho\begin{pmatrix}\bar{n}_1\bar{n}_2Q_0 & \bar{n}_2^2Q_0\\ -\bar{n}_1^2Q_0 & -\bar{n}_1\bar{n}_2Q_0\end{pmatrix}$$

and

$$Q_0=2\bar{n}_1\bar{n}_2\frac{\partial^2u_1(X)}{\partial x^2}-(\bar{n}_1^2-\bar{n}_2^2)\left(\frac{\partial^2u_1(X)}{\partial y\partial x}+\frac{\partial^2u_2(X)}{\partial x^2}\right)-2\bar{n}_1\bar{n}_2\frac{\partial^2u_2(X)}{\partial y\partial x}.$$

Finally, inserting (4.2.32) into (4.2.27), the desired result can be deduced. □

Proceeding as in the proof of Theorem 4.2.1, by Lemma 4.2.7, the following theorem holds.

Theorem 4.2.2. *For any $T\in\mathcal{T}_h^i$ and $\boldsymbol{u}\in\tilde{\boldsymbol{H}}^2(T)$, it holds*

$$\|\partial_s(I_{h,T}\boldsymbol{u}-\boldsymbol{u})\|_{0,T^{*,-}}\lesssim h\|\boldsymbol{u}\|_{2,T},\qquad s=x,y.$$

Arguing as Lemma 4.2.6, Theorem 4.2.1 and Lemma 4.2.6, we have similar result on $T^{*,+}$.

Theorem 4.2.3. *For any $T\in\mathcal{T}_h^i$ and $\boldsymbol{u}\in\tilde{\boldsymbol{H}}^2(T)$,*

$$\|\boldsymbol{u}-I_{h,T}\boldsymbol{u}\|_{0,T^{*,+}}\lesssim h^2\|\boldsymbol{u}\|_{2,T},$$

$$\|\partial_s(\boldsymbol{u}-I_{h,T}\boldsymbol{u})\|_{0,T^{*,+}}\lesssim h\|\boldsymbol{u}\|_{2,T},\qquad s=x,y.$$

Using the same argument in [52], the following theorem holds.

Theorem 4.2.4. *For any $\boldsymbol{u}\in\tilde{\boldsymbol{H}}^2(T)$ and $p>1$, we have*

$$\|I_{h,T}\boldsymbol{u}-\boldsymbol{u}\|_{0,T^*}\lesssim h^2\|\boldsymbol{u}\|_{2,T}+Ch^{5/2-3/p}\|\boldsymbol{u}\|_{1,p,T^*},$$

$$\|\partial_s(I_{h,T}\boldsymbol{u}-\boldsymbol{u})\|_{0,T^*}\lesssim h\|\boldsymbol{u}\|_{2,T}+Ch^{3/2-3/p}\|\boldsymbol{u}\|_{1,p,T^*},\qquad s=x,\ y,$$

where $T\in\mathcal{T}_h^i$ is an arbitrary interface element.

Finally, combining Theorems 4.2.1-4.2.4, arguing as Theorem 3.7 in [52], we can deduce our main results of the interpolation error estimate.

Theorem 4.2.5. *For any $\boldsymbol{u} \in \tilde{\boldsymbol{H}}^2(\Omega)$ and $h > 0$ small enough,*

$$\|I_h \boldsymbol{u} - \boldsymbol{u}\|_{0,\Omega} \lesssim h^2 \|\boldsymbol{u}\|_{\widetilde{H}^2(\Omega)},$$

$$\|\partial_s (I_h \boldsymbol{u} - \boldsymbol{u})\|_{0,\Omega} \lesssim h \|\boldsymbol{u}\|_{\widetilde{H}^2(\Omega)}, \qquad s = x,\ y.$$

For the pressure space, as we mentioned in Chapter 3, we choose extension operators $E_k^s : H^k(\Omega^s) \to H^k(\Omega)$ such that $(E_1^s q)|_{\Omega^s} = q$ and

$$\|E_k^s w\|_{k,\Omega} \le C\|w\|_{k,\Omega^s},\ \ \forall w \in H^k(\Omega^s),\ s = +,-.$$

Let C_h be the local projection on the piecewise constants. Define

$$C_h q \doteq \begin{cases} C_h^- q^- & \text{in } \Omega^-, \\ C_h^+ q^+ & \text{in } \Omega^+, \end{cases}$$

where $C_h^s q_s \doteq (C_h E_1^s q^s)|_{\Omega^s}$, $s = +, -$. Then,

Theorem 4.2.6. *For any $(\boldsymbol{v}, q) \in \tilde{\boldsymbol{H}}^2(\Omega_1 \cup \Omega_2) \times H^1(\Omega_1 \cup \Omega_2)$,*

$$\|(\boldsymbol{v} - \boldsymbol{I}_h \boldsymbol{v}, q - C_h q)\|_{\boldsymbol{U}\times M} \lesssim h(\|\boldsymbol{v}\|_{\tilde{\boldsymbol{H}}^2(\Omega_1\cup\Omega_2)} + \|q\|_{H^1(\Omega_1\cup\Omega_2)}). \tag{4.2.33}$$

4.3 Stability analysis

By the same technique in [57], we derive the trace inequality to IFE functions in $\boldsymbol{U}_h^i(T)$ for $T \in \mathcal{T}_h^i$ through the following lemmas.

Lemma 4.3.1. *For any $\boldsymbol{v} \in \boldsymbol{U}_h^i(T)$ in the interface element T defined as* (4.1.2)*, we have*

$$\|(b_1^-, c_1^-, b_2^-, c_2^-)\| \lesssim \|(b_1^+, c_1^+, b_2^+, c_2^+)\|, \tag{4.3.1}$$

where $\|\cdot\|$ is a Euclidean norm.

Proof. We only prove the right inequality in (4.3.1), the left inequality can be proved similarly. By the interface conditions, we have

$$M^-(a_1^-, b_1^-, c_1^-, a_2^-, b_2^-, c_2^-)^t = M^+(a_1^+, b_1^+, c_1^+, a_2^+, b_2^+, c_2^+),$$

where

$$M^s = \begin{pmatrix} 1 & 0 & e & 0 & 0 & 0 \\ 1 & d & 0 & 0 & 0 & 0 \\ 0 & 0 & 0 & 1 & 0 & e \\ 0 & 0 & 0 & 1 & d & 0 \\ 0 & \mu^s ed & \alpha\mu^s/2 & 0 & \alpha\mu^s/2 & \mu^s ed \\ 0 & 1 & 0 & 0 & 0 & 1 \end{pmatrix}, \ s = +, -.$$

Since $(d, e) \neq (0, 0)$, we have $\det(M^s) \neq 0$ $(d \neq e)$. Then, by solving above equations system, we derive

$$b_1^+ = (1 - 2\xi^2\eta)b_1^- - \xi\eta(c_1^- + b_2^-) - 2\xi^2\eta c_2^-,$$

$$b_2^+ = \frac{2e}{d}\xi^2\eta b_1^- + \frac{e}{d}\xi\eta c_1^- + (1 + \frac{e}{d}\xi\eta)b_2^- + \frac{2e}{d}\xi^2\eta c_2^-,$$

$$c_1^+ = -\frac{d}{e}\xi^2\eta b_1^- + (1 - \frac{d}{e}\xi\eta)c_1^- - \frac{d}{e}\xi\eta b_2^- - \frac{d}{e}\xi^2\eta c_2^-,$$

$$c_2^+ = 2\xi^2\eta b_1^- + \xi\eta(c_1^- + b_2^-) + (1 + 2\xi^2\eta)c_2^-,$$

where $\xi = \frac{de}{e^2 - d^2}$, $\eta = \frac{\mu^- - \mu^+}{\mu^+}$. Therefore, there exists a constant C that depends on μ^s $(s = +, -)$ such that (4.3.1) holds. □

By the same technique in Lemma 5.2 of [57], we have the trace inequality.

Lemma 4.3.2. *For any linear IFE function $\boldsymbol{v}$,*

$$\|\mu\boldsymbol{\epsilon}(\boldsymbol{v}) \cdot \mathbf{n}\|_{0,e} \lesssim h^{1/2}|T|^{-1/2}\|\mu\boldsymbol{\epsilon}(\boldsymbol{v})\|_{0,T}, \tag{4.3.2}$$

where $e \in \varepsilon_h^i$ is an interface edge and $T \in \mathcal{T}_h^i$ is an interface element.

Define norms for the spaces $\boldsymbol{U}_h$, M_h and $\boldsymbol{U}_h \times M_h$

$$\|\boldsymbol{v}_h\|_h = \left(\sum_{T\in\mathcal{T}_h} \big(\mu\boldsymbol{\epsilon}(\boldsymbol{v}_h), \boldsymbol{\epsilon}(\boldsymbol{v}_h)\big)_T + \sum_{e\in\varepsilon_h^i} h^{-1}(\mu[\boldsymbol{v}_h],[\boldsymbol{v}_h])_e \right)^{\frac{1}{2}}, \quad \forall \boldsymbol{v}_h \in \boldsymbol{U}_h, \tag{4.3.3}$$

$$\|q_h\|_{0,h} = (\|q_h^-\|^2_{L^2(\Omega^-_{h,E})} + \|q_h^+\|^2_{L^2(\Omega^+_{h,E})})^{1/2}, \quad \forall q_h \in M_h, \tag{4.3.4}$$

$$\|(\boldsymbol{v}_h, q_h)\|_H = (\|\boldsymbol{v}_h\|_h^2 + \|q_h\|^2_{0,h})^{1/2}, \quad \forall (\boldsymbol{u}_h, p_h) \in \boldsymbol{U}_h \times M_h. \tag{4.3.5}$$

Now, we prove the coercivity of the bilinear form $a_h(\boldsymbol{u}_h, \boldsymbol{v}_h)$ in the IFE space with respect to the energy norm.

Theorem 4.3.1. *There exists a constant $\kappa > 0$ such that*

$$\kappa \|\boldsymbol{v}_h\|_h^2 \le a_h(\boldsymbol{v}_h, \boldsymbol{v}_h) \quad \forall \boldsymbol{v}_h \in S_{h,0}(\Omega). \tag{4.3.6}$$

Proof. For each $e \in \varepsilon_h^i$, by Cauchy-Schwarz inequality and Lemma 4.3.2, there exists a constant $\delta > 0$ such that

$$\begin{aligned} 2\sum_{e\in\varepsilon_h^i}(\{\boldsymbol{n}\cdot\boldsymbol{\epsilon}(\boldsymbol{v}_h)\},[\boldsymbol{v}_h])_e &\le \sum_{e\in\varepsilon_h^i}(2\delta h(\boldsymbol{n}\cdot\boldsymbol{\epsilon}(\boldsymbol{v}_h), \boldsymbol{n}\cdot\boldsymbol{\epsilon}(\boldsymbol{v}_h))_e + \frac{4}{\delta h}\|[\boldsymbol{v}_h]\|^2_{0,e}) \\ &\le \sum_{T\in\mathcal{T}_h^i} C\delta\,(\boldsymbol{\epsilon}(\boldsymbol{v}_h), \boldsymbol{\epsilon}(\boldsymbol{v}_h))_T + \sum_{e\in\varepsilon_h^i}\frac{4}{\delta h}([\boldsymbol{v}_h],[\boldsymbol{v}_h])_e. \end{aligned}$$

Finally,

$$\begin{aligned} a_h(\boldsymbol{v}_h, \boldsymbol{v}_h) \ge \sum_{T\in\mathcal{T}_h} \big(\mu\boldsymbol{\epsilon}(\boldsymbol{v}_h), \boldsymbol{\epsilon}(\boldsymbol{v}_h)\big)_T - 2\sum_{T\in\mathcal{T}_h^i} C\delta\,(\mu\boldsymbol{\epsilon}(\boldsymbol{v}_h), \boldsymbol{\epsilon}(\boldsymbol{v}_h))_T \\ - 2\sum_{e\in\varepsilon_h^i}\frac{4}{\delta h}(\mu[\boldsymbol{v}_h],[\boldsymbol{v}_h])_e + \sum_{e\in\varepsilon_h^i} h^{-1}(\mu[\boldsymbol{v}_h],[\boldsymbol{v}_h])_e. \end{aligned}$$

Therefore, there exists a constant κ such that $a_h(\boldsymbol{v}_h, \boldsymbol{v}_h) \ge \kappa\|\boldsymbol{v}_h\|_h^2$ by choosing a proper δ. $\square$

Theorem 4.3.2. *For $(\boldsymbol{v}_h, q_h), (\boldsymbol{\omega}_h, \lambda_h) \in \boldsymbol{U}_h \times M_h$, there exists a constant C_μ which only depends on μ, such that*

$$A_h((\boldsymbol{v}_h, q_h), (\boldsymbol{\omega}_h, \lambda_h)) \leq C_\mu \|(\boldsymbol{v}_h, q_h)\|_H \|(\boldsymbol{\omega}_h, \lambda_h)\|_H. \tag{4.3.7}$$

The proof is same as the process in Theorem 3.2.1.

Denote the nonconforming P_1-P_0 element space pair on $\Omega^s_{h,F}$ by $\boldsymbol{V}_h(\Omega^s_{h,F}) \times Q_{h,0}(\Omega^s_{h,F})$, where

$$\boldsymbol{V}_h(\Omega^s_{h,F}) = \{\boldsymbol{w}_h \in (L^2(\Omega^s_{h,F}))^2; \boldsymbol{w}_h|_T \in P_1(T), \int_e [\boldsymbol{w}_h] ds = 0, \ \forall e \in \varepsilon_h\},$$

$$Q_{h,0}(\Omega^s_{h,F}) = Q_h(\Omega^s_{h,F}) \cap L^2_0(\Omega^s_{h,F}).$$

For any $q_h \in Q_{h,0}(\Omega^s_{h,F})$, there exists $\boldsymbol{v}^s_0 \in \boldsymbol{V}_h(\Omega^s_{h,F})$ satisfies

$$\|\nabla \boldsymbol{v}_0\|_{L^2(\Omega^s_{h,F})} \lesssim b_h(\boldsymbol{v}^s_0, q^s_h), \tag{4.3.8}$$

$$\|q_h\|_{L^2(\Omega^s_{h,F})} \lesssim b_h(\boldsymbol{v}^s_0, q^s_h). \tag{4.3.9}$$

We derive the inf-sup stability of $b_h(\cdot,\cdot)$ on $\boldsymbol{V}_h \times Q_h$.

Lemma 4.3.3. *For any given $q_h \in Q_h$, there exists a function $\boldsymbol{v}_0 \in \boldsymbol{V}_h$ satisfies $\boldsymbol{v}_0|_{\Omega^s_{h,F}} = 0$ $(s = +, -)$ such that*

$$c_1 \|q_h\|^2_{Q_h} \leq b_h(\boldsymbol{v}_0, q_h) + j_h(q_h, q_h), \tag{4.3.10}$$

where c_1 is independent of the mesh size, the viscosity parameters and the position of interface with respect to the mesh.

Proof. By the inequality (4.3.9), we obtain

$$C \sum_{i=1,2} \|q_h\|_{L^2(\Omega^s_{h,F})} \leq b_h(\boldsymbol{v}_0, q_h). \tag{4.3.11}$$

Moveover,

$$C \sum_{i=1,2} \|q_h\|_{L^2(\Omega^s_{h,F})} + j_h(q_h, q_h) \leq b_h(\boldsymbol{v}_0, q_h) + j_h(q_h, q_h). \tag{4.3.12}$$

Combining with Lemma 3.2.4, it holds

$$min\{C, 1\} \sum_{i=1,2} \|q_h\|_{L^2(\Omega^s_{h,E})} \leq b_h(\boldsymbol{v}_0, q_h) + j_h(q_h, q_h). \tag{4.3.13}$$

Let $c_1 = min\{C, 1\}$, the proof is completed. □

By the same technique in Theorem 3.2.2, we could show the stability of the discrete formulation.

Theorem 4.3.3. *If h is sufficient small, for any $(\boldsymbol{v}_h, q_h) \in \boldsymbol{U}_h \times M_h$, there exists a positive constant C_μ independent of h and the location of interface relative to the mesh such that*

$$\sup_{(\boldsymbol{\omega}_h, \lambda_h) \in \boldsymbol{U}_h \times M_h} \frac{A_h((\boldsymbol{v}_h, q_h), (\boldsymbol{\omega}_h, \lambda_h))}{\|(\boldsymbol{\omega}_h, \lambda_h)\|_H} \geq C_\mu \|(\boldsymbol{v}_h, q_h)\|_H. \tag{4.3.14}$$

4.4 Error analysis

We start by proving the interpolation error estimate in the energy norm.

Lemma 4.4.1. *For $\boldsymbol{u} \in \tilde{\boldsymbol{H}}^2(\Omega)$, it holds*

$$\|\boldsymbol{u} - I_h \boldsymbol{u}\|_h \lesssim h \|\boldsymbol{u}\|_{\widetilde{H}^2(\Omega)}. \tag{4.4.1}$$

Proof. We first note

$$\|\boldsymbol{u} - I_h\boldsymbol{u}\|_h^2 = \sum_{T \in \mathcal{T}_h} \big(\mu \boldsymbol{\epsilon}(\boldsymbol{u} - I_h\boldsymbol{u}), \boldsymbol{\epsilon}(\boldsymbol{u} - I_h\boldsymbol{u})\big)_T + \sum_{e \in \varepsilon_h^i} h^{-1} (\mu[\boldsymbol{u} - I_h\boldsymbol{u}], [\boldsymbol{u} - I_h\boldsymbol{u}])_e, \tag{4.4.2}$$

According to Theorem 4.2.5,

$$\sum_{T\in\mathcal{T}_h}\big(\mu\boldsymbol{\epsilon}(\boldsymbol{u}-I_h\boldsymbol{u}),\boldsymbol{\epsilon}(\boldsymbol{u}-I_h\boldsymbol{u})\big)_T\lesssim h^2\|\boldsymbol{u}\|^2_{\widetilde{H}^2(\Omega)}. \tag{4.4.3}$$

Therefore, we only need to estimate the last term in (4.4.2). By the standard trace inequality,

$$\begin{aligned}\|[\boldsymbol{u}-I_h\boldsymbol{u}]\|^2_{0,e}&\le(\|(\boldsymbol{u}-I_h\boldsymbol{u})|_{T_1}\|_{0,e}+\|(\boldsymbol{u}-I_h\boldsymbol{u})|_{T_2}\|_{0,e})^2\\&\lesssim\sum_{i=1}^{2}|e||T_i|^{-1}(\|(\boldsymbol{u}-I_h\boldsymbol{u})\|_{0,T_i}+h\|\nabla(\boldsymbol{u}-I_h\boldsymbol{u})\|_{0,T_i})^2\\&\lesssim\sum_{i=1}^{2}|e|(h\|\boldsymbol{u}\|_{\widetilde{H}^2(T_i)})^2.\end{aligned} \tag{4.4.4}$$

Combining (4.4.4), (4.4.2) with (4.4.3), we can deduce the desired result. □

Theorem 4.4.1. *The problem* (4.1.13) *has a unique solution pair* $(\boldsymbol{u_h},p_h)\in\boldsymbol{U}_h\times M_h$. *Furthermore, assume that the solution pair* $(\boldsymbol{u},p)$ *of the problem* (4.1.11) *belongs to* $\tilde{\boldsymbol{H}}^2(\Omega_1\cup\Omega_2)\times H^1(\Omega_1\cup\Omega_2)$. *There exists a constant* $C_\mu>0$ *such that*

$$\|(\boldsymbol{u}-\boldsymbol{u}_h,p-p_h)\|_H\le C_\mu h(\|\boldsymbol{u}\|_{\tilde{\boldsymbol{H}}^2(\Omega^+\cup\Omega^-)}+\|p\|_{H^1(\Omega^+\cup\Omega^-)}). \tag{4.4.5}$$

Proof. From Theorem 4.3.3, we conclude the problem (4.1.13) has a unique solution pair $(\boldsymbol{u_h},p_h)\in\boldsymbol{U}_h\times M_h$. By the triangle inequality,

$$\|(\boldsymbol{u}-\boldsymbol{u}_h,p-p_h)\|_H\lesssim\|(\boldsymbol{u}-\boldsymbol{I}_h\boldsymbol{u},p-C_hp)\|_H+\|(\boldsymbol{I}_h\boldsymbol{u}-\boldsymbol{u}_h,C_hp-p_h)\|_H.$$

According to Green's formula,

$$\begin{aligned}F((\boldsymbol{v}_h,q_h))=&a_h(\boldsymbol{u},\boldsymbol{v}_h)-b_h(\boldsymbol{v}_h,p)+b_h(\boldsymbol{u},q_h)+c(p_h,q_h)\\&-\sum_{e\in\varepsilon_h^n}\langle\{(\mu\epsilon(\boldsymbol{u})-p\boldsymbol{I})\boldsymbol{n}\},[\boldsymbol{v}_h]\rangle_e+\gamma j_h(p_h,q_h)\\=&A_h((\boldsymbol{u},p),(\boldsymbol{v}_h,q_h))-E((\boldsymbol{u},p),(\boldsymbol{v}_h,q_h)),\end{aligned}$$

where

$$E((\boldsymbol{u},p),(\boldsymbol{v}_h,q_h)) = \sum_{e\in\varepsilon_h^n}\langle\{(\mu\epsilon(\boldsymbol{u})-p\boldsymbol{I})\boldsymbol{n}\},[\boldsymbol{v}_h]\rangle_e - \gamma j_h(C_hp,q_h). \tag{4.4.6}$$

From Theorem 4.3.3, we obtain

$$\begin{aligned}
&\|(\boldsymbol{I}_h\boldsymbol{u}-\boldsymbol{u}_h, C_hp-p_h)\|_H \\
&\le \frac{1}{C_\mu}\sup_{(\boldsymbol{v}_h,q_h)\in\boldsymbol{U}_h\times M_h}\frac{A_h((\boldsymbol{\Pi}_h\boldsymbol{u}-\boldsymbol{u}_h,C_hp-p_h),(\boldsymbol{v}_h,q_h))}{\|(\boldsymbol{v}_h,q_h)\|_H} \\
&= \frac{1}{C_\mu}\sup_{(\boldsymbol{v}_h,q_h)\in\boldsymbol{U}_h\times M_h}\frac{A((\boldsymbol{I}_h\boldsymbol{u}-\boldsymbol{u},C_hp-p),(\boldsymbol{v}_h,q_h))+E((\boldsymbol{u},p),(\boldsymbol{v}_h,q_h))}{\|(\boldsymbol{v}_h,q_h)\|_H}.
\end{aligned} \tag{4.4.7}$$

For any edge $e\in\varepsilon_h^n$, it is easy to derive that

$$\sum_{e\in\varepsilon_h^n}\langle\{(\mu\epsilon(\boldsymbol{u})-p\boldsymbol{I})\boldsymbol{n}\},[\boldsymbol{v}_h]\rangle_e \lesssim h\|\boldsymbol{v}_h\|_{\boldsymbol{U}_h}(\|\boldsymbol{u}\|_{\tilde{\boldsymbol{H}}^2(\Omega^+\cup\Omega^-)}+\|p\|_{H^1(\Omega^+\cup\Omega^-)}). \tag{4.4.8}$$

Moreover, by the same technique in Theorem 3.2.1,

$$j_h(C_hp,q_h)\lesssim h\|p\|_{H^1(\Omega^-\cup\Omega^+)}\|q_h\|_{0,h}. \tag{4.4.9}$$

Combining (4.4.6), (4.4.7), (4.4.8) with (4.4.9), we have the desired estimate,

$$\begin{aligned}
&\|(\boldsymbol{I}_h\boldsymbol{u}-\boldsymbol{u}_h,C_hp-p_h)\|_H \\
&\le C_\mu(\|(\boldsymbol{u}-\boldsymbol{I}_h\boldsymbol{u},p-C_hp)\|_{\boldsymbol{U}\times M}+h(\|\boldsymbol{u}\|_{\tilde{\boldsymbol{H}}^2(\Omega^+\cup\Omega^-)}+\|p\|_{H^1(\Omega^+\cup\Omega^-)})).
\end{aligned} \tag{4.4.10}$$

Finally, by Theorem 4.2.6,

$$\|(\boldsymbol{v}-\boldsymbol{I}_h\boldsymbol{v},p-C_hp)\|_H\lesssim h(\|\boldsymbol{v}\|_{\tilde{\boldsymbol{H}}^2(\Omega^+\cup\Omega^-)}+\|p\|_{H^1(\Omega^+\cup\Omega^-)}). \tag{4.4.11}$$

Combining (4.4.11) with (4.4.10), the proof is completed. □

Chapter 5 Conclusions and future works

In my dissertation, we mainly develop the nonconforming immersed finite element methods for elasticity interface problem. Optimal approximation capability for the broken Sobolev space $H^2(\Omega_1 \cup \Omega_2)$ and the optimal finite element error estimate are both proved. Moreover, a relatively new approach for interface problems, enriched finite element method, is also developed. Before we give the nonconforming enriched finite element method, this method is merely applied on conforming elements. Finally, we first present the approximation capability and the optimal finite element error estimate of immersed finite element method for the stokes interface problem.

We have shown that the immersed finite element method is an efficient method for interface problems. However, there are many interface problems still unsolved. We list a few research topics beyond this dissertation.

- IFEMs for fourth order planar interface problems.
- How to solve the parabolic interface problems with moving interfaces.
- Apply IFEMs to other interface problems, such as fluid-structure interactions.

Bibliography

[1] R. A. Adams and J. J. Fournier. Sobolev Spaces. *Academic press,* 2003.

[2] S. Adjerid, N. Chaabane and T. Lin. An immersed discontinuous finite element method for Stokes interface problems. *Computer Methods in Applied Mechanics and Engineering*, 293(2015), 170–190.

[3] S. Adjerid, T. Lin and J. Wang. Higher-order immersed discontinuous Galerkin methods. *Int. J. Inf. Syst. Sci.*, 3(2007), 555-568.

[4] D. M. Anderson, G. B. McFadden and A. A. Wheeler. Diffuse interface methods in fluid mechanics. *Annual Review of Fluid Mechanics*, 30(1998), 139–165.

[5] P. F. Antonietti and B. Ayuso. Two-level Schwarz preconditioners for super penalty, discontinuous Galerkin methods. *Communications in Computational Physics*, 5(2009), 398-412.

[6] D. N. Arnold. An interior penalty finite element method with discontinuous elements. *SIAM J. Numer. Anal.*, 19(1982), 742–760.

[7] J. M. Arrieta, A. Rodríguez-Bernal and J. D. Rossi. The best Sobolev trace constant as limit of the usual Sobolev constant for small strips near the boundary. *Proc. R. Soc. Edinb. Sect. A*, 138(2008), 223-237.

[8] I. Babuška. The finite element method for elliptic equations with discontinuous coefficients. *Computing*, 5(1970), 207–213.

[9] I. Babuška and M. Zlámal. Nonconforming elements in the finite element method with penalty. *SIAM J. Numer. Anal.*, 10(1973), 863-875.

[10] T. Belytschko and T. Black. Elastic crack gorth in finite elements with minimal remeshing. *Int. J. Numer. Meth. Engng.*, 45(1999), 601-620.

[11] M. Bendsoe and O. Sigmund. Topology Optimization: Theory, Method, and Applications. *Springer Science and Business Media*, 2003.

[12] P. B. Bochev, C. R. Dohrmann and M. D. Gunzburger. Stabilization of lower order mixed finite elements for the Stokes equations. *SIAM J. Numer. Anal.*, 44(2006), 82–101.

[13] J. H. Bramble and J. T. King. A robust finite element method for nonhomogeneous Dirichlet problems in domains with curved boundaries. *Math. Comp.*, 63(1994), 1-17.

[14] J. H. Bramble and J. T. King. A finite element method for interface problems in domains with smooth boundaries and interfaces. *Advances in Computational Mathematics*, 6(1996), 109–138.

[15] S. Brenner. Korn's inequalities for piecewise H^1 vector fields. *Math. Comp.*, 73(2004), 1067–1087.

[16] S. Brenner, and L. Sung. Linear finite element methods for planar linear elasticity. *Math. Comp*, 59(1992), 321-338.

[17] S. Brenner and R. Scott. The Mathematical Theory of Finite Element Methods. *Springer-Verlag*, New York.

[18] F. Brezzi and M. Fortin. Mixed and Hybrid Finite Element Methods. *Springer-Verlag*, Berlin, 1991.

[19] F. Brezzi and A. Russo. Discontinuous Galerkin approximations for elliptic problems. *Numerical Methods for Partial Differential Equations*, 16(2015), 365-378.

[20] E. Burman. Ghost penalty. *Comptes Rendus Mathematique*, 348(2010), 1217–1220.

[21] E. Burman, J. Guzmán, M. A. Sánchez and M. Sarkis. Robust flux error estimation of an unfitted Nitsche method for high-contrast interface problems. *IMA Journal of Numerical Analysis*, 2016.

[22] E. Burman and P. Hansbo. Fictitious domain finite element methods using cut elements: Ii. A stabilized Nitsche method. *Applied Numerical Mathematics*, 62(2012), 328–341.

[23] E. Burman and P. Hansbo. Fictitious domain methods using cut elements: Iii. A stabilized Nitsche method for Stokes problem. *ESAIM: Mathematical Modelling and Numerical Analysis*, 48(2014), 859–874.

[24] L. Cattaneo, L. Formaggia, G. F. Iori, A. Scotti and P. Zunino. Stabilized extended finite elements for the approximation of saddle point problems with unfitted interfaces. *Calcolo*, 52(2015), 123–152.

[25] Z. Chen, Z. Wu and Y. Xiao. An adaptive immersed finite element method with arbitrary Lagrangian-Eulerian scheme for parabolic equations in time variable domains. *International Journal of Numerical Analysis and Modeling*, 12(2015), 567–591.

[26] Z. Chen and J. Zou. Finite element methods and their convergence for elliptic and parabolic interface problems. *Numer. Math.*, 79(1998), 175-202.

[27] S. H. Chou. An immersed linear finite element method with interface flux capturing recovery. *Discrete & Continuous Dynamical Systems-Series B*, 17(2012), 2343–2357.

[28] S. H. Chou, D. Y. Kwak and K. T. Wee. Optimal convergence analysis of an immersed interface finite element method. *Advances in Computational Mathematics*, 33(2010), 149–168.

[29] M. Crouzeix and P. Raviant. Conforming and nonconforming finite element methods for solving the stationary Stokes equations. *RARIO Anal. Numér*, 7.R3(1973), 33-75.

[30] R. S. Falk. Nonconforming finite element methods for the equations of linear elasticity. *mathematics of computation*, 57(1991), 529–550.

[31] T. P. Fries and T. Belytschko. The extended/generalized finite element method: an overview of the method and its applications. *International Journal for Numerical Methods in Engineering*, 84(2010), 253–304.

[32] H. Gao, Y. Huang and F. F. Abraham. Continuum and atomistic studies of intersonic crack propagation. *Journal of the Mechanics and Physics of Solids*, 49(2001), 2113–2132.

[33] Y. Gong, B. Li and Z. Li. Immersed-interface finite element methods for elliptic interface problems with nonhomogeneous jump conditions. *SIAM J. Numer. Anal.*, 46(2008), 472-495.

[34] Y. Gong and Z. Li. Immersed interface finite element methods for elasticity interface problems with non-homogeneous jump conditions. *Numerical Mathematics: Theory, Methods & Applications* 3(2010), 23–39.

[35] J. Guzmán, M. Sánchez and M. Sarkis. On the accuracy of finite element approximations to a class of interface problems. *Mathematics of Computation*, 85(2016), 2071–2098.

[36] R. Guo, T. Lin and Q. Zhuang. Improved error estimation for the partially penalized immersed finite element methods for elliptic interface problem. *International Journal of Numerical Analysis and Modeling*, 16(2019), 575–589.

[37] A. Hansbo and P. Hansbo. An unfitted finite element method, based on Nitsche's method, for elliptic interface problems. *Computer Methods in Applied Mechanics and Engineering*, 191(2002), 5537–5552.

[38] A. Hansbo and P. Hansbo. A finite element method for the simulation of strong and weak discontinuities in solid mechanics. *Computer Methods in Applied Mechanics and Engineering*, 193(2004), 3523–3540.

[39] P. Hansbo, M. G. Larson and S. Zahedi. A cut finite element method for a Stokes interface problem. *Applied Numerical Mathematics*, 85(2014), 90–114.

[40] X. He, T. Lin and Y. Lin. Approximation capability of a bilinear immersed finite element space. *Numerical Methods for Partial Differential Equations*, 24(2008), 1265–1300.

[41] X. He, T. Lin and Y. Lin. Immersed finite element methods for elliptic interface problems with non-homogeneous jump conditions. *International Journal of Numerical Analysis & Modeling*, 8(2011), 284–301.

[42] X. He, T. Lin and Y. Lin. The convergence of the bilinear and linear immersed finite element solutions to interface problems. *Numerical Methods for Partial Differential Equations*, 28(2012), 312–330.

[43] S. Hou, P. Song, L. Wang and H. Zhao. A weak formulation for solving elliptic interface problems without body fitted grid. *Journal of Computational Physics*, 249(2013), 80–95.

[44] P. Huang, J. Chen and M. Cai. A mortar method using nonconforming and mixed finite elements for the coupled Stokes-Darcy model. *Advances in Applied Mathematics and Mechanics*, 9(2017), 596–620.

[45] D. Jacqmin. Calculation of two-phase Navier-Stokes flows using phase-field modeling. *Journal of Computational Physics*, 155(1999), 96–127.

[46] R. Kafafy, T. Lin and J. Wang. Three-dimensional immersed finite element methods for electric field simulation in composite materials. *Internat. J. Numer. Methods. Engrg.*, 64(2005), 940-972.

[47] K. Kergrene, I. Babuška and U. Banerjee. Stable generalized finite element method and associated iterative schemes; application to interface problems. *Computer Methods in Applied Mechanics and Engineering*, 305(2016), 1–36.

[48] M. Kirchhart, S. Gross and A. Reusken. Analysis of an XFEM discretization for Stokes interface problems. *SIAM Journal on Scientific Computing*, 38(2016), 1019–1043.

[49] R. Kouhia and R. Stenberg. A linear nonconforming finite element method for nearly incompressible elasticity and Stokes flow. *Computer Methods in Applied Mechanics and Engineering*, 124(1995), 195–212.

[50] Z. Li. The immersed interface method using a finite element formulation. *Applied Numerical Mathematics*, 27(1998), 253–267.

[51] Z. Li, T. Lin and X. Wu. New Cartesian grid methods for interface problems using the finite element formulation. *Numerische Mathematik*, 96(2003), 61–98.

[52] Z. Li, T. Lin Y. Liu and R. C. Rogers. An immersed finite element space and its approximation capability. *Numerical Methods for Partial Differential Equations*, 20(2004), 338-367.

[53] T. Lin, Y. Lin and X. Zhang. Partially penalized immersed finite element methods for elliptic interface problems. *SIAM Journal on Numerical Analysis*, 53(2015), 1121–1144.

[54] T. Lin, D. Sheen and X. Zhang. A locking-free immersed finite element method for planar elasticity interface problems. *J. Comput. Appl. Math.*, 236(2012), 4681-4699.

[55] Z. Li and X. Yang. An Immersed interface finite element methods for elasticity equations with interfaces. *Contemporary Mathematics*, 383(2005), 285-298.

[56] T. Lin and X. Zhang. Linear and bilinear immersed finite elements for planar elasticity interface problems. *Journal of Computational and Applied Mathematics*, 236(2012), 4681–4699.

[57] A. Liu and J. Chen. A partially penalized P_1/CR immersed finite element method for planar elasticity interface problems. *Numerical Methods for Partial Differential Equations*, 48(2019), 2117–2134.

[58] A. Massing, M. G. Larson, A. Logg and M. E. Rognes. A stabilized nitsche overlapping mesh method for the stokes problem. *Numerische Mathematik*, 128(2014), 73–101.

[59] F. Qin, J. Chen, Z. Li and M. Cai. A Cartesian grid nonconforming immersed finite element method for planar elasticity interface problems. *Computers and Mathematics with Applications*, 73(2017), 404-418.

[60] A. Reusken. Analysis of an extended pressure finite element space for two-phase incompressible flows. *Comput. Vis. Sci.*, 11(2008), 293-305.

[61] A. Reusken and T. Nguyen. Nitsche's method for a transport problem in two-phase incompressible flows. *J. Fourier. Anal. Appl.*, 15(2009), 663-683.

[62] A. Sutton and R. Balluffi. Interfaces in Crystalline Materials. *Clarendor Press*, 1995.

[63] I. S. Sokolnikoff. Mathematical Theory of Elasticity. *McGraw-Hill Book Company, New York*, 1956.

[64] B. Wang, K. Xia and G. W. Wei. Second order method for solving 3d elasticity equations with complex interfaces. *Journal of Computational Physics*, 294(2015), 405–438.

[65] H. Wang, J. Chen, P. Sun and F. Qin. A conforming enriched finite element method for elliptic interface problems. *Applied Numerical Mathematics*, 127(2018), 1–17.

[66] H. Wang, J. Chen, P. Sun, and N. Wang. A conforming enriched finite element method for Stokes interface problems. *Comp. Math. Appl.*, 75:4256-4271 2018.

[67] Q. Wang and J. Chen. A new unfitted stabilized Nitsche's finite element method for Stokes interface problems. *Computers & Mathematics with Applications*, 70(2015), 820–834.

[68] C. Wu, Z. Li and M. Lai. Adaptive mesh refinement for elliptic interface problems using the non-conforming immersed finite element method. *Int. J. Numer. Anal.*, 8(2011), 466-483.

[69] J. Xu. Estimate of the convergence rate of finite element solutions to elliptic equations of second order with discontinuous coefficients. *Natural Science Journal of Xiangtan University (in Chinese)*, 1(1982), 84–88.

[70] J. Xu and S. Zhang. Optimal finite element methods for interface problems. *Comp. Sci. Engng.*, 104, 2016.

[71] X. Yang, B. Li and Z. Li. The immersed interface method for elasticity problems with interface. *Dynamics of Continuous, Discrete and Impulsive Systems*, 10(2003), 783–808.

[72] X. Zhang. Nonconforming immersed finite element methods for interface problems. *Thesis (Ph.D.)-Virginia Polytechnic Institute and State University*, 2013.

Publications and completed papers

1. A partially penalized P_1/CR immersed finite element method for planar elasticity interface problems. Numer Methods Partial Differential Eq., 35(2019), 2318 - 2347.
2. An immersed finite element method for planar elasticity interface problem. Journal of Advances in Mathematics and Computer Science. 34(2019), 1-16.
3. A partially super penalty nonconforming enriched finite element method for elasticity interface problems in mixed formulation. (finished)
4. An immersed finite element method for Stokes interface problems. (being modified)

Acknowledgements

On the completion of my thesis, I appreciate all those who made this possible with advice and kindness. First and foremost, I am greatly indebted to my advisor Professor Jinru Chen. In these three years, I learned a lot from him. He not only gave me guidance in my process of research, but also taught me how to behave in many things. His effective advice and comments have kept the thesis in the right way. He gave me the opportunity to make everything possible.

Thanks to other Professors and the classmates in our seminar, they shared a lot of valuable experiences and ideas with me. I also want to show my gratitude to my roommate Yujie Wang, my friends Lijun Yan and Qilian Zheng, my girlfriend Siying Feng for their spiritual support and help in life.

At last, I would like to thank my mother and sister for her support in my whole life. Without their love, I couldn't be where I am now. Once again, thanks to all of you, I will continue to work hard and live up to your expectations.

Angran Liu

2019-3-25